SELECTIVE SEPARATION OF ELEMENTS AND RADIOISOTOPES BY ION EXCHANGE CHROMATOGRAPHY

CLIVE NAIDOO

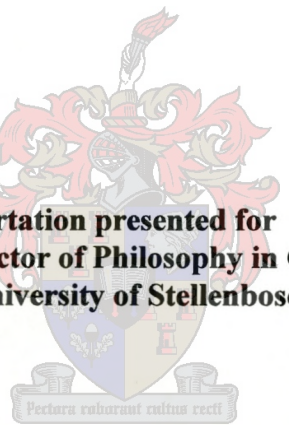

Dissertation presented for
the Degree of Doctor of Philosophy in Chemistry
at the University of Stellenbosch

Promoter: Dr TN van der Walt

Co-Promoter: Prof HG Raubenheimer

December 2002

DECLARATION

I, the undersigned, hereby declare that the work contained in this dissertation is my own original work and has not previously in its entirety or in part been submitted to any university for a doctoral degree in chemistry.

Signature:

Date:

ABSTRACT

The equilibrium distribution coefficients of 32 metal ions [Al(III), As(V), Cd(II), Ce(III), Ce(IV), Co(II), Cr(III), Cu(II), Fe(III), Ga(III), Ge(IV), In(III), La(III), Mn(II), Mo(VI), Nb(V), Ni(II), Pr(III), Sb(V), Sc(III), Se(IV), Sn(IV), Ta(V), Tb(III), Te(IV), Ti(IV), V(V), W(VI), Y(III), Yb(III), Zn(II) and Zr(IV)] on a cation exchanger (Bio-Rad® AG50W-X8) and an anion exchanger (Bio-Rad® AG1-X8) in varying oxalic acid - sulphuric acid mixtures were successfully determined. The equilibrium distribution coefficients of these selected metal ions were determined in both 0.05 M and 0.25 M oxalic acid at various concentrations of sulphuric acid (0.005 M, 0.05 M, 0.10 M, 0.25 M, 0.50 M, 1.00 M, 1.50 M and 2.00 M). Attempts to explain the sorption behaviour of the selected metal ions were made by using MINEQL+, a speciation modelling program, and the speciation systems for Al(III), Cd(II), Co(II) and Zn(II) in varying oxalic acid – sulphuric acid mixtures were determined. Two component [Zr(IV)-La(III); Al(III)-La(III); Ga(III)-Zn(II); As(V)-Zn(II); Cu(II)-Ce(IV); Ga(III)-Ce(IV); Ge(IV)-Ce(III); Mo(VI)-Y(III); Nb(V)-Y(III); Ga(III)-Co(II); As(V)-Co(II) and Fe(III)-Mn(II)] and three component [Fe(III)-Ga(III)-Zn(II) and Zr(IV)-Ta(V)-Yb(III)] mixtures on a 10 ml or 13 ml cation exchange resin in a variety of oxalic acid – sulphuric acid mixtures were successfully separated. Two component [As(V)-Zr(IV); Co(II)-Fe(III); Ni(II)-Co(II) and Ni(II)-Fe(III)] and three component [Ni(II)-As(V)-Se(IV); Al(III)-Zn(II)-Ge(IV) and As(V)-Cu(II)-Ge(IV)] mixtures on a 10 ml or 13 ml anion exchange resin in a variety of oxalic acid – sulphuric acid mixtures were also successfully separated and studied. It was also shown how some of the elution curves developed above could easily be adapted for radiochemical separations.

Using the relevant data from the above study, a separation for ^{68}Ge from a Ga_2O target was developed according to a method based on acid dissolution of the target and chromatography on an anion exchange resin (Bio–Rad® AG1–X8). The separated ^{68}Ge showed high radionuclidic purity and an acceptable chemical purity.

OPSOMMING

Die ewewigsverdelingskoëffisiënte van 32 metaalione [Al(III), As(V), Cd(II), Ce(III), Ce(IV), Co(II), Cr(III), Cu(II), Fe(III), Ga(III), Ge(IV), In(III), La(III), Mn(II), Mo(VI), Nb(V), Ni(II), Pr(III), Sb(V), Sc(III), Se(IV), Sn(IV), Ta(V), Tb(III), Te(IV), Ti(IV), V(V), W(VI), Y(III), Yb(III), Zn(II) en Zr(IV)] op 'n katioonruiler (Bio-Rad® AG50W-X8) en 'n anioonruiler (Bio-Rad® AG1-X8) in veranderende oksaalsuur-swaelsuurmengsels is met welslae bepaal. Die ewewigsverdelingskoëffisiënte van hierdie geselekteerde elemente is in beide 0.05 M en 0.25 M oksaalsuur by verskeie konsentrasies swaelsuur (0.005 M, 0.05 M, 0.10 M, 0.25 M, 0.50 M, 1.00 M, 1.50 M en 2.00 M) bepaal. Daar is gepoog om die sorpsiegedrag van die geselekteerde metaalione te verklaar deur die gebruik van MINEQL+, 'n spesiëring-modelleringsprogram, en die spesiëringsisteme vir Al(III), Cd(II), Co(II) en Zn(II) in veranderende oksaalsuur-swaelsuurmengsels is bepaal. Tweekomponent [Zr(IV)-La(III); Al(III)-La(III); Ga(III)-Zn(II); As(V)-Zn(II); Cu(II)-Ce(IV); Ga(III)-Ce(IV); Ge(IV)-Ce(III); Mo(VI)-Y(III); Nb(V)-Y(III); Ga(III)-Co(II); As(V)-Co(II) en Fe(III)-Mn(II)] en driekomponent [Fe(III)-Ga(III)-Zn(II) en Zr(IV)-Ta(V)-Yb(III)] mengsels op 'n 10 ml of 13 ml katioonruilhars in 'n verskeidenheid oksaalsuur-swaelsuurmengsels is met welslae geskei. Tweekomponent [As(V)-Zr(IV); Co(II)-Fe(III); Ni(II)-Co(II) en Ni(II)-Fe(III)] en driekomponent [Ni(II)-As(V)-Se(IV); Al(III)-Zn(II)-Ge(IV) en As(V)-Cu(II)-Ge(IV)] mengsels op 'n 10 ml of 13 ml anioonruilhars in 'n verskeidenheid oksaalsuur-swaelsuurmengsels is ook met welslae geskei en bestudeer. Daar is ook aangetoon hoe sommige van die elueringskrommes wat hierbo ontwikkel is, maklik vir radiochemiese skeidings aangepas sou kon word.

Deur gebruik te maak van die relevante data uit die studie hierbo, is 'n skeiding vir ^{68}Ge uit 'n Ga_2O-teiken ontwikkel volgens 'n metode gebaseer op suurdissolusie van die teiken en chromatografie op 'n anioonruilhars (Bio-Rad® AG1-X8). Die geskeide ^{68}Ge het hoë radionukliedsuiwerheid en 'n aanvaarbare chemiese suiwerheid getoon.

ACKNOWLEDGEMENTS

I would like to extend my sincere thanks and appreciation to:

My promoter, Dr Nico van der Walt, Head of the Radionuclide Production Group, iThemba LABS, for his enthusiastic and continued contributions throughout the duration of this project. His encouraging and thorough approach has been immensely inspiring to me.

My co-promoter, Prof HG Raubenheimer, Head of the Chemistry Department, University of Stellenbosch, for his enthusiastic interest and sound guidance that contributed to the completion of this thesis.

Prof GE Jackson, Chemistry Department, University of Cape Town, for his assistance with the speciation study of this project.

My fellow colleagues at the iThemba LABS, Mr S Dolley, Ms Z Buthelezi, Mr J Hanekom and Mr S Ngatshe, who have contributed in one way or another to the completion of this project.

My parents and especially my wife, Krishnee, and son, Sachin, for their love, support and encouragement during the course of this project.

Finally, I would like to declare that without the guidance and strength of the Lord, none of this work would have been possible.

CONTENTS

LIST OF FIGURES

LIST OF TABLES

CHAPTER 1

GENERAL INTRODUCTION AND AIMS OF THE STUDY

1.1 BACKGROUND OF THE iTHEMBA LABS

This study was carried out at the iThemba LABS (formerly, the National Accelerator Centre), Faure, South Africa. The iThemba LABS is a multidisciplinary scientific research laboratory, established in 1977 under the control of the Council for Scientific and Industrial Research. Since 1988 it has been one of several National Facilities administered by the National Research Foundation (NRF), and provides facilities for:

- the training of students in basic and applied research using accelerated particle beams
- particle radiotherapy for the treatment of cancer
- the supply of accelerator-produced radioisotopes for diagnostic studies in nuclear medicine and for research.

The iThemba LABS is organized so as to bring together people working in medical, biological and physical sciences who are interested in the use of accelerated particle beams, by providing opportunities for research and postgraduate training in these disciplines, and also by stimulating mutual interest in the interdisciplinary areas.

The accelerators operated by the iThemba LABS are a 6 MV Van der Graaff accelerator, an 8 MeV injector cyclotron which provides light ions for a 200 MeV cyclotron, a second injector

cyclotron which provides heavy ions and polarised ions for the 200 MeV machine, and the 200 MeV Separated-Sector Cyclotron (SSC) itself.

The Van der Graaff accelerator is a high-precision, variable-energy machine, capable of accelerating light ions to energies of between 0.5 and 20 MeV with an energy spread of less than one part in 10 000. The accelerator can also produce pulsed beams of particles with 0.2-nanosecond pulses every 500 nanoseconds, which makes it particularly useful for research with neutrons. The iThemba LABS Van der Graaff accelerator is used almost exclusively for materials research and for solid-state physics. This work is done in close collaboration with South African universities and technikons, as well as with overseas laboratories.

The (SSC) at the iThemba LABS is a variable-energy machine capable of accelerating protons to a maximum energy of 200 MeV. This gives the protons sufficient velocity to travel a distance equivalent to four times around the earth in only one second. Protons of 200 MeV can just pass through the human body, making them especially suitable for cancer therapy.

Two small conventional cyclotrons, designed and constructed by the iThemba LABS, are used as injectors (pre-accelerators) for the much larger SSC. The first injector uses an internal ion source to produce the intense beams of light ions required for radiotherapy and radioisotope production. The second is designed both for heavy ions, such as those of carbon, argon and krypton, and for polarised proton and deuteron beams, and has therefore been provided with two external ion sources. It also provides an alternative source of protons for therapy.

The SSC has a diameter of 13.2 metres and a height of 7 metres. The four sector magnets together weigh 1400 tons, and are positioned to an accuracy of one-tenth of a millimetre. The cyclotron is housed in a vault surrounded by concrete walls more than 4 metres thick to provide shielding against neutrons. The entire facility contains over 30 000 cubic metres of concrete in the form of floor slabs, shielding walls or removable shielding roof beams. The accelerated particle beams are guided to specific areas within the shielded building for radiotherapy, radioisotope production or for basic research in a number of disciplines, including nuclear physics and radiobiology.

Radiotherapy facilities are provided by the iThemba LABS at the Medical Radiation Group, together with the 30-bed Faure Hospital. The facilities at the iThemba LABS are specifically designed to provide beams of high-energy protons and neutrons for radiotherapy and for related radiobiological experiments. Neutrons are potentially more effective in controlling certain types of tumour than the radiation from linear accelerators, which are routinely used in radiotherapy. Protons have the advantage that much more of the dose delivered can be accurately localised within the tumour volume, which minimises damage to surrounding healthy tissue. Since 1989, cancer patients have regularly received treatment with neutron therapy, while the first facilities for proton therapy were commissioned in 1993. For proton therapy a computerised system has been developed which uses video cameras to locate the patient automatically, and then precisely positions the patient for therapy by using a motor driven treatment couch.

Radioisotopes have been manufactured in South Africa since 1965. This started at the 32 MeV CSIR cyclotron in Pretoria, and since its closure in 1988 the radioisotope production

programme has been continued with the SSC, supported by a strong research and development programme. The 66 MeV proton beam of the SSC and its superior facilities make it possible to produce a wide variety of short-lived isotopes, such as ^{18}F, $^{81}Rb/^{81m}Kr$, ^{67}Ga, ^{111}In, ^{123}I, ^{201}Tl, as well as radiolabelled compounds for medical purposes. In addition, long-lived radioisotopes such as ^{22}Na, ^{55}Fe, ^{68}Ge, ^{82}Sr and ^{139}Ce are manufactured.

1.2 BACKGROUND OF THE RADIONUCLIDE PRODUCTION GROUP

Cyclotron produced radioisotopes, which have to be in a specific chemical form or incorporated in an organic compound, are often used as tracers to monitor various bodily functions. Highly sophisticated equipment such as gamma cameras and positron emission tomographs are then used to detect gamma rays and form images showing the tracer locations. This is one of the techniques used in diagnosing and localising malignant tumours.

The high purity radioisotopes which are produced at the iThemba LABS on a weekly basis satisfy South Africa's entire demand for certain important cyclotron-produced medical radioisotopes and radiopharmaceuticals. More than 1000 consignments are supplied to about fifty provincial hospitals, private nuclear medicine practices and research institutions throughout the country and are used in nearly 10 000 patients per year. In addition, a number of other radiopharmaceutical products are under development and some are available on request from the iThemba LABS for patient use, on prescription, or for clinical trials and evaluations. None of these radioisotopes can be produced anywhere else in South Africa. Furthermore, they cannot be imported cost-effectively from abroad because of their short half-lives, and, in most instances, they cannot be replaced satisfactorily with other (reactor-produced

or imported) radioisotopes. In order to obtain a perspective of the production procedures, a brief explanation of the facility layout and production sequence is given.

- The first step in the production of a specific radioisotope is the preparation of the target material (solid, liquid or gaseous) into a form suitable for bombardment with the proton beam. Solid targets of various materials are prepared by one or more of the following processes: cutting, machining, cold or hot sintering. Because of the heating of targets under the bombardment, all targets have to be water-cooled, and therefore all water-soluble or highly corrosive target materials have to be encapsulated. Solid targets or target capsules are mounted in standardised target holders, while liquids and gases have to be contained in special target holders with high integrity, since leakage can cause serious contamination problems.

- Since radioisotope production targets become highly radioactive when bombarded, they are a radiation health hazard to personnel and therefore have to be handled remotely. For this purpose target holders are transported by means of a remotely-controlled target transport system. The transport system comprises a microcomputer control system, motorised trolleys and transportation rails connecting the target bombardment station (in the bombardment vault) to the hot-cell complex, parking loop and target storage area.

- The target bombardment station is a complex microcomputer-controlled system and consists of three rotary target magazines behind one another, mounted inside a cylindrical radiation shield. Each magazine has the capacity to load five target holders, and a maximum of three targets can be bombarded in tandem. A pneumatic robot arm facilitates transfer between the

transport trolleys and the target magazines, and a pneumatic pusher arm connects the targets to the beamline. Cooling water to the target holders is also provided via the pusher arm. The various targets are bombarded for different time periods, varying from approximately 5 minutes up to a few months.

- After bombardment, the target holders are transported to one of the reception hot-cells, where the target material is removed from them.

- The chemical separation of the desired radioisotopes is performed in the chemical processing hot-cells. These hot-cells are lead shielded chambers where "hot" chemistry is performed under negative pressure atmospheric conditions.

- After separation, the radioisotopes are transported to the dispensing laboratory where the pharmacist performs the dispensing in aseptic conditions and performs the quality control, i.e. checks the chemical purity, radionuclidic purity, etc. of the final product.

- After dispensing, the vials containing the radioisotopes are sealed and then packed into lead pots and tins, and thereafter into boxes, before being dispatched to the various local hospitals or to Cape Town International Airport for transport to remote hospitals.

Cyclotron-produced radioisotopes have become increasingly popular in medical and industrial research fields despite their relatively high cost when compared to reactor-produced radioisotopes [1-5]. The two production methods are used to create two fundamentally different classes of radionuclides. Cyclotron-produced radioisotopes are generally neutron

deficient whilst reactor-produced radioisotopes are neutron rich. The main advantage derived from cyclotron-produced radioisotopes is that they usually have a high specific activity. Additionally it is more difficult to produce several isotopes with convenient half-lives and decay characteristics, by neutron bombardment [6] compared to cyclotron irradiation [7,8].

The cyclotron invented by Lawrence (1934) can, from the chemist's point of view, be considered as a source of reagents, namely energetic protons, deuterons, helium (III) and alpha particles, which are used to induce nuclear reactions to form the required product. In short, it realises the eternal dream of the ancient alchemist: the transmutation of one element into another.

For the production of radiopharmaceuticals the following points play a very important role:

- The production method must be economically viable.
- The product must have a high specific activity.
- The chemical separation must be simple and easy to carry out in a hot-cell, with minimum radiation exposure to the operator.
- The radiopharmaceutical must comply with specifications and be registered with the South African Medicines Control Board.

A carrier-free radioisotope is usually characterised by: a high specific activity, a high radionuclidic purity (free from other radioisotopes), a high radiochemical purity (free from other chemical forms, for example $^{123}I^-$ must be free of $^{123}IO_3^-$) and a high chemical purity (the presence of non-active material). Radionuclidic purity is normally determined by a high

resolution gamma ray spectrometer while radiochemical purity is determined by paper, gel or thin layer chromatography. The chemical purity is normally determined by flame atomic absorption spectrometry, electrothermal atomisation spectrometry, induced coupled plasma emission spectrometry, or colorimetric spectrophotometry [1].

Chemistry is therefore one of the most important disciplines in the preparation, separation and quality control of carrier-free radioisotopes and other radiopharmaceuticals.

The iThemba LABS utilises a proton beam of 66 MeV for the production of a number of radioisotopes for radiopharmaceutical and other applications. A radioisotope is produced by selecting an appropriate target material, and a small disc of this material is then bombarded with the proton beam. The resulting nuclear reaction that takes place in the target produces a new element - the radioisotope. This radioisotope then has to be chemically separated from the target material, purified from all contaminants and then sterilised before it can be used as a medicine.

The chemical separation of a radioisotope from the target material is complicated not only by the very small amount (10^{-9}-10^{-12} g) of radioisotope formed compared to the amount (1–16 g) of non-radioactive target material present, but also by the presence of other radioisotopes produced by side reactions and chemical impurities in the target material. To isolate the required radioisotope a variety of chemical techniques such as precipitation, co-precipitation, gel filtration, solvent extraction, distillation, electrodeposition and ion exchange chromatography has been used [2].

This study will focus on the ion exchange chromatographic technique because of the simplicity and effectiveness of the separation procedure and because in most separations, specialised pieces of equipment (such as centrifuges and mechanical shakers) can be replaced by a single resin column. This technique works well within the confines of a hot-cell and minimises the radiation exposure to the operator.

In planning an ion exchange separation, the following points had to be taken into account. Since the specific radioisotope to be prepared is normally in picogram to nanogram quantities compared to the gram amounts of the target material, a big separation factor, α^{A}_{B}, is needed to separate a radioisotope, A, from the target material, B, or *vice versa*. In general, the radioisotope must have a large distribution coefficient ($D > 500$) and the target material a small distribution coefficient ($D < 10$). Initially the separation factor must be larger than 50. The resin column must have good kinetics so that equilibrium is reached as quickly as possible as the ions move down the resin column, to obtain a sharp separation. A relatively small resin column is always preferred to a large column, since smaller elution volumes are required to elute the sorbed elements. This also leads to a short chemical separation process, which is often an important factor in the final product yield, which is dependent on the half-life of the specific radioisotope. Less radioactive waste is also generated [7].

1.3 MOTIVATION FOR THE STUDY

Systematic information about the ion exchange behaviour of elements is indispensable for planning separations and estimating optimum conditions. The more extensive the systematic information on distribution coefficients, the more variables the analyst has at his disposal when looking for selective elemental separations. These separations would then normally serve as a basis for radioisotopic separations.

Systematic surveys of the behaviour of a large number of elements on a strong acid cation exchange resin have been reported for hydrochloric acid [9,10], nitric acid [11], sulphuric acid [11], hydrobromic acid [12,13], perchloric acid [10,14] and hydrochloric acid – perchloric acid [15], hydrochloric acid – ethanol [16], hydrochloric acid – acetone [17,18,19] and hydrobromic acid – acetone [12,20] mixtures. Various other organic complexing systems, which include citrate [21], formate [22], tartrate [23,24], succinate [25,26] and malate [27] media have also been reported. Systematic surveys of the behaviour of elements on a strong base anion exchange resin have also been reported for hydrochloric acid [28], nitric acid [29], hydrofluoric acid [30], phosphoric acid [31], sulphuric acid [32] and hydrochloric acid - hydrofluoric acid [33,34], nitric acid - hydrofluoric acid [35,36] and sulphuric acid - hydrofluoric acid [36] mixtures. Various other systems, which include EDTA [37,38], DCTA [39], malonic acid [40], ascorbic acid [40], tartaric acid [41,42] and citric acid [43] media, have also been reported.

Systematic information on distribution coefficients of elements in oxalic acid solutions or oxalic – mineral acid mixtures is limited to work done by Nozaki et al. [44] and Strelow et al. [45] with cation exchange resins, and by De Corte et al. [46] and Strelow et al. [47] with anion

exchange resins. Oxalic acid is a very promising complexing agent for certain elements to be separated by anion exchange as well as cation exchange chromatography, firstly because it's a moderately strong acid, and secondly, because it forms relatively strong metal complexes. The effective concentration of oxalate and bioxalate anions, and therefore the metal complex and ion exchange equilibria which determine the value of the distribution coefficient, can easily be modified by mixing the oxalic acid with a strong mineral acid such as hydrochloric acid [44,47], nitric acid [45] or possibly sulphuric acid, and it is assumed that this would have some influence on the sorption of elements on an ion exchange resin. The anion of the mineral acids will compete for exchange sites on the resin, and not only the concentration, but also the kind of anion, governs the strength of this competition. In addition, we also need to consider opposing effects: with lower pH we have not only less complexation, but also less sorption due to the anion effect. No addition of buffer solutions, which introduce unwanted cations, is necessary. Nozaki et al. [44] presented a systematic study of cation exchange distribution coefficients of 19 elements with the Amberlite® IR-120 resin in the oxalic acid - hydrochloric acid mixture. Unfortunately, the results were presented as curves that allow only for an approximate estimation of the actual values of the distribution coefficients. Strelow et al. [45] presented only the distribution coefficients for Mg and Al with the cation exchangers, Bio-Rad® AG50W-X4 and AG50W-X8, in the oxalic acid and oxalic acid – nitric acid mixtures. The oxalic acid concentrations varied from 0.1 M to 0.5 M and the nitric acid concentrations from 0.1 M to 0.2 M and, unfortunately, this work was limited to only two elements. De Corte et al. [46] presented a systematic study of anion exchange distribution coefficients of 12 elements with the Dowex® 1-X8 resin in pure oxalic acid solutions. The oxalic acid concentrations varied from 0.001 M to 0.98 M. However, this work involved radioactive tracers and thus was not useful for large-scale separations. Strelow et al. [47] presented a

systematic study of anion exchange distribution coefficients of 36 elements (1 mmole) with the Bio-Rad® AG1-X8 resin in the oxalic acid – hydrochloric acid mixture. Two oxalic acid concentrations of 0.05 M and 0.25 M were selected and the hydrochloric acid concentrations varied from 0.01 M to 4 M. The same authors carried out a systematic study of anion exchange distribution coefficients of 29 elements (1 mmole) with the Bio-Rad® AG1-X8 resin in the oxalic acid – nitric acid mixture. Again, two oxalic acid concentrations of 0.05 M and 0.25 M were selected and the nitric acid concentrations were varied from 0.01 M to 4 M. The work of Strelow et al. [47] was the first comprehensive and systematic study of elements involving oxalic acid. However, this work did not involve certain other elements (As, Ce, Ge, Pr, Sb, Se, Sc, Tb, Te, Y and Yb) that are commonly involved in radioisotopic separations. Applications of cation and anion exchange separations in oxalic acid or oxalic acid – mineral acid mixtures are known [48-51]. According to a literature survey, no cation or anion exchange behaviour of elements in oxalic acid – sulphuric acid mixtures has been published. It is conceivable that the sulphate anion will also have an influence in controlling the ion exchange equilibria of the oxalic acid – sulphuric acid system. The H^+ of the H_2SO_4 can also suppress the dissociation of the oxalic acid system. Therefore, a detailed systematic cation as well as anion exchange study in the oxalate – sulphate mixture of selected elements was necessary and such an investigation was planned and carried out. The oxalic acid concentrations of 0.05 M and 0.25 M, and the sulphuric acid concentrations of 0.005 M – 2 M, were chosen so that this study could be comparable with the work of Strelow et al. [45,47]. A number of the possibilities of this oxalic acid – sulphuric acid system for separation applications using a cation and an anion exchanger, needed attention. In addition, the adaptation of these separations for radioisotopic separations was also foreseen and is described in detail in this thesis.

1.4 OBJECTIVES OF THE STUDY

I. To investigate the equilibrium distribution coefficients for metal ions [Al(III), As(V), Cd(II), Ce(III), Ce(IV), Co(II), Cr(II), Cu(II), Fe(III), Ga(III), Ge(IV), In(III), La(III), Mn(II), Mo(VI), Nb(V), Ni(II), Pr(III), Sb(V), Sc(III), Se(IV), Sn(IV), Ta(V), Tb(III), Te(IV), Ti(IV), V(V), W(VI), Y(III), Yb(III), Zn(II) and Zr(IV)] on a cation exchange resin (Bio-Rad® AG50W-X8) in 0.05 M and 0.25 M oxalic acid at various concentrations of sulphuric acid (0.005 M, 0.05 M, 0.10 M, 0.25 M, 0.50 M, 1.00 M, 1.50 M and 2.00 M). The above metal ions were selected because they are commonly used in the production of various types of radioisotopes in the form of a target material, and/or in the form of the involved radiocontaminants produced during the nuclear bombardment of a target material or by decay of some of these radioisotopes. Often the radiochemist is faced with the problem of separating the target material from the radiocontaminants. As mentioned previously, earlier investigations were limited to only a few elements [44-47], and it was foreseen that an investigation involving a larger selection of elements in varying oxalic acid – sulphuric acid mixtures would provide the analyst with additional variables for radiochemical separations. The strong acid cation exchange resin (AG50W-X8) was chosen because it could, in contrast to many other studies involving this type of resin, be used under a variety of conditions. In addition, elemental separations were investigated to indicate the separation possibilities of the oxalic acid – sulphuric acid system and how it could be adapted for radioisotopic separations.

II. To investigate the equilibrium distribution coefficients for the above selected metal ions on an anion exchange resin (Bio-Rad® AG1-X8) in 0.05 M and 0.25 M oxalic acid at various concentrations of sulphuric acid (0.005 M, 0.05 M, 0.10 M, 0.25 M, 0.50 M, 1.00 M, 1.50 M and 2.00 M). The same metal ions with the AG1-X8 resin were chosen for the purpose of comparisons with {I} above and with the work of Strelow et al. [47]. Again, elemental separations were carried out to indicate the separation possibilities of the oxalic acid – sulphuric acid system and how it could be adapted for radioisotopic separations.

III. To investigate the quantitative separation of mixtures [Ge(IV) in combination with Al(III), As(V), Co(II), Cu(II), Ga(III), In(III), La(III), Ni(II), Y(III), Yb(III) and Zn(II)] on an anion exchange resin in 0.25 M oxalic acid – 1 M sulphuric acid mixture. This study could serve as preliminary work to the study in {IV} below, i.e. the separation of ^{68}Ge radioisotope from a proton-irradiated Ga_2O target. The separation of Ge(IV) from the above selected elements is based on the possible radiocontaminants that could be produced under proton bombardment of the Ga_2O target.

IV. To investigate a radiochemical separation for the purification of ^{68}Ge radioisotope from a proton-irradiated Ga_2O target using ion exchange chromatography. Various nuclear reactions leading to ^{68}Ge production are cited in the literature, varying in target material, nuclear raction pathway and type of radiochemical separation [53-65]. In this study, Ga_2O (initially proposed by van der Walt [66]) is chosen as the target material because it can be encapsulated in an inexpensive aluminium canister while Ga has to be encapsulated in an inert metal canister such as niobium. The nuclear reaction pathway

is limited to the high energy proton (66 MeV) beam with high beam currents (>65 μAH) available at iThemba LABS. Ion exchange chromatography is used as a method for radiochemical separations because it can easily be prepared in a hot-cell.

V. To investigate whether the sorption behaviour of the elements in the varying oxalic acid – sulphuric acid systems on the selected resins can be explained by a computer speciation program, namely MINEQL+.

VI. To adapt analytical methods, such as electrothermal atomisation spectrometry and induced coupled plasma emission spectrometry, for elemental analysis when applying the various techniques used above in accordance with the relevant matrix.

1.5 SUMMARY

Chapter 1 outlines the facilities that were used during the investigations. The background of the iThemba LABS, and in particular the Radionuclide Production Group, is briefly discussed. An explanation as to why the ion exchange chromatographic principle is still currently being used by this Group for the production of radioisotopes is given here. In addition, this Chapter outlines the motivation and objectives of this study. The specific metal ions selected, the conditions (oxalic acid – sulphuric acid system using a strong acid cation exchange resin and a strong base anion exchange resin) and also why alternative ^{68}Ge production routes are still being investigated, are discussed.

In Chapter 2 an overview of the theory of ion exchange chromatography will be given. The various types of ion exchangers are classified. Various properties of the ion exchangers, for example particle size and form, temperature, crosslinkage and swelling, Donnan theory, stability, exchange capacity and selectivity, are discussed in relation to influences on the ion exchange process. In addition, the principles of chemical speciation, and in particular the speciation program used in this study, are discussed.

The following Chapter (3) outlines the experimental conditions used in the study, for example the ion exchange chromatographic methods, ion exchangers, reagents and apparatus, and analytical techniques used.

Chapter 4 contains the results and a discussion of the sorption behaviour of 32 metal ions on a cation exchanger (AG50W-X8) in 0.05 M and 0.25 M oxalic acid at various concentrations of sulphuric acid (0.005 M, 0.05 M, 0.10 M, 0.25 M, 0.50 M, 1.00 M, 1.50 M and 2.00 M).

Similarly, the results of the study on the sorption behaviour of the same 32 metal ions on an *anion exchanger* (AG1-X8) in 0.05 M and 0.25 M oxalic acid at various concentrations of sulphuric acid (0.005 M, 0.05 M, 0.10 M, 0.25 M, 0.50 M, 1.00 M, 1.50 M and 2.00M) are presented in Chapter 5.

In Chapter 6 it is shown how the results of the previous two chapters could be adapted for radioisotope production. In particular, a detailed account is given of the production of ^{68}Ge from a Ga_2O target material. In addition, by using the elution curves in Chapter 4 and 5, a few other radiochemical separations are proposed.

Finally, Chapter 7 reviews how the results detailed in Chapters 4, 5 and 6 meet the objectives of this study and also serves to identify areas requiring further investigation.

1.6 REFERENCES

1. Nayak D., *Int. J. Appl. Radiat. Isot.,* 54, 195, 2001.
2. Chunfu Z., Wang Y., Yongping Z. and Xiuli Z., *Int. J. Appl. Radiat. Isot.,* 55, 441, 2001.
3. Ma D., McDevitte M.R., Finn R.D. and Scheinberg D.A., *Int. J. Appl. Radiat. Isot.,* 55, 463, 2001.
4. Inoue H., *Int. J. Appl. Radiat. Isot.,* 54, 595, 2001.
5. Chen F., Covas D.T. and Baffa O., *Int. J. Appl. Radiat. Isot.,* 55, 13, 2001.
6. Khalid M., Mushtaq A. and Iqbal M.Z., *Int. J. Appl. Radiat. Isot.,* 52, 19, 2000.
7. Guin R., Das S.K. and Saha S.K., *Int. J. Appl. Radiat. Isot.,* 52, 185, 2000.
8. Alcaraz Pelegrina J.M. and Martinez-Aguirre A., *Int. J. Appl. Radiat. Isot.,* 55, 419, 2001.
9. Strelow F.W.E., *Anal. Chem.*, 32, 1185, 1960.
10. Nelson F., Murase T. and Kraus K., *J. Chromatogr.*, 13, 503, 1964.
11. Strelow F.W.E., Rethemeyer R. and Bothma C.J.C., *Anal. Chem.* 37, 106, 1965.
12. Strelow F.W.E., Hanekom M.D., Victor A.H. and Eloff C., *Anal. Chim. Acta.*, 76, 377, 1975.
13. Nelson F. and Michelson D.J., *J. Chromatogr.*, 25, 414, 1966.
14. Strelow F.W.E. and Sondorp H., *Talanta*, 19, 113, 1972.
15. Nelson F. and Kraus K., *J. Chromatogr.*, 178, 163, 1979.
16. Strelow F.W.E., Van Zyl C.R. and Bothma C.J.C., *Anal. Chim. Acta.*, 45, 81, 1969.
17. Fritz J.S. and Retting T.A., *Anal. Chem.*, 34, 1562, 1962.
18. Strelow F.W.E., Victor A.H., Van Zyl C.R. and Eloff C., *Anal. Chem.*, 43, 870, 1971.

19. Korkisch J. and Ahluwahia S.S., *Talanta,* 14, 155, 1967.

20. Korkisch J. and Klakl E., *Talanta,* 16, 377, 1969.

21. Frache R., Dadone A. and Baffi F., *VII Convegno Nazionale di Chimica Inorganica*, Pesaro, Italy, 1974.

22. Frache R., Dadone A. and Baffi F., *Atti del XII Congresso Nazionale Societa Chimica Italiana*, S. Margherita di Pula, Cagliari, Italy, 1975.

23. Dadone A., Baffi F. and Frache R., *Talanta*, 23, 593, 1976.

24. Dadone A., Baffi F., Frache R. and Mazzucotelli A., *Chromatographia*, 12, 38, 1979.

25. Alumaa P. and Pentchuk J., *Chromatographia*, 47, 77, 1998.

26. Dadone A., Baffi F., Frache R. and Mazzucotelli A., *II Convegno Nazionale di Chimica Analitica*, Pedavo, Italy, 1979.

27. Dadone A., Baffi F., Frache R., Cosma B. and Mazzucotelli A., *Chromatographia*, 14, 32, 1981.

28. Kraus K.A. and Nelson F., *Proc. Intern. Conf. Peaceful Uses at Energy,* Vol. 7 U.N., Geneva, 1956.

29. Buchanan R.F. and Faris J.P., *Radioisotopes in the Physical Sciences and Industry*, Vol. 2, I.A.E.A., Vienna, 1962.

30. Faris J.P., *Anal. Chem.*, 32, 520, 1960.

31. Polkowska-Motrenko H. and Dybezynski R., *J. Chrom.*, 88, 387, 1974.

32. Danielson L., *Acta. Chem. Scand.*, 19, 670, 1965.

33. Faris J.P., *Pittsburgh Conf. on Anal. Chem. and Applied Spectroscophy*, Feb. 1961.

34. Nelson F., Rush R.M. and Kraus K.A., *J. Am. Chem. Soc.*, 82, 339,1960.

35. Huff E.A., *Anal. Chem.*, 36, 1921, 1964.

36. Danielson L., *Acta. Chem. Scand.*, 19, 1859, 1965.

37. Wodkiewicz L. and Dybezynski R., *J. Chromatogr.*, 32, 394, 1973.

38. Vigneau O., Pinel C. and Lemaire M., *Anal. Chim. Acta.,* 435, 75, 2001.

39. Schoebrechts F., Merciny E. and Duyckaerts G., *J. Chromatogr.*, 79, 293, 1973.

40. Chakrovorty M. and Khopkar S.M., *Chromatographia*, 10, 100, 1977.

41. Morie G.P. and Sweet T.R., *J. Chromatogr.*, 16, 201, 1964.

42. Strelow F.W.E. and van der Walt T.N., *Anal. Chem.,* 54, 457, 1982.

43. Huffman E.H. and Oswalt R.L., *J. Am. Chem. Soc.*, 72, 3323, 1950.

44. Nozaki T., Takeuchi K., Yamauchi T and Nomura T., *Jpn. Analyst*, 27, 454, 1978.

45. Strelow F.W.E. and van der Walt T.N., *S. Afr. J. Chem.*, 37, 149, 1984.

46. De Corte F., Van Den Winkel P., Speecke A. and Hoste J., *Anal. Chim. Acta.*, 42, 67, 1968.

47. Strelow F.W.E., Weinert C.H.S.W. and Eloff C., *Anal. Chem.*, 44, 2352, 1972.

48. Korkisch J., *Handbook of ion exchange resins: applications to inorganic analytical chemisrtry*, Vol. 1, CRC Press, Florida, 1989, pp. 265.

49. Ding X. and Mou S., *J. Chromatogr.*, 920, 101, 2001.

50. Ji-Ying Ji. and Blesa M.A., *Inorg. Chem.,* 37, 3159, 1998.

51. Blesa M.A., *Inorg. Chem.,* 36, 6423, 1997.

52. Sharma S.D. and Sharma S.C., *J. Chromatogr.*, 841, 263, 1999.

53. Iwata Y., Kawamoto M. and Yoshizawa Y., *Int. J. Appl. Radiat. Isot.,* 31, 1537, 1983.

54. Choppin G.R. and Rydberg J., *Nuclear chemistry, theory and applications*, Pergamon Press, New York, 1985, pp. 35.

55. Hughes E., *Material in Engineering*, 2, 34, 1980.

56. Lambrecht R.M. and Sajjad M., *Radiochim Acta*, 43, 171, 1988.

57. Lambrecht R.M., *Radiochim Acta*, 34, 9, 1988.

58. Qaim S.M., *IAEA-SR-131/5*, Vienna, Austria, 13-17 October 1986.

59. Pao P.J., Silvester D.J. and Waters S.L., *J. Radioanal. Chem.*, 64, 267, 1981.

60. Gleason G.I., *Int. J. Appl. Radiat. Isot.*, 8, 90, 1960.

61. Mirzadeh S., Kahn M., Grant P.M. and O'Brien H.A., *Radiochim. Acta*, 28, 47, 1981.

62. Barong B. and Yinsong W., *Nucl. Sci. Tech.*, 3, 202, 1992.

63. Loc'h C., Maziere B., Comar D. and Knipper R., *Int. J. Appl. Radiat. Isot.*, 33, 267, 1982.

64. Grant P.M., Miller D.A., Gilmore J.S. and O'Brien H.A., *Int. J. Appl. Radiat. Isot.*, 33, 415, 1982.

65. Kopecky P., Mudrova B. and Svoboda K., *Int. J. Appl. Radiat. Isot.*, 24, 73, 1973.

66. van der Walt T.N., personal communication.

CHAPTER 2

ION EXCHANGE CHROMATOGRAPHY

2.1 INTRODUCTION

Ion exchange chromatography is of great significance in separations of ions with similar properties, i.e. systems which are difficult or impossible to analyse by other methods. The separation is based on the difference in sorbabilities of the ionic species on an ion exchanger to be separated. Very often the selectivities in complex-free media are too small to permit an effective separation, but, by taking advantage of complex formation and other equilibria in the solution, the separability can be increased. The principle in ion exchange chromatography is largely the same as in chromatographic analysis with other sorbents. Ion exchange chromatography has proved an excellent method for solving troublesome separation problems both in inorganic chemistry and with certain organic substances. The availability of suitable resinous exchangers, together with improved knowledge of them and the development of chromatographic working methods, has stimulated the vast expansion of ion exchange chromatography. Of special interest are investigations, carried out under the Plutonium Project, on the separation of the fission fragments formed during fission of the heavy elements. Among the fission products are different rare earths. By using cation exchange resins, these can be separated from one another [1]. Several other separations of very similar elements can be performed by this technique.

Ion exchange phenomena have been observed since about the middle of the 19^{th} century, but the practical significance of ion exchange was not recognised immediately, and it was not until

early in the 20th century that natural or synthetic ion exchangers were widely known. By then a number of relatively pure minerals such as zeolites and clays had been found or synthesised that exhibited ion exchange characteristics. Although these exchangers were commonly used in water treatment and are still employed today, some of them are unstable in acid and alkaline solutions and can be used satisfactorily only under nearly neutral conditions. Their exchange kinetics are also slow and very slow flow rates have to be used. Consequently these aluminosilicates are of little significance for the analytical separation of metal ions [1].

A more significant development took place in 1934, however, when it was discovered that some synthetic high molecular weight organic polymers containing a large number of functional groups, as an integral part, could be employed as ion exchange resins, which can be considered as gel-like dispersed systems. The dispersed medium is usually water and the dispersed portion is the three-dimensional polymer of the ion exchange resin, which is of organic origin. Cross-linked bonds (e.g., divinylbenzene bridges) between the polymer chains form a three-dimensional matrix (network, skeleton), which hinders the motion of the polymer chains and formation of a solution in contact with the solvent (water). Only swelling of the matrix in contact with the solvent occurs. This swelling is governed especially by the character, number and length of the cross-linked bonds [1].

An important feature differentiating the ion exchange resins from other types of gels is the presence of functional groups (also called exchangeable groups). The groups (e.g., $-SO_3^-H^+$ and $-N^+R_3$) are attached to the matrix. The ion exchange process between the ions in the solution takes place on these functional groups.

The exchange of ions between the ion exchange resin and the solution is governed by the following two principles:

1. The process is reversible (only rare exceptions are known).
2. The exchange reactions take place on the basis of equivalency in accordance with the principle of electroneutrality. The number of millimoles of an ion sorbed by an exchanger should correspond to the number of millimoles of an equally charged ion that has been released from the ion exchanger.

Ion exchange resins, on account of their property of exchanging ions in solutions, can be applied in various fields of chemistry. Concerning analytical chemistry, ion exchangers can not only be successfully applied in the quantitative separation of complex ionic mixtures (which is the main application of ion exchange resins), but also be used for other analytical purposes, e.g. for the microchemical detection of elements [2].

2.2 CLASSIFICATION OF ION EXCHANGERS

Ion exchange resins are divided into two groups, namely inorganic and organic ion exchangers. The latter is commonly used in analytical chemistry. The matrix of the vast majority of these ion exchange resins is a cross-linked copolymer consisting of styrene and divinylbenzene that is prepared by pearlpolymerisation. The particle size and particle size distribution of the spherical beads thus obtained depend on the extent of mechanical agitation and on reaction conditions during the polymerisation. A summary of the synthetic processes that are utilised

for the preparation of the analytically most important ion exchange resins, is presented in Figure 2.1 [3].

Figure 2.1. Preparation of ion exchange resins.

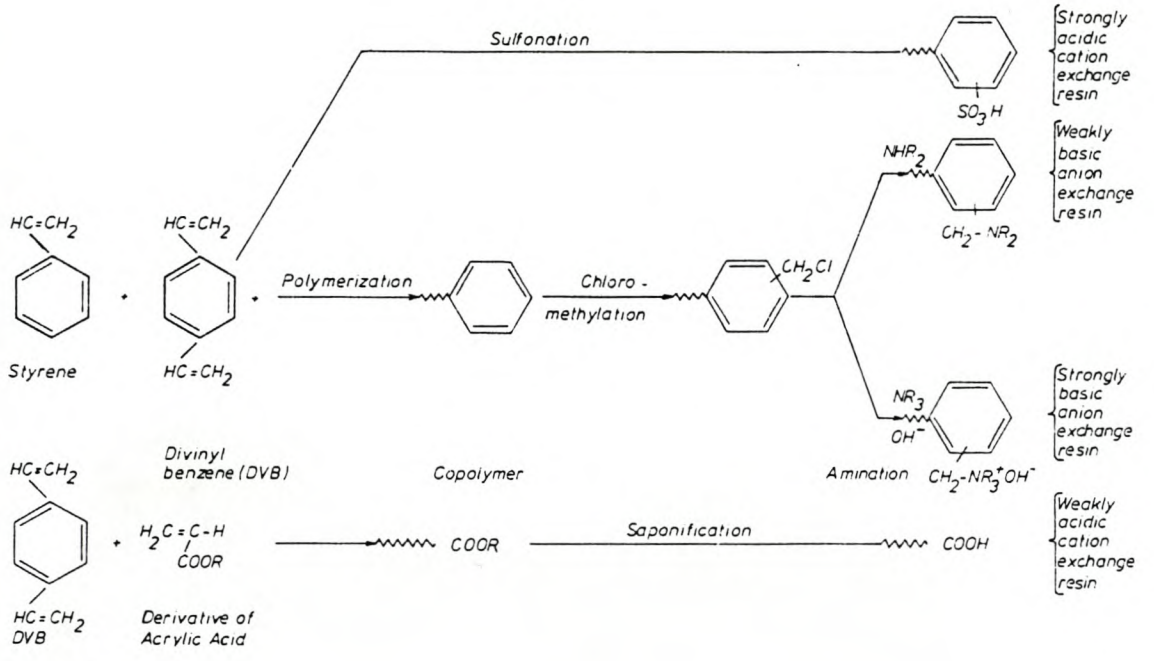

At present, the majority of ion exchanger manufacturers indicate their own products by the company name (Bio-Rad®, Dowex®, etc.). Symbols and numbers describing the type of the exchanger supplement the name. Additional symbols or abbreviations are used in order to describe the products more exactly. These symbols or abbreviations reflect the purity of the starting raw materials, the methods of treatment, the grain size of the resulting products, or other special properties of the materials. For example, the Bio-Rad® resin *AG1-X8, 100-200*

mesh, chloride form, which was used in this study, contains all of the following information [3]:

AG indicates that the resin is a purified Analytical Grade ion exchange resin specially prepared by Bio-Rad® from a Dowex® ion exchange resin. The starting material, Dowex® resin, is a technical grade product not generally acceptable for analytical work. The designation AG means that extensive purification and sizing have been performed at Bio-Rad® Laboratories.

The number 1 means that the resin is a type 1 (strongly basic) anion exchanger containing quaternary ammonium (NR_4^+) groups.

X8 refers to the extent of crosslinkage within the resin bead. In this case, there is 8% divinylbenzene crosslinkage of the styrene divinylbenzene copolymer.

100-200 refers to the bead size expressed in U.S. standard dry mesh designation. The actual hydrated bead diameter varies slightly from one resin to another.

Cl^- refers to the ionic form of the resin. In this case, the chloride is the negative counterion that is associated with the fixed positive quaternary ammonium functional groups on the resin.

The organic ion exchangers are divided into three groups, namely cation exchange resins, anion exchange resins and chelating resins. This study will be limited to cation and anion exchange resins [3].

2.2.1 Cation Exchange Resin

The first commercial sulfonic acid resins were produced at the Wolfen factory in Germany under the trade name Wofatit®. The products were made by the condensation of aromatic sulfonic acids, e.g. phenolsulfonic acid with formaldehyde. Since the resins contain both sulfonic acid groups and phenolic groups, they are bifunctional. The resins are produced in the form of hard dark granules of irregular shape. Data concerning the manufacture and properties of these resins have been reported by Griessbach [4]. These phenolic resins have been used for a number of analytical applications, but the more modern styrene-divinylbenzene resins are for several reasons more attractive to the analytical chemist. These resins are produced by sulfonation of a co-polymer of styrene with divinylbenzene. In this co-polymer, the divinylbenzene forms crosslinkages between the chains of polymerised styrene (Figure 2.1). It should be noted that the relative amount of divinylbenzene can be varied and commercial resins with varying degrees of cross-linking are available. The more divinylbenzene used, the harder and more brittle is the polymerisate. The degree of crosslinkage is defined in terms of the percentage divinylbenzene added during the polymerisation. Most commercial resins are made from co-polymers of styrene, ethylvinylbenzene and divinylbenzene [5], but in all respects of interest in this context, the resins behave as styrene-divinylbenzene resins. The co-polymer can be prepared in a pearl-polymerisation, from which it is obtained in the form of nearly spherical beads; and after introduction of the functional groups, the particles remain in bead form.

Although many commercial products contain a large number of cracked particles, much effort has been expended to eliminate resin breakage and cracking. Successful results have been reported by Wheaton and Harrington [6] and by Abrams [7]. The sulfonation is achieved with

sulphuric acid with, on average, about one sulfonic acid group per benzene ring present in commercial products of this type. This corresponds to an exchange capacity of approximately five milliequivalents per gram of dry resin in the H^+ form. The functional groups are, however, not all structurally equivalent. This dissimilarity may have some effect on certain phenomena, but as a practical matter it is of no great consequence. These resins can, therefore, be considered as monofunctional, provided, of course, that no other functional groups are present. As a matter of fact, several commercial resins of this type contain appreciable amounts of carboxyl groups formed by oxidation in the sulfonation step, but it is possible to prepare monofunctional resins if proper conditions are chosen [7]. Detailed studies of the preparation of sulfonated styrene-divinylbenzene resins have been published by Pepper [8] and Gregor [9]. Several methods have been suggested for the manufacture of resins whose exchange capacity is a result of carboxylic acid groups. Wofatit® C is the first commercial resin of this type. It is prepared by the condensation of 1,3,5-resorcylic acid with formaldehyde in alkaline medium. Other carboxylic resins can be prepared by the co-polymerisation of methacrylic or acrylic acid with divinylbenzene. The degree of crosslinkage can be varied within wide limits [10]. The structure of this type of resin is illustrated in Figure 2.1. Such resins can be manufactured in bead form by a pearl-polymerisation technique or in rods or plates by bulk polymerisation.

Other types of cation exchangers, e.g., resins containing phosphonic acid groups, $-PO(OH)_2$, have been prepared and are available commercially [11].

2.2.2 Anion Exchange Resin

The first commercial anion exchange resins were of the weakly basic type. Wofatit® M is a weakly basic resin obtained by the condensation of m-phenylenediamine and polyethylene-imine with formaldehyde. Similar condensation products were later manufactured in several countries and such products are still produced commercially. The preparation of weakly basic resins has been described by Topp and Pepper [12]. Most anion exchangers are produced by the introduction of structurally bound exchange groups into polystyrene-divinylbenzene resins. The most important method for the preparation of strongly basic anion exchange resins is based on the following principle [13]: First, methylene chloride groups are introduced into the co-polymer by treatment with chloromethyl ether in the presence of a swelling agent. Treatment of the chloromethylated resins with a tertiary amine, e.g., trimethylamine, will produce a quaternary ammonium salt, i.e., the chloride form of a strongly basic anion exchange resin.

Dowex® 1 is produced according to the method described above. The resin is so strongly basic that a considerable quantity of caustic soda is required to convert the resin into the free-base form. For certain purposes it is desirable to have a resin which regenerates more easily, but which still behaves as a stongly basic anion exchanger. Such a resin (e.g., Dowex® 2) is obtained when a hydroxyethyl group ($-C_2H_4OH$) is attached to the nitrogen atom in place of one of the methyl groups, i.e., when amination is made with N,N-dimethyl-ethanolamine instead of trimethylamine. If the chloromethylated product is treated with ammonia or with primary or secondary amines, it is, of course, possible to obtain weakly basic resins. Dowex® 3 is a resin of this type. It is made by amination with a mixture of aliphatic polyamines and

contains a mixture of primary, secondary and tertiary amine groups. Zerolit® G and H are examples of monofunctional weakly basic resins which possess polystyrene networks [14].

Anion exchangers of the styrene-divinylbenzene type are now available with varying degrees of crosslinkage. A low degree is preferred for the uptake of large ions. Other types of porous resins have also been suggested, and some phenolic resins which are made for the sorption of colouring substances of an acidic nature and other large molecules, have been brought onto the market (Decolorite®, Duolite® S-30). The structure of these resins is unknown. The structural formulas of the ion exchange resins used in this study (Bio-Rad AG50W- and Bio-Rad AG1-) are shown in Table 2.1 [15].

Table 2.1 Structural formulas of ion exchange resins used in this study.

Trade name (®)	Structural formula	Classification (resin type)
Bio-Rad AG 50W, Dowex 50, Amberlite IRA 120, Zeo-Karb 225, Cationite KU-2, Diaion SK1, Wofatit KPS, Lewatit S-100, Ostion KS	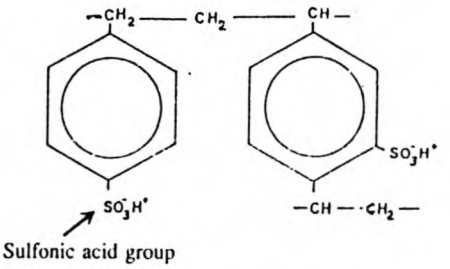 Sulfonic acid group	Monofunctional strongly acidic cation exchange resin (H^+ form)
Bio-Rad AG1, Dowex 1, Amberlite IRA-400, Deacidite FF, Anionite AV-17, Diaion SA1, Wofatit SBW, Lewatit M 500, Ostion AT, Resin 717	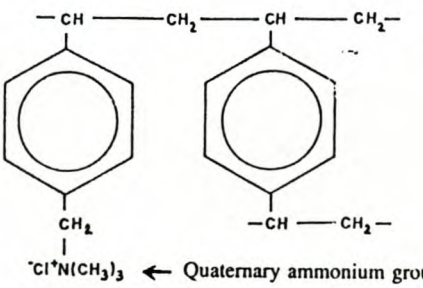 ← Quaternary ammonium group	Monofunctional strongly basic anion exchange resin (Cl^- form) (type 1)

2.3 GENERAL PROPERTIES OF ION EXCHANGE RESINS

Ion exchange resins perform efficiently in a variety of applications, in part because of their valuable chemical and physical properties. The physical properties of an ion exchange resin include matrix, functional group, ionic form, particle size distribution, particle shape, swelling, porosity for macroporous resins, permeability for gel type resins, and crosslinkage. The chemical properties include exchange capacity, water retention capacity, thermal stability, resistance to reduction and oxidation, solvent stability and response to ionic strength. Because of the high permeability and high concentration of functional groups within their chemical structure, ion exchange resins normally have a high effective capacity. Small volumes of resin can retain high molecular amounts of ionic material when used for concentrating substances of interest or for scavenging ions to be eliminated from a solution.

Ion exchange resins also provide high resolution chromatographic separations, because many interactions take place per unit of column volume. In addition, the remarkable chemical stability of ion exchange resins makes them usable with a variety of chromatographic conditions including high temperatures, organic solvents and strong reducing and some oxidising agents. The resin matrix remains chemically unchanged by the ionic interactions which take place at the functional groups, and the resins can be regenerated [16].

2.3.1. Particle Size and Form

Most Analytical Grade (AG) and Dowex® resins are available in several particle size ranges, although the ranges in Analytical Grade resins are more precisely controlled than the

commonly used Dowex® resins. The flow rate in a column increases with increasing resin particle size. The attainable resolution, however, increases with decreasing particle size i.e., less tailing is evident. The particle size of Analytical Grade resins is generally specified as dry mesh, mesh referring to the number of openings per inch on the screens used to size ion exchange resins. As the particle size of an ion exchanger decreases, the time required to reach equilibrium decreases, the flow rate is reduced, the settling rate of the resin is decreased and the efficiency of a given volume of resin increases. Generally 200-400 mesh and finer mesh resins are used for high resolution chromatography, 100-200 mesh (used in this study) for general purpose ion exchange techniques, and 50-100 mesh and coarser meshes for large scale applications and batch operations where the resin and sample are slurred together.

Most resins are available in several ionic forms and can be converted from one form to another. In the most straightforward example, the resin is used in an ionic form with a lower selectivity for the functional group than the sample ions to be sorbed. The sample ions are then sorbed when introduced, and can be desorbed by introducing an ion with high affinity for the resin, or a high concentration of an ion with equivalent or lower affinity. In many cases, a high concentration of the original counterion can be used for desorption, thus regenerating the resin at the same time the sample is eluted. In general, the lower the selectivity of the counterion, the more readily it exchanges for another ion of like charge. The order of selectivity can be used to estimate the effectiveness of different ions as eluants, with the most highly selective being the most efficient. The order of selectivity can also be used to estimate the difficulty of converting the resin from one form to another. Conversion from a highly selected to a less highly selected form requires an excess of the new ion [16].

2.3.2 Crosslinkage and Swelling

The styrene divinylbenzene ion exchange resins have a relatively rigid gel type structure. The porosity depends on the hydration of the matrix, which, in turn, is controlled by the hydration of the functional groups. Ion exchange resins are most hydrated and therefore most swollen, in water. Their swelling decreases as the ionic strength of the solvent is increased, or as increasingly non-polar solvents are added. Swelling is also affected by the ionic form of the resin and the hydrophilic nature of the functional group. The copolymer matrix of ion exchange resins consists of polystyrene chains tied together at intervals by divinylbenzene groups. The percentage of crosslinkage used determines the solubility, swelling, selectivity as well as other physical and chemical properties for a given type of ion exchanger. As the crosslinkage decreases, the permeability increases, and the ability of the resin to accommodate larger ions is increased. Low crosslinked resins (2%-4% styrene divinylbenzene) have a high degree of permeability, reach equilibrium more rapidly, and are able to accommodate larger ions. High crosslinked resins (8%-16% styrene divinylbenzene) that are used in this study exhibit properties in the opposite direction.

Ion exchange resins swell or shrink in different aqueous media. The solubility of a resin is limited by its crosslinked organic backbone. In a specific ionic form, the resin will be swollen to its greatest degree in water. This is caused primarily by the hydration of the functional groups with water, which is directly proportional to the number of hydrophilic functional groups on the polymer matrix. Most of the water retained by an ion exchange resin is held internally due to the hydration of the functional group. The amount of water is more or less

dependent upon the hydrophobic nature of the functional group and the ionic form of the resin [16].

2.3.3 Donnan Theory

The penetration of electrolytes can be calculated from the Donnan equation. For the distribution of an electrolyte, A_cC_a, between a homogeneous exchanger and an external electrolyte solution, we have:

$$\{A\}^{c}_{r} . \{C\}^{q}_{r} = \{A\}^{c} . \{C\}^{a}$$

where { } represents the ion activities in the external solution (no subscript) and the resin phase (subscript r). It should be stressed that this simple formulation of the Donnan equation is thermodynamically consistent, but that the influence of the swelling pressure on the chemical potential is included in the activity coefficient of the electrolyte inside the resin. The application of the Donnan theory to the penetration of electrolytes into cation exchange resins was first studied by Samuelson [16]. As predicted by theory, the following rules were found to hold true:

1. The concentration of movable electrolyte in the resin phase increases with increasing electrolyte concentration in the external solution, and approaches the external concentration in concentrated solutions.
2. For a given electrolyte and a given external concentration, the penetration decreases with decrease in swelling (increased degree of crosslinkage) of the resin.
3. For resins with a high degree of crosslinkage (low swelling), the electrolyte penetration can be neglected, provided that the external concentration is low.

For a given cation exchanger and a given equivalent concentration in the external solution, the penetration decreases with increase in valence of the co-ion [17].

2.3.4 Stability of Ion Exchange Resins

The chemical, thermal and radiation stability of ion exchange resins depends on the type of resin matrix, its degree of crosslinkage, the type of the functional group, and their counter ion. In addition to these fundamental factors, the stability of ion exchangers is affected by their synthesis. Also important are the purity of the original raw material and the method of preparation. The change in resin stability becomes especially evident in the change of the volume exchange capacity, the loss of functional groups, swelling changes and the formation, eventually, of new groups (especially weakly acidic) or the destruction of the resin matrix to varying degrees [18].

2.3.4.1 Chemical stability

According to the nature of degradation processes that occur during the chemical corrosion of ion exchangers, the following reaction types can occur:

1. Degradation of the macromolecular chain between the spatial bridges.
2. Chemical changes in groups belonging indirectly to the macromolecular chain (the functional groups remain unaffected).
3. Substitution or degradation of the functional groups.
4. Formation of new (especially weakly acidic) functional groups.

From the point of view of chemical stability of ion exchangers, the most important characteristic is their resistance towards oxidising agents. If the resin is degraded in its polymer matrix because of insufficient oxidation resistance, its crosslinkage is decreased. The resin swelling increases and, in a limited case, the resin is dissolved. Strongly basic anion exchange resins, the resins used in this study, are especially sensitive to H_2O_2. Resins containing the pyridinium groups are more resistant than other strongly basic exchangers. If the resins are in contact with acidic solutions of chromates, permanganates and vanadates, these anions are reduced with the oxidation of some components of the resin. However, cation exchangers styrene – divinylbenzene - SO_3H: heated to 70^0C in 3% H_2O_2 in the presence of Fe (III), resulted in weight losses of 1% divinylbenzene - 62% weight loss, 2% divinylbenzene - 46% weight loss, 4% divinylbenzene - 26% weight loss, and 8% divinylbenzene - 11,6% weight loss. Macroreticular, strongly basic anion exchange resins exhibit a higher stability to alkaline solutions than do gel-like resins [19].

2.3.4.2 Thermal stability

Sulfonated cation exchangers of the phenol-formaldehyde type (in the H^+ form) show the first symptoms of desulfonation at 100^0C. No change in the exchange capacity was found when this type of resin was heated to 70^0C in sealed ampules for 60 days. The opposite behaviour was found for a styrene-divinylbenzene strongly acidic cation exchanger, the resin used in this study. The exchange capacity of the latter resin decreases with increasing temperature due to increased desulfonation:

$$R_sSO_3H \rightarrow R_sH + H_2SO_4 \qquad (R_s = \text{resin matrix})$$

Increasing the temperature accelerates the desulfonation process, and at high temperatures (150^0C), a reaction between the sulphuric acid formed and oxidisable resin components begins and sulphur dioxide is formed.

$$R_{red} + H_2SO_4 \rightarrow R_{ox} + H_2O + SO_2$$

Desulfonation, together with other reactions, as a consequence of the air heating of the resin, was also observed for styrene-divinylbenzene cation exchangers. For this type of exchange resin in the H^+ form, differential thermal analysis revealed three endothermic changes: dehydration at 100 to 120^0C, desulfonation at 270 to 310^0C, and oxidative degradation for the matrix at temperatures above 430^0C. In addition to these three endothermic effects, an exothermic effect at 370^0C was observed corresponding to the depolymerisation of the matrix. The evidence suggests that at the higher temperatures, the $-SO_3H$ groups react, resulting in the formation of sulfones and additional cross-links. Further rise in temperature causes the breakdown in the sulfone to SO_2 as well as an extensive degradation of the polymer matrix form. The destructive reactions always occur in the functional groups first, since bonds in these groups are usually weaker than those in the polymer chains.

Air drying at room temperature of type 1 strongly basic anion exchange resins in the OH^- form, leads to a decrease in the volume exchange capacity of their functional groups. The loss of capacity accelerates with increasing temperature [20].

2.3.4.3 Radiation Stability

The interaction of radioactive radiation with ion exchange resins leads to their radiation damage. In the presence of a solvent (water), this primary degradation is accompanied by

secondary damage as a consequence of the reaction of the solvent radiolytic products with the resin. The consequences of radiation damage of the resin can be summarised as the following effects:

1. Loss in the exchange capacity due to the degradation of functional groups.
2. Formation of new functional groups.
3. Degradation of the resin matrix (Solubility of the resin increases due to the decrease in the molecular weight. On the other hand, the reverse effect occurs when the crosslinkage of the matrix increases {especially in resins of low crosslinkage}).
4. All the above effects (1 to 3) leading to a change in resin swelling.
5. Gaseous products also formed by radiolytic degradation of the resins.

Considerable changes appear at doses $>10^6$ Gy. Only 5% of the exchange capacity remained when Dowex® 50W-X8 had been irradiated by 3.9×10^7 Gy. The total extent of damage is given by a series of resin properties and structures. The effect of the cross-linking agent is that resin crosslinkages with divinylbenzene are less stable than those cross-linked with butadiene. If divinylbenzene is used for the resin preparation, the radiation stability of the exchanger will also depend on the ratio of the divinylbenzene isomers present. The effect of the amount of the cross-linking agent is that resins with a higher content of cross-linking agent are relatively more stable. The effect of the ionic form is that resins in the H^+ form are the most sensitive. Their stability can be increased by converting them to a suitable ionic form. If the resin is irradiated in air, new functional groups (predominantly carboxylic) are formed. Radiolysis of dry resins leads to the formation of gases (SO_2, SO_3 and especially H_2). On irradiating the swollen resin, new functional groups are also formed. However, the formation of hydroxyl groups

predominates. It can be concluded from numerous literature references that substantial changes occur for this type of resin at integral doses $>10^6$ Gy. Doses higher than 10^7 Gy usually cause such great damage that the resin cannot be used. The stability of the macroporous-type resins towards ionising radiation does not differ appreciably from that of gel-like resins.

The radiation stability of anion exchange resins depends on the matrix type and on the nature of the functional groups. The stability of resins containing aromatic cores in their matrix is higher than that of anion exchange resins based purely on aliphatic hydrocarbons. They are appreciably resistant towards ionising radiation. The stability of the functional groups of anion exchangers increases with decreasing basicity of the groups. The exchange capacity of strongly basic anion exchange resins (e.g., types 1 and 2) is appreciably reduced at doses of 10^5 to 10^6 Gy. They cannot be used at doses around 10^7 Gy. Weakly basic anion exchange resins are very sensitive towards ionising radiation. A remarkable degradation occurs usually at a dose of 10^5 Gy. However, several anion exchangers are substantially damaged even at doses of 10^2 Gy [21].

2.3.5 Exchange Capacity of Ion Exchangers

The exchange capacity of an ion exchange resin is the number of ion exchange sites per unit mass per volume of resin. The exchange capacity of an ion exchange resin is expressed both as the number of equivalents per gram of oven dried resin and the number of equivalents per unit volume of the hydrated (packed) resin. These data are often expressed as milliequivalents per gram of dry resin (ECD), and milliequivalents per gram of hydrated resin (ECV). For crosslinked polystyrene resins, the ECV for a particular resin type and ionic form increases

with crosslinkage, while the ECD is nearly independent of crosslinkage. The ECD for a class of ion exchange resin, for example, AG 1 resin, is relatively constant. When all the water is removed, the dry resin has approximately the same number of functional groups per unit mass of resin, regardless of the degree of crosslinkage.

The water retention capacity (WRC) for ion exchange resins is often given as the percentage of water. The WRC varies with crosslinkage and the ionic form. The WRC increases with decreasing crosslinkage because of the reduced physical strength of the crosslinkaged lattice. The resin may be more soluble as crosslinkages decrease and therefore it may be able to adsorb more water than increased crosslinkaged resins. If there were no crosslinkage, the resin would be completely soluble in water [22].

2.3.6 Selectivity of Ion Exchange Resins

If the ion exchange resin is added to an aqueous solution (free from complex-forming substances of an electrolyte), an exchange reaction between the ion exchanger and the ions in the solution takes place. The exchange reaction of ions of the same charge can be written as

$$R_sA + B^+ \leftrightarrow R_sB + A^+ \qquad (R_s = \text{resin matrix})$$

If this reaction is carried out in a closed system, the reaction goes to equilibrium due to the fact that the ion exchange is a reversible process. Equilibrium concentrations of ions taking part in the exchange are not identical under equilibrium conditions. They are dependent on the value of relative affinity of the reacting ions to the ion exchanger as well as on their initial concentration. It has been shown experimentally that the affinity (or ion exchange potential) of various ions to the same resin (in dilute solutions, <0.1 M) increases with ionic charge of the

ion investigated. Polyvalent ions are, therefore, attached to the exchange resin more firmly (under the same conditions) compared with monovalent ions. For ions of the same charge, it has been found that affinities are inversely proportional to the radius of the hydrated ions. This has general validity, but exceptions do exist. The affinity of cations to a series of cation exchange resins is similar or identical to the so-called lyotropic series. The affinity of anions is governed by similar rules. Moreover, it increases with increasing polarisability of the anions.

The difference in affinity between individual ions is called selectivity. The selectivity depends on the type and concentration of the reacting ions as well as on the quality of the solvent and the nature of the exchange resin. In principle, the selectivity of an ion exchange resin depends on the factors mentioned below (selectivity rules) [23]:

1. Selectivity of the resin increases with increasing content of the crosslinkage substance, e.g., divinylbenzene.
2. Ions with a smaller effective hydrated ionic radius are preferentially adsorbed.
3. If the ionogenic group of resin forms an ionic pair with the reacting ion, the selectivity of the resin to this type of ion is increased.
4. If substances in the solution form slightly dissociated compounds, then ions forming a more dissociated compound are preferentially adsorbed.
5. Selectivity of the resin decreases with increasing temperature. This effect can be explained as a consequence of the decrease in the ionic hydration shells leading to a diminishing of the difference between the effective hydrated ionic radii of the reacting ions.

From the point of view of analytical practice, the control of resin selectivity is of great importance. The most convenient way is to add a complex-forming agent to the ion exchange system. By choosing a suitable agent, it is possible to separate a mixture of ions easily (either by selective sorption or by selective elution) as a result of the change in the selectivity of the ionogenic groups of the resin. For the theoretical and practical description of ion exchange equilibria and hence of selectivities, the so-called selectivity coefficients (quotients), distribution coefficients and separation factors can be used. While the selectivity coefficients are mainly employed for theoretical purposes, the distribution coefficients are of enormous practical significance as will be shown in this study [23].

2.4 ION EXCHANGE EQUILIBRIUM

2.4.1 Selectivity Coefficient

If the exchange reaction of two ions A and B is described by the equation

$$bR_sA + aB^{b+} \leftrightarrow aR_sB + bA^{a+}$$

then the selectivity coefficient, $k_{B,A}$, is expressed by the relation

$$k_{B,A} = [R_sB]^a[A]^b / [R_sA]^b[B]^a$$

where [ ] is the analytical concentration (molarity) of the ion A or B, and a and b are the absolute charges of ions A and B respectively. The batch method is used for the determination of the selectivity coefficients as it is employed in connection with the determination of the distribution coefficients [23].

2.4.2 Equilibrium Distribution Coefficient

The equilibrium state in the system, electrolyte solution – ion exchange resin, can be expressed in various ways. Ion exchange equilibria are very often expressed in terms of the "distribution coefficient". This quantity is given by the ratio of the equilibrium concentrations of the same ion in the exchanger phase and in the solution. The equilibrium distribution coefficient, D, is defined by the following equation [23]:

$$D = \frac{\text{amount of component in ion exchanger phase at equilibrium}}{\text{amount of component in liquid phase at equilibrium}}$$

If the distribution coefficient is related to a unit mass (g) of the exchanger and to a unit volume (ml) of the solution, it is denoted by the symbol D_g, K_d or K_D (the latter two are most frequently used). If this quantity is related to a unit volume (ml) of the exchanger, the symbol D_v is used. However, no uniform symbol exists for this quantity as yet, and therefore a wide variety of symbols is found in the literature. The relation between the "mass" and "volume" distribution coefficients can be expressed by the equation [23]

$$D_g = D_v \cdot p$$

where p is the specific mass of the ion exchanger (the mass of the dry residue of the exchanger in 1 ml of the column filling). The distribution coefficients are determined either by the static (batch) method or by the dynamic (column) method.

In the batch method, the method used in this study, a known amount of the ion exchange resin in a known ionic form is added to a solution of known volume and qualitative and quantitative

composition. After equilibration (mechanical shaking machine), the change in concentration of the cation in question is determined (usually by analyzing the filtrate). For more precise measurements, the amount of ion sorbed by the resin should also be determined. The occluded solution is removed from the exchanger by centrifuging, and the sorbed ion is eluted with an appropriate solution. At the same time, the dry residue of the exchanger is determined. Resin quantities up to 1 g and solution volumes up to 250 ml are most frequently used for laboratory, static measurements. The concentration of the ions studied varies between trace carrier free amounts (for radioactive elements) and 10^{-3} to 10^{-2} M. The results are expressed as the weight distribution coefficient, defined according to the following equation:

$$D_g(K_d) = \frac{\text{mass of component / gram of dry exchanger}}{\text{mass of component / millilitre of liquid phase}}$$

This method is especially well suited for the determination of distribution coefficients in the order of 0.5 to 10^6 [23].

2.4.3 Separation Factor

The separation factor, α, is given by the ratio of the distribution coefficients or retention volumes of two different elements that were determined under identical experimental conditions.

$$\text{Separation factor} = \alpha = D_g\,(K_d)(a) / (D_g)(K_d)\,(b) = V_{max}\,(a) / V_{max}$$

where a and b may, for instance, be Na and K or any other pair of elements. This ratio determines the separability of two elements by ion exchange. Separations can be achieved only

if this ratio shows a value which is different from unity, i.e., the more α differs from 1 for a given ion pair, the easier the two ions will separate on an ion exchange column. The separation factor will play a vital role in this study when devising elemental separations [23].

2.5 THE ION EXCHANGE PROCESS

In order to initiate the desired ion exchange process, the ion exchange resin should be in contact with a solution containing ions capable of being retained by it. Two methods exist for bringing an ion exchanger into contact with ions in solution: the batch method and the column method.

Batch ion exchange is never complete, but in certain cases it can be accepted as practically quantitative. Ion exchange resins are nearly always used in columns. As a solution passes down an exchanger column, it continually meets fresh unreacted exchanger, so that equilibrium is shifted in the desired direction. By this multistage effect, even an unfavourable equilibrium can give exchange which is complete within the limits of analytical detection.

In addition to true ion exchange, other interactions can take place between the solute and the resin, which may either supplement the ion exchange interaction or be used in place of ion exchange to separate either ionic or non-ionic species [23]. There are: sorption, complex formation, partition, ion exclusion, ligand exchange and molecular sieving.

2.6 CHEMICAL SPECIATION

2.6.1 Analytical Techniques in Chemical Speciation

Most analytical methods used in the study of chemical speciation are concerned with the identification and quantification of a particular chemical species in a sample as well as the numerical description of the distribution or abundance of different species containing the same central element. Analytical techniques that have been developed and used in speciation studies can be divided into two broad groups: those that detect total metal concentrations, and those that detect a specified fraction of the total [24].

There are numerous methods for the detection of total concentrations in a given sample. The most widely used include inductively coupled plasma spectrometry, atomic absorption spectrometry and atomic emission spectrometry [24-26]. These methods, however, are usually coupled with techniques that separate or fractionate the sample to detect the different species present effectively. The samples are separated according to their size by filtration/ultrafiltration, gel filtration or a combination of size and charge through dialysis, ion exchange and solvent extraction. In order for these techniques to be utilised effectively, and in order to avoid changes in concentration during the separation stage of the procedure, the complexes being studied must be inert.

In contrast, there are few techniques available which can detect a specified fraction of the total metal concentration in a sample at levels sensitive enough to be used in a speciation analysis. These include high performance liquid chromatography, gas chromatographic techniques and

anodic stripping voltametry (ASV) [27-29]. ASV seems to be the most promising analytic tool for direct or *in situ* metal species detection in solution. This electrochemical procedure allows the measurement of different fractions of the total concentration by simply adjusting the electrochemical parameters. However, although this technique is the most sensitive analytical method available, it is restricted to metals that form an amalgam with mercury. The interpretation of the data generated by ASV is often difficult.

The analytical study of speciation is riddled with problems that need to be overcome by the investigator. The reliability of the technique is dependent on the extent to which these problems affect the chosen method. The main challenge in the analytical method of speciation study lies in the disturbance of the equilibrium state during the sampling stage. In order to ascertain species distribution accurately, one must obtain a sample of the solution under investigation when all the complexes that have formed are at equilibrium or quasi-equilibrium. This is a paradox as the very act of sampling disrupts this equilibrium, changing the concentration of the species present. This in turn leads to a misinterpretation of the species distribution in the sample. Separation techniques also play an important part in the perturbation of the equilibrium state. In the physical fractionation of a sample, for example, certain species may be adsorbed onto the filters being used. This not only alters the equilibrium state, but also leads to the adsorbed species not being detected. Though investigators strive to minimise these effects by using centrifugation where feasible, sorption losses are unavoidable. Ion exchange resins, which are used to separate species according to their charge, are also a source of error, as they retain some of the unstable charged species. In addition, the detection limits or the analytical window that a specific analytical technique possesses can often be a limiting factor in speciation studies. Some techniques are not sensitive enough to detect a particular fraction of

the metal at a particular concentration. Although the occurrence of these errors can be reduced to some extent, the effects cannot be completely nullified. It remains for the chemist to carefully select a technique that will adequately represent the species distribution at equilibrium state. In an attempt to avoid such sources of error associated with sampling and sample preparation, some analytical chemists have found ways to predict the most likely species distribution pattern in a sample by calculation (chemical speciation modelling) [28].

2.6.2 Principles of Chemical Speciation Modelling

Chemical speciation modelling is based on the study of thermodynamic equilibria. Therefore, in order to understand the intricacies of speciation modelling fully, it is important to grasp the basics of thermodynamic equilibrium [30,31]. Before speciation calculations can be carried out, it is important to define correctly the equilibrium problem that is to be solved. The first step in the definition of the problem is that each of the chemical species involved in the reactions must be expressed as a set of components. Once the chemical components have been identified, the necessary chemical reactions for the formation of the relevant chemical species must be compiled. Speciation calculations are algebraic and are based on a wide range of variables that must be expressed numerically for the calculation to be performed. After the components have been identified, the mass action terms that define the formation of the various possible species must be collated. The final expressions are a re-arrangement of equilibrium equations in terms of the formation constants of all the possible species in a system. The most difficult and tedious part of solving equilibrium problems is the compilation and solving of the numerous algorithms. The increase in the sophistication of the modern personal computer (PC) has led to the development of computer speciation programs, which set up the speciation

problem, carry out the difficult calculations and predict the species distribution in a specified medium [32].

Although several computer models have been developed over many years, it is possible to categorise each one by tracing the developmental stages of computer modelling [33-35]. Initially, the computer speciation models that were designed, differed in the thermodynamic assumptions on which they were based. This, in turn, influenced the numerical techniques used to execute the speciation calculations [30]. There are two distinct thermodynamic frameworks on which computer speciation models may be based. These are the equilibrium constant approach [36] and the Gibbs free energy of reaction approach [37]. While both approaches are valid methods in speciation calculations, the Gibbs free energy approach, which requires a database of free energy values, presents the user with a fundamental limitation, which is the unavailability of reliable free energy values. Thus for the purposes of this study, we shall confine ourselves to the evolution of computer models that utilise the equilibrium constant approach.

The equilibrium constant approach employs the Newton-Raphson iteration with the added feature of a curve-crawler technique that allows for rapid solution to the iteration. Although the development of this approach was general and only the reactions taking place in the specified solution could be computed, it was later welcomed by the scientific community, as it could be easily adapted to suit digital computers. The use of this general and multipurpose model became a foundation on which more sophisticated and specific programs were developed [36].

2.6.3 Speciation Programs in Analytical Chemistry

Computer speciation programs that used the equilibrium constant approach to solve equilibrium problems in physical and analytical chemistry were the three main first generation programs WATEQ, SOLMNEQ and EQ3 [30]. These programs had a very small and limited thermodynamic database.

A major breakthrough in the development of computer speciation programs occurred when Morel and Morgan [38] designed REDEQL, a program written in the FORTRAN language. REDEQL has the capacity to calculate multi-component, multi-ligand systems and possesses a large thermodynamic database containing a large number of metal-ligand interactions. Furthermore, REDEQL has the capacity to specify saturation values, which allows dissolution or precipitation of solids in solution to be taken into account.

REDEQL uses the Newton-Raphson method to compare the difference between the total calculated component concentration and the total analytical concentration, and solves by iteration. The program does not impose charge balance or proton balance on the calculation, which results in the inability to solve certain problems. Modification of REDEQL has led to the development of programs such as REDEQL2, GEOCHEM and MINEQL [36]. These programs have improved the reliability of the Newton-Raphson method by employing additional mathematical techniques such as under-relaxation and curve-crawling. Each program has its own advantages and variations to suit its particular function. Other useful programs that have followed include MINEQL+, MINTEQA2 and PHREEQC and many hundreds of derivative programs that assume a fairly advanced knowledge of computers and

programming [33]. In all the programs available, 95% of the numerical algorithms are the same. MINTEQA2 and PHREEQC, although excellent models, do not allow the modeler to interact with the program.

MINEQL+, already developed in the mid-1970's in its initial format [38, 39], was used in this study, because it is a powerful and user-friendly chemical equilibrium modelling system that can be used to perform calculations in aqueous systems of low to moderate ionic strength (<0.5 M). MINEQL+ is a data-driven program, so there is no need for programming. In the simplest scenario, systems are created by selecting chemical components from a menu, scanning the thermodynamic database and running the calculation. MINEQL+, over the years, has maintained such robustness and elegance that it is hard to beat. All the improvements that have come to MINEQL+ over the years have not tampered with its core numerical techniques.

2.6.4 Problems Associated with Chemical Modelling

Speciation modelling is not without its drawbacks and constraints. The strengths of a computer speciation program are often offset by inadequacies that must be considered when selecting an appropriate speciation model. The majority of computer speciation programs are based on the equilibrium approach as described earlier. Therefore, the correct use of equilibrium constants in order to perform the speciation calculation is very important. A computer model is only as accurate as its thermodynamic database [38]. Problems arise chiefly from the absence of equilibrium constant values, the numerous incorrect values recorded in the literature, as well as the manner in which the computer program handles its thermodynamic database. The incorrect values, in turn, find their way into the thermodynamic databases of computer speciation

programs, affecting the results of the calculations. In addition, values found in the literature vary greatly from one author to another. Nordstrom et al. [31] reported that for a single species, the values for equilibrium constants may differ by as much as three orders of magnitude. There are several factors that contribute to the inaccuracy of formation constants present in the literature. These are:

1. Data generated through poor and irreproducible analytical techniques that were appropriate at one stage, are often shown to be inadequate as newer methods and knowledge become available.
2. In some literature references, the presence of impurities in the reagents used is a major cause of inaccurate results. The impurities in the system are involved in unexpected side reactions that inadvertently lead to the lowering of measured constants in that particular system.
3. The selection of an appropriate background electrolyte in which the complex formation reactions are performed, can be a source of error. Some electrolytes interact significantly with the system under investigation, leading to competing side reactions and cause an underestimation of the formation constants.

Although the scientific community is still in the process of re-determining and re-evaluating current thermodynamic data, a considerable effort is still required until a satisfactory standard is achieved. This onerous task has fallen on the US National Bureau of Standards, which has taken responsibility for funding studies that evaluate available thermodynamic data and select the most reliable values. However, some computer speciation models still have incorrect or missing values in their thermodynamic databases which have not been updated or re-

determined. The manner in which speciation models handle the thermodynamic database is also a source of error. Weaknesses in this regard include the limited size of the thermodynamic database, the manner in which data is transformed according to unspecified predetermined criteria, and the lack of information on the methods and sources from which the constants were obtained [38].

2.7 REFERENCES

1. Korkisch J., *Handbook of ion exchange resins*, Vol. 1, CRC Press, Inc., Florida, USA, 1989, pp. 1.
2. Korkisch J., *Handbook of ion exchange resins*, Vol. 1, CRC Press, Inc., Florida, USA, 1989, pp. 10.
3. Korkisch J., *Handbook of ion exchange resins*, Vol. 1, CRC Press, Inc., Florida, USA, 1989, pp. 4.
4. Griessbach R., *Angew Chem.*, Beifte, 31, 1939.
5. Pepper K.W. and Reichenberg D, *Z. Electrchem*, 57,183, 1953.
6. Wheaton R.M. and Harrington D.F., *Ind. Eng. Chem.*, 44, 1796, 1952.
7. Abrams J.M., *Ind. Eng. Chem.*, 48,1469, 1956.
8. Pepper K.W., *J. Appl. Chem.*, 1, 124, 1951.
9. Gregor H.P., Bregman J.I., Gutoff F., Broadley R.D., Baldwin D.E. and Overberger C.G., *J. Colloid Sci.*, 6, 20, 1951.
10. Howe P.C. and Kitchener J.A., *J. Chem. Soc.*, 2143, 1955.
11. Bregman J.I., *Ann.* N.Y. *Acad. Sci.,* 57, 125, 1953.
12. Topp N.E. and Pepper K.W., *J. Chem. Soc.*, 3299, 1949.
13. Samuelson O., *Ion exchange separations in analytical chemistry*, John Wiley & Sons Inc., New York, 1963, pp. 327.
14. Samuelson O., *Ion exchange separations in analytical chemistry*, John Wiley & Sons Inc., New York, 1963, pp. 31-32.
15. Korkisch J., *Handbook of ion exchange resins*, Vol. 1, CRC Press, Inc., Florida, USA, 1989, pp. 5.

16. Bio-Rad, *Guide to ion exchange*, Catalogue No. 140-9997, 1997, pp. 5-7.

17. Samuelson O., *Ion exchange separations in analytical chemistry*, John Wiley & Sons Inc., New York, 1963, pp. 45-46.

18. Korkisch J., *Handbook of ion exchange resins*, Vol. 1, CRC Press, Inc., Florida, USA, 1989, pp. 21.

19. Korkisch J., *Handbook of ion exchange resins*, Vol. 1, CRC Press, Inc., Florida, USA, 1989, pp. 22.

20. Korkisch J., *Handbook of ion exchange resins*, Vol. 1, CRC Press, Inc., Florida, USA, 1989, pp. 23.

21. Korkisch J., *Handbook of ion exchange resins*, Vol. 1, CRC Press, Inc., Florida, USA, 1989, pp. 27-28.

22. Bio-Rad, *Guide to ion exchange*, Catalogue No. 140-9997, 1997, pp. 8.

23. Korkisch J., *Handbook of ion exchange resins*, Vol. 1, CRC Press, Inc., Florida, USA, 1989, pp. 30-35.

24. Sarzanini C., *J. Chromatogr.,* 850, 213, 1999.

25. Do B., Robinet S., Pradeau D. and Guyon F., *J. Chromatogr.,* 918, 87, 2000.

26. Zheng J., Ohata M., Furuta N. and Kosmus W., *J. Chromatogr.,* 874, 55, 2000.

27. Michalke B. and Schramel P., *J. Chromatogr.,* 834, 341, 1999.

28. Liu W. and Lee H.K., *J. Chromatogr.,* 834, 45, 1999.

29. Murimboth J., Lam M.T. Hassan N.M. and Chakrabarti C.L., *Anal. Chim. Acta.*, 423, 115, 2000.

30. Ball J.W. and Nordstrom D.K., *U.S. Geological Survey Open –File Report,* 91, 189, 1992.

31. Nordstrom D.K., Plummer L.N and Jones B.F., *American Chemical Society Symposium Series, Washington D.C.,* 416, 398, 1990.

32. Parkhurst D.L. and Plummer L.N., *Geochemical models,* Van Nostrand Reinhold, New York, 1993, pp. 199.

33. Parkhurst D.L., *U.S Geological Survey Water-Resources Investigations Report*, 95, 143, 1995.

34. Barak P., *J. Agron. Educ.,* 19, 44, 1990.

35. Plummer L.N., Prestemon E.C. and Parkhurst D.L., *U.S Geological Survey Water-Resources Investigations Report*, 94, 130, 1994.

36. Tao S., Wen Y., Long A., Dawson R., Cao J. and Xu F., *Comp. and Chem.,* 25, 215, 2001.

37. Pesavento M., Alberti G. and Profumo A., *Anal. Chim. Acta.,* 405, 309, 2000.

38. Morel F.M.M., *Principles and applications of aquatic chemistry*, Wiley-Interscience, New York, 1983, pp. 25.

39. Westall J.C., Zachary J.L. and Morel F.M.M., *MINEQL, A computer program for the calculation of chemical equilbrium composition of aqueous system,* Massachusetts Institute of Technology (MIT), Tech. No. 18, 1976.

CHAPTER 3

EXPERIMENTAL SECTION

The aim of this Chapter is to outline the ion chromatographic methods, ion exchangers, reagents, apparatus and analytical instrumentation used in this study. The experimental procedures and parameters are directly related to the results presented in Chapter 4, 5 and 6.

3.1 ION EXCHANGE CHROMATOGRAPHIC METHODS

To study the sorption behaviour of elements on different ion exchangers, various ion exchange chromatographic methods exist, as described in Chapter 2. The methods used in this study were the equilibrium distribution coefficient, elemental separations (elution curves) and quantitative separation of mixtures determinations. In addition, in an attempt to explain the sorption behaviour of elements, a computer speciation program was used.

3.1.1 Equilibrium Distribution Coefficient Determination

Equilibrium distribution coefficients were obtained by equilibrating 100 ml of oxalic acid – sulphuric acid mixtures (at specified concentration ratios) containing two concentrations (0.1 or 1 mmole) of the specific element to be determined, with 1 g of the dry resin by shaking for 24 hours at 20 ^{0}C. After equilibration, the resin was separated from the aqueous phase by filtration, the filtrate was collected in a 250 ml volumetric flask and diluted with water to volume, and the amount of the specific element in the aqueous phase was determined by the appropriate analytical techniques as described later in this Chapter. The element retained on

the resin was eluted with 2 M or 4 M HNO_3 (50 ml) in a 250 ml volumetric flask, diluted with water to volume, and the concentration of the element was determined by using appropriate analytical techniques. Equilibrium distribution coefficients (K_D) were calculated according to equation (1),

$$K_D = \frac{\text{mass of element in resin}}{\text{mass of element in solution}} \text{ X } 100 \quad \text{(ml/g)} \quad (1)$$

The experimental parameters are illustrated for both 0.05 M and 0.25 M oxalic acid with varying sulphuric acid concentration, in Tables 3.1 and 3.2 respectively.

3.1.2 Elemental Separations (Elution Curves) Determination

In this study, an elution curve is generally obtained by equilibrating a 10 ml (ca. 3.1 g dry resin) or a 13 ml (ca. 4 g dry resin) resin column (the preparation of a resin column is described later in the Chapter) with 50 ml of the appropriate solution. The loading solution containing the dissolved elements in the appropriate media passes through the resin column. The appropriate eluent is used to remove any impurities remaining on the column whilst the retained elements are eluted with a low molarity acid (~1 M – 4 M). Fractions are collected from the sorption step. The excess acid is evaporated on a water bath, the residue diluted with water to an appropriate volume, and the amounts of each element in all fractions are determined by using the appropriate analytical techniques.

Table 3.1 Distribution coefficient experimental parameters for 0.05 M oxalic acid at varying H_2SO_4 concentration (0.005 M – 2.00 M)

	[H_2SO_4]							
	0.005M	0.05M	0.10 M	0.25 M	0.50 M	1.00 M	1.50 M	2.00 M
[Metal] = 0.1 M or 0.01 M	10.0 ml	10.0 ml	10.0 ml	10.0 ml	10.0 ml	10.0 ml	10.0 ml	10.0 ml
Oxalic acid (0.5 M)	10.0 ml	10.0 ml	10.0 ml	10.0 ml	10.0 ml	10.0 ml	10.0 ml	10.0 ml
H_2SO_4	0.5 ml	5.0 ml	10.0 ml	2.5 ml	5.0 ml	10.0 ml	15.0 ml	20.0 ml
(10 M or 1 M)	(1 M)	(1 M)	(1 M)	(10 M)	(10 M)	(10 M)	(10 M)	(10 M)
Deionised water	79.5 ml	75.0 ml	70.0 ml	77.5 ml	75.0 ml	70.0 ml	65.0 ml	60.0 ml
Resin (dry)	1.000 g	1.000 g	1.000 g	1.000 g	1.000 g	1.000 g	1.000 g	1.000 g

Table 3.2 Distribution coefficient experimental parameters for 0.25 M oxalic acid at varying H_2SO_4 concentration (0.005 M – 2.00 M)

	[H_2SO_4]							
	0.005 M	0.05 M	0.10 M	0.25 M	0.50 M	1.00 M	1.50 M	2.00 M
[Metal] = 0.10 M or 0.01 M	10.0 ml	10.0 ml	10.0 ml	10.0 ml	10.0 ml	10.0 ml	10.0 ml	10.0 ml
Oxalic acid (0.5 M)	50.0 ml	50.0 ml	50.0 ml	50.0 ml	50.0 ml	50.0 ml	50.0 ml	50.0 ml
H_2SO_4	0.5 ml	5.0 ml	10.0 ml	2.5 ml	5.0 ml	10.0 ml	15.0 ml	20.0 ml
(10 M or 1 M)	(1 M)	(1 M)	(1 M)	(10 M)	(10 M)	(10 M)	(10 M)	(10 M)
Deionised water	39.5 ml	35.0 ml	30.0 ml	37.5 ml	35.0 ml	30.0 ml	25.0 ml	20.0 ml
Resin (dry)	1.000 g	1.000 g	1.000 g	1.000 g	1.000 g	1.000 g	1.000 g	1.000 g

3.1.3 Quantitative Separation of Mixtures

A series of 13 ml resin columns was prepared (described later in the Chapter). Appropriate volumes of a standard solution, for example Ge(IV) [10 µg] ion, and one other ion, for example Al(III) [ca. 0.01 g], which were made up in minimal amounts of acidic solution separately, were accurately measured out in triplicate, mixed and adjusted to an appropriate matrix to be studied (for example, an oxalic acid – sulphuric acid system). Three equivalent aliquots of each solution were measured out and kept separately as standards for comparison with the solutions obtained after separations, using similar dilutions or volumes for the final determinations of the elements in the standards and separated solutions. The mixed solution was passed through the equilibrated resin columns and washed onto the resin with a small portion of the appropriate acid mixture (100 ml in total). When separating larger portions, 200 ml of the appropriate acid mixture were used. The different fractions were collected from the beginning of the sorption step, and after the excess acid had been removed by evaporation, they were made up to convenient volumes and were then measured by using the appropriate analytical methods.

3.2 ION EXCHANGERS

The ion exchange resins used in this study were the strongly basic quaternary ammonium anion exchanger, AG1–X8 (chloride form, 100–200 mesh particle size), and the strongly acidic sulphonated polystyrene cation exchanger, AG50W-X8 (hydrogen form, 100-200 mesh particle size), supplied by the Bio–Rad® Laboratories, Richmond, California.

3.2.1 Resin Preparation

The required resin was slowly added to three volumes of deionised water and mixed gently with overhead stirring while adding the resin. The resin was allowed to swell and to settle and the supernatant was decanted and a fresh volume of deionised water was added. This process was repeated until all the fines in the gel had been removed. The resins were then dried in the oven at 75 ^{0}C for 1 hour and thereafter dried overnight at 60 ^{0}C in a Gallenkamp vacuum pistol with an anhydrous silica gel as a drying agent, and stored in a desiccator over the same drying agent.

3.2.2 Column Preparation

Polyethylene tubes [25 mm inner diameter and 140 mm length (13 ml column) and 25 mm inner diameter and 110 mm length (10 ml column)], fitted with 70 μm polyethylene frits at the bottom, were used as ion exchange columns in the determination of the elution curves and in the quantitative separation of synthetic mixtures. For elution curves and quantitative separations, the columns were filled with a slurry of the resin until the settled resin reached the indicated mark. A 70 μm polyethylene frit was placed on top of the resin in the column. A plunger made of a Teflon® rod [25 mm diameter, 45 mm length, with a hole (1 mm bore) drilled through the length, fitted with an O–ring near the bottom and a Luer fitting at the top] was used to seal the column at the top end. The plunger was pushed firmly onto the frit until the resin column was compacted to the required volume. A typical ion exchange resin column is presented in Figure 3.1.

Figure 3.1 A typical ion exchange resin column.

Scale: 5 mm :1 mm

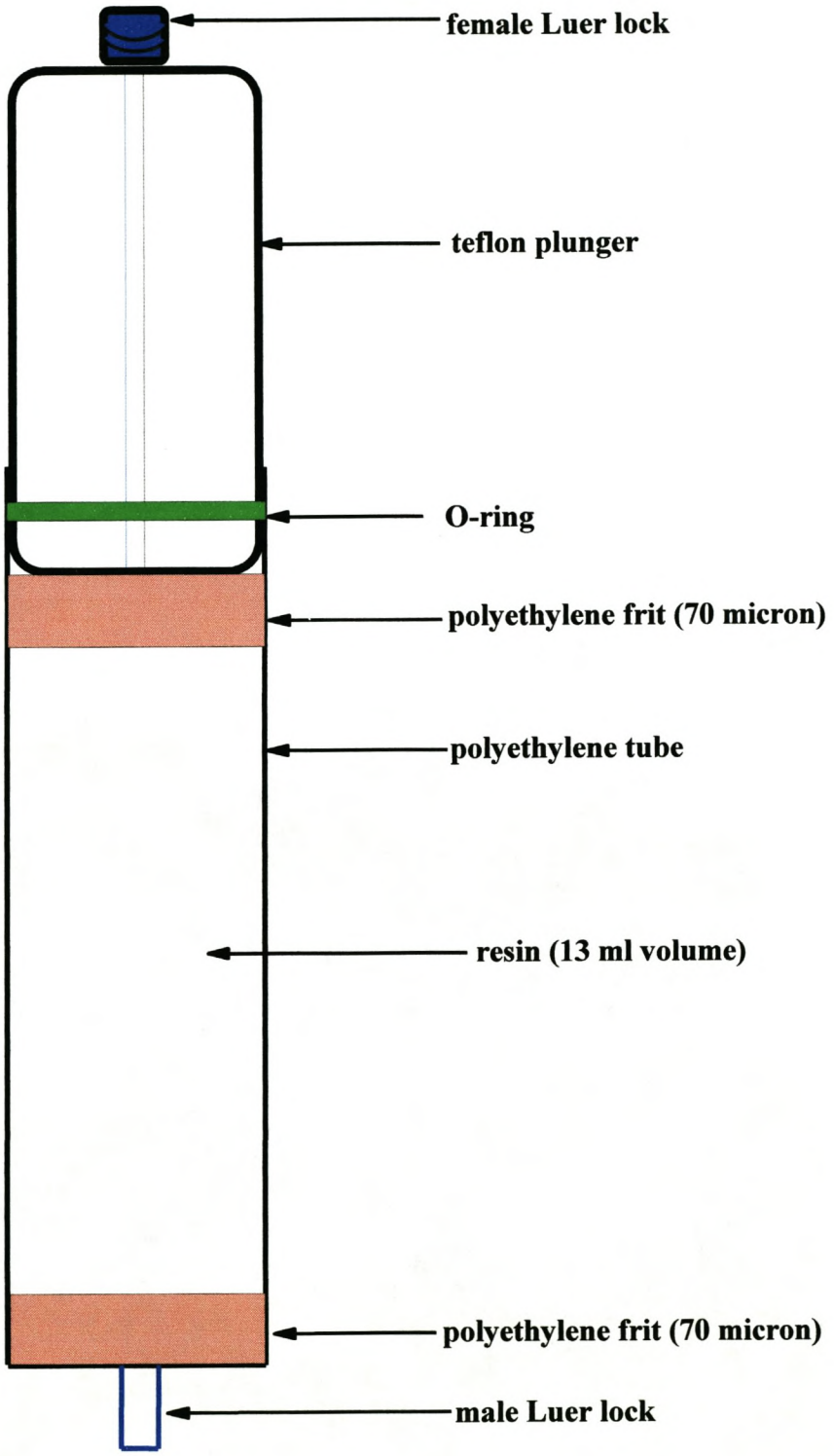

3.3 REAGENTS AND APPARATUS

3.3.1 Reagents

The reagents were of analytical grade and were supplied by Merck (SA). Deionised water was used and was obtained from a Millipore Milli-Z water system (>10 megaohm.cm^{-1}). Gallium metal (99.99%) and gallium oxide (99.99%) were obtained from Koch Chemicals Ltd., Heartford Hearts, England. The oxides of Al(III), As(V), Ce(IV), Fe(III), In(III), La(III), Mo(VI), Nb(V), Sc(III), Se(IV), Sn(IV), Ta(V), Tb(III), Te(IV), Ti(IV), V(V), W(VI), Y(III), Yb(III) and Zr(IV) were supplied by Merck (SA). The oxide of Pr(III) and the chloride of Sb(V) were supplied by Aldrich (SA). The pure metals (99.9%) of Cd(II), Co(II), Cr(II), Cu(II), Mn(II), Ni(II) and Zn(II) were also supplied by Merck (SA). Standard solutions containing 1 millimole of the element in 10 ml of 0.1 M H_2SO_4 were prepared. Solutions of Ce(IV), Mo(VI), Ta(V), Ti(IV), V(V), W(VI) and Zr(IV) also contained 0.1% of hydrogen peroxide. Less concentrated solutions (0.1 millimole per 10 ml) were prepared by dilution when required.

The prepared 0.5 M oxalic acid solution went through the following purification process before use: firstly, a 60 ml AG50W-X8 ion exchange resin column was purified by passing through 300 ml of 3 M hydrochloric acid solution followed by 200 ml of deionised water. One litre of 0.5 M oxalic acid was then passed through the resin column. The first 60 ml of the eluate was discarded and the rest of the eluate was collected in a polypropylene container.

Suprapur nitric acid (0.5 M) was used in all standards and samples make-up in the analytical investigations.

3.3.2 Radiotracers

The radiotracers ^{67}Ga ($t_{½}$=72.4 h) and ^{69}Ge ($t_{½}$=39 h) used in this study were readily available on site (iThemba LABS). The ^{67}Ge and ^{67}Ga radiotracers were prepared in a 0.01 M sulphuric acid matrix.

3.3.3 Apparatus

For this study, the following apparatus was used: A-grade glassware (inclusive of volumetric flasks, pipettes, beakers, etc.) and a Pyrex® borosilicate glass desiccator. Polypropylene bottles (250 ml) with leakproof caps for equilibration studies. Polyethylene tubes (15 ml) fitted with 70 μm polyethylene frits at the bottom, were used for filtration purposes in the equilibration studies and also adapted as ion exchange columns. A mechanical shaker (GFL 3015) with an electronic speed control (range 6-66 rpm) with a timer able to function on a continuous 24 hour cycle. Eppendorf micropipettes (0.1 ml – 1 ml and 2 ml – 10 ml range). Mettler analytical electronic weighing balance (AE240) for micro (0 - 50 g) measurements and a Mettler electronic weighing balance (PM600) for macro (>50 g) measurements.

3.4 ANALYTICAL INSTRUMENTATION

Extensive literature on trace analysis is documented [1], so there is no need to expand on the theoretical background of analytical principles. The procedures outlined in this section focus chiefly on the optimisation of instrument parameters that would produce reduced interferences and good sensitivity for the specific elements to be analysed. The determination of the elements at microgram levels in the eluates or the fractions when determining the equilibrium distribution coefficients, elution curves, quantitative separation of mixtures and the final product ^{68}Ge analysis, which will be described in Chapters 4, 5, and 6, were done with the following analytical instruments: a Perkin Elmer 400 induced coupled plasma emission spectrometer and a Varian Spectra AA-600 spectrophotometer with a Varian GTA100 graphite tube atomiser. The methods were developed according to the guidelines of the instruments' manuals [2, 3] and adapted according to the matrix of the element or radioisotope to be investigated.

3.4.1 Electrothermal Atomisation Spectrometry

Graphite furnace atomic absorption methods for sub-micro level analysis were developed for Ga, Al and Fe, the only possible inactive contaminants that could be found in the ^{68}Ge final product. A summary of the recommended instrument parameters for the Varian GTA 100 for Ga, Al and Fe is given in Table 3.3, Table 3.4 and Table 3.5 respectively. All the standards and the solutions to be analysed were in a 0.1% HNO_3 matrix, and the pyrolytically coated partitioned graphite tube was used in all analyses. For the preparation of the stock solutions (1000 µg/ml), the required amounts of oxides or pure metal were dissolved in minimal amounts

Table 3.3 Varian GTA100 operating parameters for Ga analysis.

Element	**Ga**
Instrument Mode	Absorbance
Instrument Type	Furnace
Calibration Mode	Concentration
Calibration Algorithm	New Rational
Measurement Mode	Peak Height
Sampling Mode	Automix
Lamp Position	1
Lamp Current (mA)	4
Slit Width (nm)	0.5
Slit Height	Normal
Wavelength (nm)	294.4
EHT	305
Minimum reading	0.000
Replicates All	3
Background Correction	On
Reslope Rate	0
Reslope Standard	1
Standard 1 concentration (µl)	10.000
Standard 2 concentration (µl)	15.000
Standard 3 concentration (µl)	25.000
Smoothing	5 Point
Expansion Factor	1.0
QC Protocol	Off

Sample parameters	Volume (µl)
Bulk Standard Concentration	25
Sample Volume	10
Total Volume	25
Standard 1 volume	5
Standard 2 volume	10
Standard 3 volume	15
Modifier	2

Furnace Parameters

Step No.	*Temperature (^{0}C)*	*Time (s)*	*Flow (l/min)*	*Gas Type*	*Read*
1	85	5	3	Nitrogen	No
2	95	50	3	Nitrogen	No
3	110	20	3	Nitrogen	No
4	125	5	3	Nitrogen	No
5	800	10	3	Nitrogen	No
6	800	5	3	Nitrogen	No
7	800	1	3	Nitrogen	No
8	2300	2	0	Argon	Yes
9	2300	2	0	Argon	Yes
10	2300	2	3	Nitrogen	No
11	40	10	3	Nitrogen	No

Table 3.4 Varian GTA100 operating parameters for Al analysis.

Element	**Al**
Instrument Mode	Absorbance
Instrument Type	Furnace
Calibration Mode	Concentration
Calibration Algorithm	New Rational
Measurement Mode	Peak Height
Sampling Mode	Automix
Lamp Position	2
Lamp Current (mA)	10
Slit Width (nm)	0.5
Slit Height	Normal
Wavelength (nm)	309.3
EHT	275
Minimum reading	0.000
Replicates All	3
Background Correction	On
Reslope Rate	0
Reslope Standard	1
Standard 1 concentration (µl)	10.000
Standard 2 concentration (µl)	15.000
Standard 3 concentration (µl)	25.000
Smoothing	5 Point
Expansion Factor	1.0
QC Protocol	Off

Sample parameters	Volume (µl)
Bulk Standard Concentration	25
Sample Volume	10
Total Volume	25
Standard 1 volume	5
Standard 2 volume	10
Standard 3 volume	15
Modifier	0

Furnace Parameters

Step No.	*Temperature (^{0}C)*	*Time (s)*	*Flow (l/min)*	*Gas Type*	*Read*
1	85	5	3	Nitrogen	No
2	95	50	3	Nitrogen	No
3	110	20	3	Nitrogen	No
4	125	5	3	Nitrogen	No
5	800	10	3	Nitrogen	No
6	800	5	3	Nitrogen	No
7	800	1	3	Nitrogen	No
8	2300	2	0	Argon	Yes
9	2300	2	0	Argon	Yes
10	2300	2	3	Nitrogen	No
11	40	10	3	Nitrogen	No

Table 3.5 Varian GTA100 operating parameters for Fe analysis.

Element	**Fe**
Instrument Mode	Absorbance
Instrument Type	Furnace
Calibration Mode	Concentration
Calibration Algorithm	New Rational
Measurement Mode	Peak Height
Sampling Mode	Automix
Lamp Position	3
Lamp Current (mA)	5
Slit Width (nm)	0.2
Slit Height	Normal
Wavelength (nm)	248.3
EHT	275
Minimum reading	0.000
Replicates All	3
Background Correction	On
Reslope Rate	0
Reslope Standard	1
Standard 1 concentration (µl)	10.000
Standard 2 concentration (µl)	15.000
Standard 3 concentration (µl)	25.000
Smoothing	5 Point
Expansion Factor	1.0
QC Protocol	Off

Sample parameters	Volume (µl)
Bulk Standard Concentration	25
Sample Volume	10
Total Volume	25
Standard 1 volume	5
Standard 2 volume	10
Standard 3 volume	15
Modifier	2

Furnace Parameters

Step No.	*Temperature (^{0}C)*	*Time (s)*	*Flow (l/min)*	*Gas Type*	*Read*
1	85	5	3	Nitrogen	No
2	95	50	3	Nitrogen	No
3	110	20	3	Nitrogen	No
4	125	5	3	Nitrogen	No
5	800	10	3	Nitrogen	No
6	800	5	3	Nitrogen	No
7	800	1	3	Nitrogen	No
8	2300	2	0	Argon	Yes
9	2300	2	0	Argon	Yes
10	2300	2	3	Nitrogen	No
11	40	10	3	Nitrogen	No

of acid (10 M HNO_3) and taken up in deionised water in a volumetric flask (100 ml). The required dilutions were made thereafter. The samples were prepared in a similar way. For Ga and Fe, a palladium solution (500 μg/ml - 2000 μg/ml) plus a reducing agent such as ascorbic acid was often used to permit the use of a higher ashing temperature. This palladium modifier also resulted in the enhancement of the analyte signal, and thereby improved the sensitivity. Nitrogen gas was used in the ashing step and argon gas in the atomisation step [2].

3.4.2 Induced Coupled Plasma Spectrometry

The induced coupled plasma emission methods were developed whenever a large amount of a specific element required analysis, because of the better sensitivity it had over a large working range (1 μg/ml - 9000 μg/ml). This minimised sample dilutions, thereby minimising sample handling errors compared to electrothermal methods. More importantly, with the induced coupled plasma emission method, one was able to do multi-elemental analysis and the need for expensive hollow cathode lamps was avoided. For the preparation of the stock solutions (1000 μg/ml), the required amounts of oxides or pure metal were dissolved in minimal amounts of acid (10 M HNO_3) and made up with deionised water in a volumetric flask (100 ml). The relevant dilutions were made thereafter. The samples were prepared in a similar way. A summary of the recommended instrument parameters for the methods developed for Al, As, Ce, Cd, Co, Cr, Cu, Fe, Ga, Ge, In, La, Mn, Mo, Nb, Ni, Pr, Sb, Sc, Se, Sn, Ta, Tb, Te, Ti, V, W, Y, Yb, Zn and Zr is given in Table 3.6 [3].

Table 3.6 Perkin Elmer 400 instrument parameters for induced coupled plasma emission methods.

Element	Wavelength	Primary Line (μg/ml)
Al	167.081	0.0015 – 750
As	188.985	0.12 – 6000
Cd	228.802	0.015 – 750
Ce	418.660	0.075 – 3750
Co	228.616	0.050 – 2500
Cr	267.716	0.040 – 2000
Cu	324.754	0.02 – 1000
Fe	259.940	0.0015 – 750
Ga	417.206	0.065 – 3250
Ge	265.118	0.13 – 6500
In	325.609	0.18 – 9000
La	379.478	0.002 – 10
Mn	257.610	0.003 – 150
Mo	202.030	0.040 – 2000
Nb	309.418	0.040 – 2000
Ni	231.604	0.060 – 3000
Pr	390.831	0.3 – 750
Sb	217.581	0.18 – 9000
Sc	361.384	0.004 – 200
Se	196.026	0.37 – 18500
Sn	242.949	2.15 – 7500
Ta	268.517	0.090 – 4500
Tb	350.917	0.050 – 2500
Te	214.281	0.27 – 13500
Ti	334.941	0.006 – 300
V	309.311	0.020 – 1000
W	239.709	0.17 – 8500
Y	371.030	0.002 – 100
Yb	328.937	0.003 – 150
Zn	213.856	0.009 – 450
Zr	343.823	0.01 – 2500

3.4.3 Gamma Ray Spectrometry

The radionuclidic purity of samples was determined by high resolution γ-ray spectrometry using a high purity germanium detector and a multichannel analyzer (Silena Cicero-8K channel). The gamma energy for the identification of radioisotopes and the measurement of their activity, was obtained from a gamma ray catalogue.

3.4.4 Computer Speciation Program

To be able to explain the sorption behaviour of elements in the varying oxalic acid - sulphuric acid combinations, a speciation study was required. In this study, the MINEQL+ software program was used [4-7].

For example, to develop a speciation system involving 0.01 M Al(III) in 0.05 M oxalic acid across the chosen sulphuric acid range (0.005 M – 2.00 M), the components with their respective molarities as indicated in Table 3.7, were selected and highlighted on the chemical equilibrium database of the program. The program's 'run prompt' then executed all relevant reactions for the required system, and output all relevant complexes in total percentage of metal. Similarly, other systems could be developed.

Table 3.7 MINEQL+ speciation program input data for the speciation system of Al(III) in 0.05 M oxalic acid across chosen sulphuric acid range (0.005 M – 2.00 M).

Components	Molarity (M)							
Al(III)	0.01	0.01	0.01	0.01	0.01	0.01	0.01	0.01
H_2O	0.005	0.05	0.1	0.25	0.5	1.0	1.5	2.0
H^+	0.005	0.05	0.1	0.25	0.5	1.0	1.5	2.0
SO_4^{2-}	0.005	0.05	0.1	0.25	0.5	1.0	1.5	2.0
$(Oxalate)^-$	0.05	0.05	0.05	0.05	0.05	0.05	0.05	0.05

In this study, the speciation systems of 4 elements [Al(III), Cd(II), Zn(II) and Co(II)] in varying oxalic acid – sulphuric acid combinations were determined.

3.5 REFERENCES

1. Skoog D.A. and West D.M., *Fundamentals of analytical chemistry*, 4th edition, Saunders, Philadelphia, 1982, pp. 55.
2. Varian GTA100, *Instruction and procedure manual*, Australia, 1988, pp. 10.
3. Perkin Elmer ICP 4000, Instruction and procedure manual, USA, 1990, pp. 15.
4. Morel F.M.M., *Principles and applications of aquatic chemistry*, Wiley-Interscience, New York, 1983, pp. 25.
5. Westall J.C., Zachary J.L. and Morel F.M.M., *MINEQL, A computer program for the calculation of chemical equilbrium composition of aqueous system,* Massachusetts Institute of Technology, (MIT), Tech. No. 18, 1976.
6. Plummer L.N., Prestemon E.C. and Parkhurst D.L., *U.S Geological Survey Water-Resources Investigations Report*, 94, 130, 1994.
7. Tao S., Wen Y., Long A., Dawson R., Cao J. and Xu F., *Comp. and Chem.,* 25, 215, 2001.

CHAPTER 4

SORPTION BEHAVIOUR OF SELECTED ELEMENTS ON A CATION EXCHANGER

4.1 INTRODUCTION

As mentioned before, literature on the sorption behaviour of elements on a cation exchanger in oxalic acid or oxalic acid – mineral acid is limited to the work of Nozaki et al. [1] and Strelow et al. [2]. Nozaki et al. [1] presented a systematic study of the cation exchange distribution coefficients of 8 metal ions [Ti(IV), Zr(IV), Fe(III), Al(III), Ga(III), In(III), Cu(II) and Zn(II)] on an Amberlite® IR-120 resin in varying oxalic acid - hydrochloric acid mixtures. Strelow et al. [2] presented only the distribution coefficients for Mg and Al with the cation exchangers Bio-Rad® AG50W-X4 and AG50W-X8, in oxalic acid and oxalic acid – nitric acid mixtures. The oxalic acid concentrations varied from 0.1 M to 0.5 M and the nitric acid concentrations varied from 0.1 M to 0.2 M. However, many cation exchange separations involving oxalic acid and oxalic acid – mineral acid have been cited in the literature [3-13].

This Chapter focuses on the sorption behaviour of 32 metal ions [Al(III), As(V), Cd(II), Ce(III), Ce(IV), Co(II), Cr(III), Cu(II), Fe(III), Ga(III), Ge(IV), In(III), La(III), Mn(II), Mo(VI), Nb(V), Ni(II), Pr(III), Sb(V), Sc(III), Se(IV), Sn(IV), Ta(V), Tb(III), Te(IV), Ti(IV), V(V), W(VI), Y(III), Yb(III), Zn(II) and Zr(IV)] on a cation exchanger in an oxalic acid - mineral acid mixture. The equilibrium distribution coefficients of these selected metal ions were investigated on a cation exchange resin (Bio-Rad® AG50W-X8) in 0.05 M and 0.25 M oxalic acid at various concentrations of sulphuric acid (0.005 M, 0.05 M, 0.10 M, 0.25 M, 0.50

M, 1.00 M, 1.50 M and 2.00 M). Using the findings of the above, two component and three component elemental separations on the cation exchange resin were also investigated.

4.2 RESULTS OF CATIONIC EQUILIBRIUM DISTRIBUTION COEFFICIENT

As is evident in Table 4.1 and Table 4.2, the metal ions Al(III), Cd(II), Ce(III), Ce(IV), Co(II), Cu(II), In(III), La(III), Mn(II), Ni(II), Sc(III), Y(III), Yb(III) and Zn(II) all showed some degree of sorption, whereas the metal ions As(V), Cr(III), Fe(III), Ga(III), Ge(IV), Mo(VI), Nb(V), Pr(III), Sb(V), Se(IV), Sn(IV), Ta(V), Tb(III), Te(IV), Ti(IV), V(V), W(VI) and Zr(IV) showed absolutely no sorption on the cation exchanger at any of the chosen oxalic acid - sulphuric acid combinations. Of the sorbed metal ions, Al(III), Cd(II), Cu(II) and In(III) showed relatively weak sorption compared to the other sorbed metal ions. In addition, all the sorbed metal ions were sorbed less as the concentration of sulphuric acid increased across the chosen range. Generally, the sorbed metal ions sorbed better in 0.05 M oxalic acid compared to 0.25 M oxalic acid.

To determine whether the sorption behaviour of these metal ions correlates at all with the ionic or molecular species present under the chosen conditions, the speciation modelling program, MINEQL+, was used to develop speciation modelling systems for the metal ions Al(III), Cd(II), Co(II) and Zn(II) (Appendix, Figures 8.1 to 8.5) under the specified conditions as described in Chapter 3. These metals were chosen because of the reliability of the available thermodynamic data under the specified conditions, in the program's database. The group 3 metal ion, Al(III), showed relatively low sorption in both oxalate concentrations across the

Table 4.1 Cation exchange distribution coefficients in 0.05 M oxalic acid, at various concentrations of H_2SO_4

	Molarity H_2SO_4							
Metal ion	0.005	0.05	0.10	0.25	0.50	1.00	1.50	2.00
Al(III)	125	114	105	83	55	10.1	5.5	<0.5
As(V)[b]	<0.5	<0.5	<0.5	<0.5	<0.5	<0.5	<0.5	<0.5
Cd(II)[b]	105	89	79	49.1	23.5	10.1	3.5	<0.5
Ce(III)[b]	5600	1900	980	450	250	110	55	10.5
Ce(IV)[a, b]	4100	1300	650	300	155	85	45.5	8.5
Ce(IV)[b]	4800	1660	850	400	205	100	50.1	9.5
Co(II)	1350	532	283	95	28.2	10.1	5.2	<0.5
Cr(III)[b]	<0.5	<0.5	<0.5	<0.5	<0.5	<0.5	<0.5	<0.5
Cu(II)[b]	61	51	44.1	34.1	24.9	11.1	5.2	<0.5
Fe(III)[a,b]	<0.5	<0.5	<0.5	<0.5	<0.5	<0.5	<0.5	<0.5
Ga(III)[b]	<0.5	<0.5	<0.5	<0.5	<0.5	<0.5	<0.5	<0.5
Ge(IV)[b]	<0.5	<0.5	<0.5	<0.5	<0.5	<0.5	<0.5	<0.5
In(III)	135	110	95	65	35.1	11.1	5.1	<0.5
La(III)[b]	$>10^4$	$>10^4$	8210	3175	415	190	110	45.7
Mn(II)[b]	1295	675	295	110	55	12.3	5.5	<0.5
Mo(VI)[a,b]	<0.5	<0.5	<0.5	<0.5	<0.5	<0.5	<0.5	<0.5
Nb(V)[b]	<0.5	<0.5	<0.5	<0.5	<0.5	<0.5	<0.5	<0.5
Ni(II)[b]	3500	1250	525	98	14.4	<0.5	<0.5	<0.5
Pr(III)[b]	prec	prec	prec	prec	prec	prec	prec	prec
Sb(V)[b]	<0.5	<0.5	<0.5	<0.5	<0.5	<0.5	<0.5	<0.5
Sc(III)[b]	2755	1850	1250	650	350	75	19.5	5.5
Se(IV)[b]	<0.5	<0.5	<0.5	<0.5	<0.5	<0.5	<0.5	<0.5
Sn(IV)[b]	<0.5	<0.5	<0.5	<0.5	<0.5	<0.5	<0.5	<0.5
Ta(V)[a,b]	<0.5	<0.5	<0.5	<0.5	<0.5	<0.5	<0.5	<0.5
Tb(III)[b]	prec	prec	prec	prec	prec	prec	prec	prec
Te(IV)[b]	<0.5	<0.5	<0.5	<0.5	<0.5	<0.5	<0.5	<0.5
Ti(IV)[a,b]	<0.5	<0.5	<0.5	<0.5	<0.5	<0.5	<0.5	<0.5
V(V)[a,b]	<0.5	<0.5	<0.5	<0.5	<0.5	<0.5	<0.5	<0.5
W(VI)[a,b]	<0.5	<0.5	<0.5	<0.5	<0.5	<0.5	<0.5	<0.5
Y(III)[b]	3475	2990	2350	1045	195	41.1	16.9	6.8
Yb(III)[b]	3325	1340	750	255	107	21.4	10.1	<0.5
Zn(II)[b]	1980	1100	650	200	46.1	10.1	3.1	<0.5
Zr(IV)[a,b]	<0.5	<0.5	<0.5	<0.5	<0.5	<0.5	<0.5	<0.5

[a] 1 ml of 30% H_2O_2 present
[b] 0.1 mmol of element
prec = precipitate

Table 4.2 Cation exchange distribution coefficients in 0.25 M oxalic acid, at various concentrations of H_2SO_4

	Molarity H_2SO_4							
Metal ion	0.005	0.05	0.10	0.25	0.50	1.00	1.50	2.00
Al(III)	21.1	19.5	18.1	14.7	10.1	4.5	<0.5	<0.5
As(V)[b]	<0.5	<0.5	<0.5	<0.5	<0.5	<0.5	<0.5	<0.5
Cd(II)	89	74	62	39.4	19.6	7.5	2.5	<0.5
Ce(III)[b]	3495	1650	750	150	95	65	15.5	5.5
Ce(IV)[a, b]	2100	1350	450	110	90	50	14.1	5.1
Ce(IV)[b]	2650	1450	650	140	90	60	15.1	6.1
Co(II)	1140	560	310	100	28.1	12.1	<0.5	<0.5
Cr(III)[b]	<0.5	<0.5	<0.5	<0.5	<0.5	<0.5	<0.5	<0.5
Cu(II)[b]	18.1	10.2	5.2	2.1	<0.5	<0.5	<0.5	<0.5
Fe(III)[a,b]	<0.5	<0.5	<0.5	<0.5	<0.5	<0.5	<0.5	<0.5
Ga(III)[b]	<0.5	<0.5	<0.5	<0.5	<0.5	<0.5	<0.5	<0.5
Ge(IV)[b]	<0.5	<0.5	<0.5	<0.5	<0.5	<0.5	<0.5	<0.5
In(III)	25.1	22.5	20.1	15.1	10.1	4.1	<0.5	<0.5
La(III)[b]	$>10^4$	$>10^4$	6410	1590	375	165	90	35.5
Mn(II)	1150	585	255	155	45	15.5	7.5	<0.5
Mo(VI)[a,b]	<0.5	<0.5	<0.5	<0.5	<0.5	<0.5	<0.5	<0.5
Nb(V)[b]	<0.5	<0.5	<0.5	<0.5	<0.5	<0.5	<0.5	<0.5
Ni(II)[b]	1035	815	605	270	100	25.5	9.5	<0.5
Pr(III)[b]	prec	prec	prec	prec	prec	prec	prec	prec
Sb(V)[b]	<0.5	<0.5	<0.5	<0.5	<0.5	<0.5	<0.5	<0.5
Sc(III)	1950	1295	890	390	155	75	15.5	4.5
Se(IV)[b]	<0.5	<0.5	<0.5	<0.5	<0.5	<0.5	<0.5	<0.5
Sn(IV)[b]	<0.5	<0.5	<0.5	<0.5	<0.5	<0.5	<0.5	<0.5
Ta(V)[a,b]	<0.5	<0.5	<0.5	<0.5	<0.5	<0.5	<0.5	<0.5
Tb(III)[b]	prec	prec	prec	prec	prec	prec	prec	prec
Te(IV)[b]	<0.5	<0.5	<0.5	<0.5	<0.5	<0.5	<0.5	<0.5
Ti(IV)[a,b]	<0.5	<0.5	<0.5	<0.5	<0.5	<0.5	<0.5	<0.5
V(V)[b]	<0.5	<0.5	<0.5	<0.5	<0.5	<0.5	<0.5	<0.5
W(VI)[a,b]	<0.5	<0.5	<0.5	<0.5	<0.5	<0.5	<0.5	<0.5
Y(III)[b]	1900	1370	860	400	165	31.6	17.5	11.7
Yb(III)[b]	1375	850	350	150	65	15.5	5.5	<0.5
Zn(II)[b]	1920	890	425	110	28.1	7.2	<0.5	<0.5
Zr(IV)[a,b]	<0.5	<0.5	<0.5	<0.5	<0.5	<0.5	<0.5	<0.5

[a] 1 ml of 30% H_2O_2 present
[b] 0.1 mmol of element
prec = precipitate

chosen sulphuric acid range compared to the divalent transition metal ions, Co(II) and Zn(II). According to the distribution diagram for aluminium in 0.05 M oxalic acid (Appendix, Figure 8.1), $[Al(oxalate)_3]^{3-}$ and $[Al(oxalate)_2]^-$ are the most important complexes in the sulphuric acid range (0.005 M to ~0.1 M), after which neutral AlO(OH) becomes the dominant compound across the chosen sulphuric acid range. The $[Al(oxalate)_3]^{3-}$ reaches a maximum in ~0.005 M sulphuric acid and accounts for ~99% of the total aluminium. The $[Al(oxalate)_2]^-$ reaches a maximum in ~0.1 M sulphuric acid and accounts for ~24% of the total aluminium at that concentration. The AlO(OH) compound increases steadily from 0.1 M sulphuric acid until it accounts for >90% of the total aluminium present. The other complex, $[Al(SO_4)_2]^-$, increases from 0.005 M sulphuric acid, reaching a maximum at ~0.5 M sulphuric acid, and is limited to <3% of the total aluminium across the chosen sulphuric acid range at any given molarity. Since the speciation system for aluminium shows no cations present under these conditions, sorption must involve the sulphonate group of the cation exchanger forming strong ionic bonds with the metal ions. It is also proposed that as the concentration of the sulphuric acid increases across the chosen range (i.e. enhanced protonation of the active group on the resin), coordination decreases, justifying the effects of a decrease in the distribution coefficient of the metal ion across the chosen sulphuric acid range. The nature of the influence of protonation on coordination is dependent on the ionic strength and hydration energies of the metal complexes (metal-oxalate and metal–sulphate) [14,15].

In the distribution diagram of zinc in 0.05 M oxalic acid (Appendix, Figure 8.2), the $[Zn(oxalate)_2]^{2-}$ is the dominant complex and decreases slightly across the chosen sulphuric acid range as the $[ZnSO_4]$ complex increases across the chosen sulphuric acid range. The $[Zn(oxalate)_2]^{2-}$ is ~96% of the total zinc in 0.005 M sulphuric acid and decreases to ~69% in

2.00 M sulphuric acid. The [Zn(oxalate)] and $[Zn(SO_4)_2]^{2-}$ complexes play a less significant role and are limited to <4% of the total zinc across the chosen sulphuric acid range at any given molarity. Similarly, in the distribution diagram of cobalt in 0.05 M oxalic acid (Appendix, Figure 8.3), the $[Co(oxalate)_2]^{2-}$ is the dominant complex and decreases slightly as the $CoSO_4$ complex increases across the chosen sulphuric acid range. The $[Co(oxalate)_2]^{2-}$ is ~94% of the total cobalt in 0.005 M sulphuric acid and decreases to ~88% in 2.00 M sulphuric acid. Since speciation shows no cations present under these conditions, sorption must involve the sulphonate group of the cation exchanger forming strong ionic bonds with the metal ions. It is not clear why Co(II) and Zn(II), which have larger ionic radii than Al(III), adsorb better in the lower sulphuric acid range (0.005 M – 0.25 M) whereas Cd(II), which is larger than Co(II) and Zn(II), adsorbs more weakly. From the speciation data, the results cannot easily be rationalised. It seems that the ordinary equilibrium in aqueous solution is completely changed in the presence of the resin. A factor that could influence sorption is the hydration energies of the complexes [14,15].

In order to explain the increased sorption for a metal, for example Cd(II), in the 0.05 M oxalic acid compared to 0.25 M oxalic acid, the distribution diagrams of cadmium in both of these concentrations were used (Appendix, Figure 8.4 and 8.5 respectively). The $[Cd(oxalate)_2]^{2-}$ is the dominant complex compared to the $[Cd(SO_4)_2]^{2-}$ complex in the lower sulphuric acid range (0.005 M to 0.50 M), and thereafter the reverse occurs across the chosen sulphuric acid range. The $[Cd(oxalate)_2]^{2-}$ complex decreases steadily as the concentration of the $[Cd(SO_4)_2]^{2-}$ complex increases across the chosen sulphuric acid range. The [Cd(oxalate)] complex is ~14% of the total cadmium in 0.005 M sulphuric acid and decreases steadily to 0% across the chosen sulphuric acid range. According to the distribution diagram of cadmium in 0.25 M oxalic acid,

the $[Cd(oxalate)_2]^{2-}$ is the dominant complex across the chosen sulphuric acid range. The $[Cd(oxalate)_2]^{2-}$ complex is ~97% of the total cadmium in 0.005 M sulphuric acid and decreases to ~59% in 2.00 M sulphuric acid. Again, the concentration of the $[Cd(oxalate)_2]^{2-}$ complex decreases as the $[Cd(SO_4)_2]^{2-}$ complex increases across the chosen sulphuric acid range. As is indicated with speciation, many of the dominant complexes (metal–oxalate and metal–sulphate) are negatively charged and do not favour cation sorption. However, the difference in sorption could be attributed to a complex set of factors such as the strength of the metal ion bond with the sulphonate group of the cation exchanger, the influence of the H^+ (of the H_2SO_4) on the dissociation of the oxalic acid, and/or the equilibrium shift of the metal-oxalate complexes to free ions. Each of these factors could either suppress or enhance sorption depending on the specific conditions. For the metal ions Ni(II) and Mn(II) it is assumed that the distribution diagrams would be similar to those of Co(II) and Zn(II), because of their similar distribution coefficients across the chosen sulphuric acid range. It is expected that $[Ni(oxalate)_2]^{2-}$ and $[Mn(oxalate)_2]^{2-}$ are the dominant complexes.

It can therefore be concluded that the speciation modelling systems used in the above study were not conclusive in explaining the sorption behaviour of the above metal ions on the studied cation exchanger, because of the non-correlation between the dominant species in solution and the dominant species on the resin column.

The trivalent transition metal ions Sc(III), Cr(III), Fe(III), Y(III) and La(III) showed variable sorption on the cation exchanger. Cr(III) and Fe(III) showed absolutely no sorption compared to the other trivalent transition metal ions, which showed pronounced sorption of a similar order to that of divalent transition metal ions [Co(II), Mn(II), Ni(II) and Zn(II)]. For Cr(III), it

is expected that $[Cr(oxalate)_3]^{3-}$ and $[Cr_2(SO_4)_3.nH_2O]$ are the dominant complexes [16], and similarly, for Fe(III), $[Fe(oxalate)_3]^{3-}$ and $[Fe_2(SO_4)_3.nH_2O]$ are the dominant complexes [17]. For Sc(III), $Sc_2(SO_4)_3$ and the soluble $[Sc(oxalate)_2]^-$ are the dominant complexes [18]. As indicated above, many of the dominant complexes (metal–oxalate and metal–sulphate) are negatively charged and do not favour cation sorption. However, the variable sorption could again be attributed to a complex set of factors such as the strength of the metal ion bond with the sulphonate group of the cation exchanger, the influence of the H^+ (of the H_2SO_4) on the dissociation of the oxalic acid, and/or the equilibrium shift of the metal-oxalate complexes to free ions. Each of these factors could either suppress or enhance sorption depending on the specific conditions.

The tetravalent transition metal ions Zr(IV) and Ti(IV), the pentavalent transition metal ions Nb(V), Ta(V) and V(V), and the hexavalent transition metal ions W(VI) and Mo(VI), showed no sorption at any of the chosen oxalic acid - sulphuric acid combinations. For the metal ion Ti(IV), when TiO_2 dissolves in sulphuric acid, the $[Ti_2O(SO_4)_3.3H_2O]$, $[Ti(SO_4)_2]$ and $[TiO(SO_4)]$ complexes are evident [19]. In the presence of peroxides, the $[Ti(O_2)(OH)(H_2O)_x]^+$ complex is evident [20]. For the metal ion V(V), when V_2O_5 dissolves in sulphuric acid, $[VO_2(SO_4)_2]^{3-}$ complex is evident and in the presence of peroxide, $[VO_2(O_2)_2]^{3-}$ is also evident [21]. For the metal ion Mo(VI), when MoO_3 dissolves in sulphuric acid, $[Mo_2O(SO_4)_2.nH_2O]$ or $[MoO_2(SO_4)]$ complexes are evident [22], and when WO_3 dissolves in sulphuric acid, the $[WO_3.SO_3]$ complex is evident. The above complexes could be strongly associated with anions (ion pairs or even molecules), thus limiting their sorption in cation exchange.

Group 4 metal ions [Sn(IV) and Ge(IV)], group 5 metal ions [As(V) and Sb(V)] and group 6 metal ions [Se(IV) and Te(IV)] also showed no sorption at any of the chosen oxalic acid - sulphuric acid combinations. For the metal ion Sn(IV), when SnO_2 dissolves in sulphuric acid, the $Sn(SO_4)_2$ complex is evident [24]. The dissolution of $SbCl_5$ in sulphuric acid results in $[Sb_2(SO_3)(SO_4)_3]$ and $[Sb_2O_3.4SO_3]$ complexes [25]. The dissolution of TeO_2 in sulphuric acid results in $[2TeO_2.SO_3]$ and $[Te_2O_3(SO_4)]$ complexes [26]. Again, the above complexes could be strongly associated with anions (ion pairs or even molecules), thus limiting their sorption in cation exchange.

Lanthanide metal ions [Ce(III), Pr(III), Tb(III) and Yb(III)] studied, showed relatively strong sorption with the exception of Pr(III) and Tb(III), which formed precipitates. Lanthanide oxalates are sparingly soluble in an aqueous solution of oxalic acid [27]. The addition of oxalic acid would reduce the solubilities of these oxalates in the mineral acids. However, the solubility of these oxalates would increase with increasing concentration of the mineral acid. With a more concentrated acid, for example sulphuric acid, the solid phase changes and mixed oxalates (oxalato-sulphates) may be formed, or the oxalate may be converted to sulphate. In addition, the more basic the lanthanide, the greater the solubility of the corresponding oxalate in the acid [27]. When CeO_2 dissolves in sulphuric acid, the $[Ce(SO_4)_3]^{2-}$ complex is evident, and in the presence of peroxide, $[Ce(OH)_4]$ and $[Ce(OH)_2(COO)_2]$ complexes are evident [28,29]. Hydrogen peroxide was used in this study for the selected metal ions [Ce(IV), Mo(VI), Fe(III), Ta(V), Ti(IV), V(V), W(VI) and Zr(VI)] to ensure that during investigations the desired oxidation state is maintained. In addition, the peroxide could contribute to the stabilisation of complexes of these metal ions in solution, for example the formation of ternary complexes containing the hydrogen peroxide, as in the case of Ta(V) [2, 29]. For the metal ion

Pr(III), the $Pr_2(oxalate)_3$ complex precipitates due to its low solubility [27]. A similar behaviour for Tb(III) is assumed because of its similar chemistry to Pr(III).

Table 4.1 and Table 4.2 also show that a variety of elemental separations is possible. In both oxalate concentrations, the group 4 metal ions [Ge(IV) and Sn(IV)], group 5 metal ions [As(V) and Sb(V)], group 6 metal ions [Se(IV) and Te(IV)], and the tetravalent [Zr(IV) and Ti(IV)], pentavalent [Nb(V), Ta(V) and V(V)] and hexavalent [Mo(VI) and W(VI)] transition metal ions with a distribution coefficient of <0.5, could easily be separated from the other studied metal ions in the lower sulphuric acid range [0.005 M - 0.25 M] with the exception of Pr(III) and Tb(III), which formed precipitates. For the metal ion La(III), and to a lesser degree Ce(III), Ce(IV), and Sc(III), this could be extended to the 1.00 M sulphuric acid.

Elemental separations of group 3 metal ions [Al(III) and In(III)] could be separated only from those metal ions with a distribution coefficient of <0.5 in 0.05 M oxalic acid in the lower sulphuric acid range (0.005 M-0.50 M).

Elemental separations are possible with the divalent transition metal ions [Mn(II), Co(II), Cu(II), Zn(II) and Cd(II)], which showed relatively stronger sorption than groups 3, 4, 5 and 6 metal ions and, in addition, with the tetravalent, pentavalent and hexavalent transition metal ions in both the oxalic acid concentrations in the lower sulphuric acid range (0.005 M – 0.25 M). The only exceptions were Cu(II) and Cd(II). Similarly, elemental separations with the trivalent transition metal ions [Sc(III), Cr(III), Fe(III), Y(III) and La(III)], which showed relatively stronger sorption than the divalent transition metal ions in both the oxalic acid concentrations in the lower sulphuric acid range (0.005 M – 0.25 M), were possible. The

exceptions were Cr(III) and Fe(III), which showed absolutely no sorption in any of the oxalic acid and sulphuric acid combinations.

Elemental separations of the lanthanides Ce(IV) and Yb(III) were possible from all other metal ions with a distribution coefficient of <0.5 in both oxalic acid concentrations in the lower sulphuric acid range (0.005 M - 0.50 M). Elemental separations of Pr(III) and Tb(III) were not possible in any of the chosen oxalic acid - sulphuric acid combinations as a result of precipitation.

The significant feature of the oxalic acid - sulphuric acid system on the cation exchanger was the relatively high sorption of Zn(II) in 0.05 M oxalic acid in combination with 0.005 M, 0.05 M, 0.10 M, 0.25 M and 0.50 M sulphuric acid, which corresponded to distribution coefficients of 1980, 1110, 650, 200 and 46 respectively. This sorption was far superior to the results of Nozaki et al. [1], who used similar experimental conditions, and the corresponding distribution coefficient of ~110 was determined in the 0.05 M oxalic acid - 0.40 M hydrochloric acid mixture. The difference in sorption behaviour could be attributed to the influence of the double negatively charged sulphate anion compared to the singly charged chloride anion. In addition, the greatest shortcoming of Nozaki's work [1] is that his distribution coefficients are represented as curves, and therefore the distribution coefficients at their respective concentrations are only approximate values.

4.3 RESULTS OF ELUTION CURVES

The distribution coefficients in Tables 4.1 and 4.2 indicated numerous possibilities for separations. Some were selected for further investigation and a few of these were selected for typical multi-element elution curves using synthetic mixtures to demonstrate the versatility of the system. A series of 10 ml and 13 ml resin columns was prepared as described in Chapter 3.

4.3.1 Elution Curve of Zr(IV)-La(III)

A two component separation was possible in the 0.05 M oxalic acid – 0.005 M sulphuric acid mixture for Zr(IV) [$K_d < 0.5$] and La(III) [$K_d > 10^4$], because of a very high separation factor of $>10^5$. A 10 ml resin column was equilibrated with 50 ml of 0.05 M oxalic acid – 0.005 M sulphuric acid containing 0.01% hydrogen peroxide. A solution containing 100 mg Zr(IV) and 10 mg La(III) in 50 ml of 0.05 M oxalic acid – 0.005 M sulphuric acid containing 0.01% hydrogen peroxide, was prepared and passed through the resin column. The elements were washed onto the resin with small portions of the solution of the same composition, and the Zr(IV) was eluted with a total volume of 350 ml of solution (including washings). La(III) was then eluted with 4.00 M nitric acid (100 ml). The flow rate was 4.0 ± 0.4 ml /min throughout, and fractions (20 ml in volume) were collected from the beginning of the sorption step. The excess acid was evaporated on a water bath, and the residue was diluted with water and analysed with the appropriate analytical techniques as discussed in Chapter 3. The experimental curve is shown in Figure 4.1 and, as illustrated, complete separation was possible between Zr(IV) and La(III) with only trace amounts of Zr(IV) [15 μg] detected in the La(III) eluate. No breakthrough of La(III) was apparent in the sorption and eluting steps. In the 0.05

M oxalic acid – 0.005 M sulphuric acid mixture, a similar elemental separation behaviour is possible between La(III) and all other elements with a K_d <0.5.

4.3.2 Elution Curve of Al(III)-La(III)

A two component separation was possible in the 0.05 M oxalic acid – 1.00 M sulphuric acid mixture for Al(III) [K_d = 10.1] and La(III) [K_d = 190], because of a separation factor of ~20. A 10 ml resin column was equilibrated with 50 ml of 0.05 M oxalic acid – 1.00 M sulphuric acid. A solution containing 100 mg Al(III) and 10 mg La(III) in 50 ml 0.05 M oxalic acid – 1.00 M sulphuric acid, was prepared and passed through the resin column. The elements were washed onto the resin with small portions of the solution of the same composition, and the Al(III) was eluted with a total volume of 350 ml of solution (including washings). La(III) was then eluted with 4.00 M nitric acid (100 ml). The flow rate was 4.0 ± 0.4 ml/min throughout, and fractions (20 ml in volume) were collected from the beginning of the sorption step. The fractions were treated and analysed as described above. The experimental curve is shown in Figure 4.2 and, as illustrated, complete separation was possible between Al(III) and La(III) with only trace amounts of Al(III) [35 μg] detected in the La(III) eluate. No breakthrough of La(III) was apparent in the sorption and eluting steps. In the 0.05 M oxalic acid – 1.00 M sulphuric acid mixture, a similar elemental separation behaviour is possible between La(III) and all other metal ions in Table 4.1 with the exception of Ce(III), Ce(IV), Pr(III), Sc(III), Tb(III), Y(III) and Yb(III).

4.3.3 Elution Curve of Ga(III)-Zn(II)

A two component separation was possible in the 0.05 M oxalic acid – 0.005 M sulphuric acid mixture for Ga(III) [K_d < 0.5] and Zn(II) [K_d = 1980], because of a high separation factor of ~4000. A 13 ml resin column was equilibrated with 50 ml of 0.05 M oxalic acid – 0.005 M sulphuric acid. A solution containing 1 g Ga(III) and 10 mg Zn(II) in 50 ml of 0.05 M oxalic acid – 0.005 M sulphuric acid, was prepared and passed through the resin column. The elements were washed onto the resin with small portions of the solution of the same composition, and the Ga(III) was eluted with a total volume of 450 ml of solution (including washings). Zn(II) was then eluted with 1.00 M nitric acid (100 ml). The flow rate was 4.0 ± 0.4 ml/min throughout, and fractions (20 ml in volume) were collected from the beginning of the sorption step. The fractions were treated and analysed as described above. The experimental curve is shown in Figure 4.3 and, as illustrated, complete separation was possible between Ga(III) and Zn(II), with only trace amounts of Ga(III) [60 μg] detected in the Zn(II) eluate. No breakthrough of Zn(II) was apparent in the sorption and eluting steps. In the 0.05 M oxalic acid – 0.005 M sulphuric acid mixture, a similar elemental separation behaviour is possible between Zn(II) and all other elements with a K_d <0.5 and, to a certain extent Cu(II). This was confirmed in the next elution curve of As(V)-Zn(II) in 4.3.4.

4.3.4 Elution Curve of As(V)-Zn(II)

A two component separation was possible in the 0.05 M oxalic acid – 0.005 M sulphuric acid mixture for As(V) [K_d < 0.5] and Zn(II) [K_d = 1980], because of a high separation factor of ~4000. A 10 ml resin column was equilibrated with 50 ml of 0.05 M oxalic acid – 0.005 M

sulphuric acid. A solution containing 100 mg As(V) and 10 mg Zn(II) in 50 ml of 0.05 M oxalic acid – 0.005 M sulphuric acid, was prepared and passed through the resin column. The elements were washed onto the resin with small portions of the solution of the same composition, and the As(V) was eluted with a total volume of 350 ml of solution (including washings). Zn(II) was then eluted with 1.00 M nitric acid (100 ml). The flow rate was 4.0 ± 0.4 ml/min throughout, and fractions (20 ml in volume) were collected from the beginning of the sorption step. The fractions were treated and analysed as described above. The experimental curve is shown in Figure 4.4 and, as illustrated, complete separation was possible between As(V) and Zn(II) with only trace amounts of As(V) [5 μg] detected in the Zn(II) eluate. No breakthrough of Zn(II) was apparent in the sorption and eluting steps.

4.3.5 Elution Curve of Cu(II)-Ce(IV)

A two component separation was possible in the 0.05 M oxalic acid – 0.005 M sulphuric acid mixture for Cu(II) [K_d = 61] and Ce(IV) [K_d = 4100 in the presence of peroxide], because of a separation factor of ~70. A 10 ml resin column was equilibrated with 50 ml of 0.05 M oxalic acid – 0.005 M sulphuric acid containing 0.01% hydrogen peroxide. A solution containing 100 mg Cu(II) and 10 mg Ce(IV) in 50 ml of 0.05 M oxalic acid – 0.005 M sulphuric acid containing 0.01% hydrogen peroxide, was prepared and passed through the resin column. The elements were washed onto the resin with small portions of the solution of the same composition, and the Cu(II) was eluted with a total volume of 350 ml of solution (including washings). Ce(IV) was then eluted with 2.00 M nitric acid (100 ml). The flow rate was 4.0 ± 0.4 ml/min throughout, and fractions (20 ml in volume) were collected from the beginning of the sorption step. The fractions were treated and analysed as described above. The

experimental curve is shown in Figure 4.5 and, as illustrated, complete separation was possible between Cu(II) and Ce(IV) with only trace amounts of Cu(II) [10 μg] detected in the Ce(IV) eluate. No breakthrough of Ce(IV) was apparent in the sorption and eluting steps. In the 0.05 M oxalic acid – 0.005 M sulphuric acid mixture, in the presence or absence of peroxide, a similar elemental separation behaviour is possible between Ce(IV) and all other metal ions with the exception of Ce(III), Co(II), La(III), Mn(II), Ni(II), Pr(III), Sc(III), Tb(III), Y(III), Yb(III) and Zn(II).

4.3.6 Elution Curve of Ga(III)-Ce(IV)

A two component separation was possible in the 0.05 M oxalic acid – 0.005 M sulphuric acid mixture for Ga(III) [$K_d < 0.5$] and Ce(IV) [$K_d = 4800$ in the absence of peroxide] because of a very high separation factor of $>10^4$. A 10 ml resin column was equilibrated with 50 ml of 0.05 M oxalic acid – 0.005 M sulphuric acid. A solution containing 100 mg Ga(III) and 10 mg Ce(IV) in 50 ml of 0.05 M oxalic acid – 0.005 M sulphuric acid, was prepared and passed through the resin column. The elements were washed onto the resin with small portions of the solution of the same composition, and the Ga(III) was eluted with a total volume of 350 ml of solution (including washings). Ce(IV) was then eluted with 2.00 M nitric acid (100 ml). The flow rate was 4.0 ± 0.4 ml/min throughout, and fractions (20 ml in volume) were collected from the beginning of the sorption step. The fractions were treated and analysed as described above. The experimental curve is shown in Figure 4.6 and, as illustrated, complete separation was possible between Ga(III) and Ce(IV), with only trace amounts of Ga(III) [5 μg] detected in the Ce(IV) eluate. No breakthrough of Ce(IV) was apparent in the sorption and eluting steps. In the 0.05 M oxalic acid – 0.005 M sulphuric acid mixture, in the presence or absence of

peroxide, a similar elemental separation behaviour is possible between Ce(IV) and all other elements with the exception of Ce(III), Co(II), La(III), Mn(II), Ni(II), Pr(III), Sc(III), Tb(III), Y(III), Yb(III) and Zn(II).

4.3.7 Elution Curve of Ge(IV)-Ce(III)

A two component separation was possible in the 0.05 M oxalic acid – 0.005 M sulphuric acid mixture for Ge(IV) [$K_d < 0.5$] and Ce(III) [$K_d = 5600$ in the absence of peroxide], because of very high separation factor of $>10^4$. A 13 ml resin column was equilibrated with 50 ml of 0.05 M oxalic acid – 0.005 M sulphuric acid. A solution containing 1 g Ge(IV) and 10 mg Ce(III) in 50 ml of 0.05M oxalic acid – 0.005M sulphuric acid, was prepared and passed through the resin column. The elements were washed onto the resin with small portions of the solution of the same composition, and the Ge(IV) was eluted with a total volume of 450 ml of solution (including washings). Ce(III) was then eluted with 2 M nitric acid (100 ml). The flow rate was 4.0 ± 0.4 ml/min throughout, and fractions (20 ml in volume) were collected from the beginning of the sorption step. The fractions were treated and analysed as described above. The experimental curve is shown in Figure 4.7 and, as illustrated, complete separation was possible between Ge(IV) and Ce(III), with only trace amounts of Ge(IV) [10 µg] detected in the Ce(III) eluate. No breakthrough of Ce(III) was apparent in the sorption and eluting steps. In the 0.05 M oxalic acid – 0.005 M sulphuric acid mixture, in the presence or absence of peroxide, a similar elemental separation behaviour is possible between Ce(IV) and all other metal ions with the exception of Ce(III), Co(II), La(III), Mn(II), Ni(II), Pr(III), Sc(III), Tb(III), Y(III), Yb(III) and Zn(II).

4.3.8 Elution Curve of Mo(VI)-Y(III)

A two component separation was possible in the 0.25 M oxalic acid – 0.005 M sulphuric acid mixture for Mo(VI) [$K_d < 0.5$] and Y(III) [$K_d = 1900$], because of a high separation factor of ~4000. A 10 ml resin column was equilibrated with 50 ml of 0.25 M oxalic acid – 0.005 M sulphuric acid containing 0.01% hydrogen peroxide. A solution containing 100 mg Mo(VI) and 10 mg Y(III) in 50 ml of 0.25 M oxalic acid – 0.005 M sulphuric acid containing 0.01% hydrogen peroxide, was prepared and passed through the resin column. The elements were washed onto the resin with small portions of the solution of the same composition, and the Mo(VI) was eluted with a total volume of 350 ml of solution (including washings). Y(III) was then eluted with 2.00 M nitric acid (100 ml). The flow rate was 4.0 ± 0.4 ml/min throughout, and fractions (20 ml in volume) were collected from the beginning of the sorption step. The fractions were treated and analysed as described above. The experimental curve is shown in Figure 4.8 and, as illustrated, complete separation was possible between Mo(VI) and Y(III) with only trace amounts of Mo(VI) [10 µg] detected in the Y(III) eluate. No breakthrough of Y(III) was apparent in the sorption and eluting steps. In the 0.25 M oxalic acid – 0.005 M sulphuric acid containing 0.01% hydrogen peroxide, a similar elemental separation is possible between Y(III) and all other metal ions with the exception of Ce(III), Ce(IV), Co(II), La(III), Mn(II), Ni(II), Pr(III), Sc(III), Tb(III), Yb(III) and Zn(II). This was confirmed in the next elution curve Nb(V)-Y(III) in 4.3.9.

4.3.9 Elution Curve of Nb(V)-Y(III)

A two component separation was possible in the 0.25 M oxalic acid – 0.005 M sulphuric acid mixture for Nb(V) [K_d < 0.5] and Y(III) [K_d = 1900], because of a high separation factor of ~4000. A 10 ml resin column was equilibrated with 50 ml of 0.25 M oxalic acid – 0.005 M sulphuric acid. A solution containing 100 mg Nb(V) and 100 mg Y(III) in 50 ml of 0.25 M oxalic acid – 0.005 M sulphuric acid, was prepared and passed through the resin column. The elements were washed onto the resin with small portions of the solution of the same composition, and the Nb(V) was eluted with a total volume of 350 ml of solution (including washings). Y(III) was then eluted with 2.00 M nitric acid (100 ml). The flow rate was 4.0 ± 0.4 ml/min throughout, and fractions (20 ml in volume) were collected from the beginning of the sorption step. The fractions were treated and analysed as described above. The experimental curve is shown in Figure 4.9 and, as illustrated, complete separation was possible between Nb(V) and Y(III), with only trace amounts of Nb(V) [10 μg] detected in the Y(III) eluate. No breakthrough of Y(III) was apparent in the sorption and eluting steps.

4.3.10 Elution Curve of Ga(III)-Co(II)

A two component separation was possible in the 0.25 M oxalic acid – 0.005 M sulphuric acid mixture for Ga(III) [K_d < 0.5] and Co(II) [K_d = 1140], because of a high separation factor of ~2000. A 13 ml resin column was equilibrated with 50 ml of 0.25 M oxalic acid – 0.005 M sulphuric acid. A solution containing 1 g Ga(III) and 10 mg Co(II) in 50 ml of 0.25 M oxalic acid – 0.005 M sulphuric acid, was prepared and passed through the resin column. The elements were washed onto the resin with small portions of the solution of the same

composition, and the Ga(III) was eluted with a total volume of 450 ml of solution (including washings). Co(II) was then eluted with 2.00 M nitric acid (100 ml). The flow rate was 4.0 ± 0.4 ml/min throughout, and fractions (20 ml in volume) were collected from the beginning of the sorption step. The fractions were treated and analysed as described above. The experimental curve is shown in Figure 4.10 and, as illustrated, complete separation was possible between Ga(III) and Co(II), with only trace amounts of Ga(III) [25 μg] detected in the Co(II) eluate. No breakthrough of Co(II) was apparent in the sorption and eluting steps. In the 0.25 M oxalic acid – 0.005 M sulphuric acid, a similar elemental separation is possible between Co(II) and all other metal ions with the exception of Ce(III), Ce(IV), La(III), Mn(II), Ni(II), Pr(III), Sc(III), Tb(III), Y(III), Yb(III) and Zn(II). This was confirmed in the next elution curve As(V)-Co(II) in 4.3.11.

4.3.11 Elution Curve of As(V)-Co(II)

A two component separation was possible in the 0.25 M oxalic acid – 0.005 M sulphuric acid mixture for As(V) [$K_d < 0.5$] and Co(II) [$K_d = 1140$], because of a high separation factor of ~2000. A 10 ml resin column was equilibrated with 50 ml of 0.25 M oxalic acid – 0.005 M sulphuric acid. A solution containing 100 mg As(V) and 10 mg Co(II) in 50 ml of 0.25 M oxalic acid – 0.005 M sulphuric acid, was prepared and passed through the resin column. The elements were washed onto the resin with small portions of the solution of the same composition, and the As(V) was eluted with a total volume of 350 ml of solution (including washings). Co(II) was then eluted with 2.00 M nitric acid (100 ml). The flow rate was 4.0 ± 0.4 ml/min throughout, and fractions (20 ml in volume) were collected from the beginning of the sorption step. The fractions were treated and analysed as described above. The experimental curve is shown in Figure 4.11 and, as illustrated, complete separation was

possible between As(V) and Co(II), with only trace amounts of As(V) [5 µg] detected in the Co(II) eluate. No breakthrough of Co(II) was apparent in the sorption and eluting steps.

4.3.12 Elution Curve of Fe(III)-Mn(II)

A two component separation was possible in the 0.25 M oxalic acid – 0.05 M sulphuric acid mixture for Fe(III) [$K_d < 0.5$] and Mn(II) [$K_d = 585$], because of a separation factor of ~1200. A 10 ml resin column was equilibrated with 50 ml of 0.25 M oxalic acid – 0.05 M sulphuric acid. A solution containing 500 mg Fe(III) and 10 mg Mn(II) in 50 ml of 0.25 M oxalic acid – 0.05 M sulphuric acid, was prepared and passed through the resin column. The elements were washed onto the resin with small portions of the solution of the same composition, and the Fe(III) was eluted with a total volume of 350 ml of solution (including washings). Mn(II) was then eluted with 2.00 M nitric acid (100 ml). The flow rate was 4.0 ± 0.4 ml/min throughout, and fractions (20 ml in volume) were collected from the beginning of the sorption step. The fractions were treated and analysed as described above. The experimental curve is shown in Figure 4.11 and, as illustrated, complete separation was possible between Fe(III) and Mn(II), with only trace amounts of Fe(III) [25 µg] detected in the Mn(II) eluate. No breakthrough of Mn(II) was apparent in the sorption and eluting steps. In the 0.25 M oxalic acid – 0.05 M sulphuric acid, a similar elemental separation is possible between Mn(II) and all other elements with the exception of Ce(III), Ce(IV), Co(II), La(III), Ni(II), Pr(III), Sc(III), Tb(III), Y(III), Yb(III) and Zn(II).

4.3.13 Elution Curve of Fe(III)-Ga(III)-Zn(II)

A three component separation is possible in the 0.25 M oxalic acid – 0.10 M sulphuric acid mixture for Fe(III) [K_d < 0.5], Ga(III) [K_d <0.5] and Zn(II) [K_d = 425], because of a separation factor of 900 for both Fe(III)-Zn(II) and Ga(III)-Zn(II). A 10 ml resin column was equilibrated with 50 ml of 0.25 M oxalic acid – 0.10 M sulphuric acid. A solution containing 100 mg Fe(III), 100 mg Ga(III) and 500 mg Zn(II) in 50 ml of 0.25 M oxalic acid – 0.10 M sulphuric acid, was prepared and passed through the resin column. The elements were washed onto the resin with small portions of the solution of the same composition, and the Fe(III) and Ga(III) was eluted with a total volume of 450 ml of solution (including washings). Zn(II) was then eluted with 2.00 M nitric acid (100 ml). The flow rate was 4.0 ± 0.4 ml/min throughout, and fractions (20 ml in volume) were collected from the beginning of the sorption step. The fractions were treated and analysed as described above. The experimental curve is shown in Figure 4.13 and, as illustrated, complete separation was possible between Fe(III)/Ga(III) and Zn(II), with only trace amounts of Fe(III) [25 µg] and Ga(III) [20 µg] detected in the Zn(II) eluate. No breakthrough of Zn(II) was apparent in the sorption and eluting steps. In the 0.25 M oxalic acid – 0.1 M sulphuric acid, similar three component elemental separation is possible between Zn(II) and all other metal ions with the exception of Ce(III), Ce(IV), Co(II), La(III), Mn(II), Ni(II), Pr(III), Sc(III), Tb(III), Y(III) and Yb(III).

4.3.14 Elution Curve of Zr(IV)-Ta(V)-Yb(III)

A three component separation is possible in the 0.25 M oxalic acid – 0.25 M sulphuric acid mixture for Zr(IV) [K_d < 0.5], Ta(V) [K_d < 0.5] and Yb(III) [K_d = 150], because of a separation

factor of 300 for both Zr(IV)-Yb(III) and Ta(V)-Yb(III). A 10 ml resin column was equilibrated with 50 ml of 0.25 M oxalic acid – 0.25 M sulphuric acid. A solution containing 100 mg Zr(IV), 100 mg Ta(V) and 500 mg Yb(III) in 50 ml of 0.25 M oxalic acid – 0.25 M sulphuric acid, was prepared and passed through the resin column. The elements were washed onto the resin with small portions of the solution of the same composition, and the Zr(IV) and Ta(V) was eluted with a total volume of 450 ml of solution (including washings). Yb(III) was then eluted with 2.00 M nitric acid (100 ml). The flow rate was 4.0 ± 0.4 ml/min throughout, and fractions (20 ml in volume) were collected from the beginning of the sorption step. The fractions were treated and analysed as described above. The experimental curve is shown in Figure 4.14 and, as illustrated, complete separation was possible between Zr(IV)/Ta(V) and Yb(III), with only trace amounts of Zr(IV) [20 μg] and Ta(III) [15 μg] detected in the Yb(III) eluate. No breakthrough of Yb(III) was apparent in the sorption and eluting steps. In the 0.25 M oxalic acid – 0.25 M sulphuric acid, similar three component elemental separation is possible between Yb(III) and all other elements with the exception of Cd(II), Ce(III), Ce(IV), Co(II), La(III), Mn(II), Ni(II), Pr(III), Sc(III), Tb(III), Y(III), Yb(III) and Zn(II).

A summary of the results of the various elution curves is given in Table 4.3. As indicated, all the elution curves behaved similarly: no significant tailing was evident during any of the eluting steps; there was no breakthrough of the primary element during the sorption and eluting steps; and low levels of contaminants were detected in the final product eluate. As a result, these elution curves could easily be adapted for radiochemical separations as will be evident in Chapter 6.

Table 4.3 Summary of results of various elution curves on the cation exchange resin (AG50W-X8).

Elution curve number	Elution curve	% Breakthrough of metals in sorption step	% Breakthrough of metals in eluting step	Total contaminant in the retained metal eluate
1	Zr(IV)-La(III)	Zr(97.3%)-La(0%)	Zr(2.4%)-La(0%)	15 µg Zr(IV)
2	Al(III)-La(III)	Al(97.1%)-La(0%)	Al(2.9%)-La(0%)	35 µg Al(III)
3	Ga(III)-Zn(II)	Ga(97.4%)-Zn(0%)	Ga(2.9%)-Zn(0%)	60 µg Ga(III)
4	As(V)-Zn(II)	As(98.9%)-Zn(0%)	As(1.4%)-Zn(0%)	5 µg As(V)
5	Cu(II)-Ce(IV)	Cu(97.1%)-Ce(0%)	Cu(3.1%)-Ce(0%)	10 µg Cu(II)
6	Ga(III)-Ce(IV)	Ga(96.5%)-Ce(0%)	Ga(3.5%)-Ce(0%)	5 µg Ga(III)
7	Ge(IV)-Ce(IV)	Ge(97.3%)-Ce(0%)	Ge(2.3%)-Ce(0%)	10 µg Ge(IV)
8	Mo(VI)-Y(III)	Mo(97.8%)-Y(0%)	Mo(1.8%)-Y(0%)	10 µg Mo(VI)
9	Nb(V)-Y(III)	Nb(97.2%)-Y(0%)	Nb(2.5%)-Y(0%)	10 µg Nb(V)
10	Ga(III)-Co(II)	Ga(97.1%)-Co(0%)	Ga(2.5%)-Co(0%)	25 µg Ga(III)
11	As(V)-Co(II)	As(98.9%)-Co(0%)	As(1.2%)-Co(0%)	5 µg As(V)
12	Fe(III)-Mn(II)	Fe(98.2%)-Mn(0%)	Fe(98.2%)-Mn(0%)	25 µg Fe(III)
13	Fe(III)-Ga(III) Zn(II)	Fe(97.1%)-Ga(98.1%)-Zn(0%)	Fe(2.8%)-Ga(1.8%)-Zn(0%)	25 µg Fe(III) / 20 µg Ga(III)
14	Zr(IV)-Ta(V)-Yb(III)	Zr(96.1%)-Ta(97.1%)-Yb(0%)	Zr(3.7%)-Ta(3.9%)-Yb(0%)	20 µg Zr(IV) / 15 µg Ta(V)

Figure 4.1 Elution curve for Zr(IV)-La(III) on a AG50W-X8 resin column (10 ml) in 0.05 M oxalic acid – 0.005 M sulphuric acid. [sorption step and eluting step of Zr with 0.05 M oxalic acid – 0.005 M sulphuric acid (0 - 400 ml mark on the x-axis of the curve), La eluted with 4.0 M HNO_3 (400 - 500 ml mark on the x-axis of the curve)].

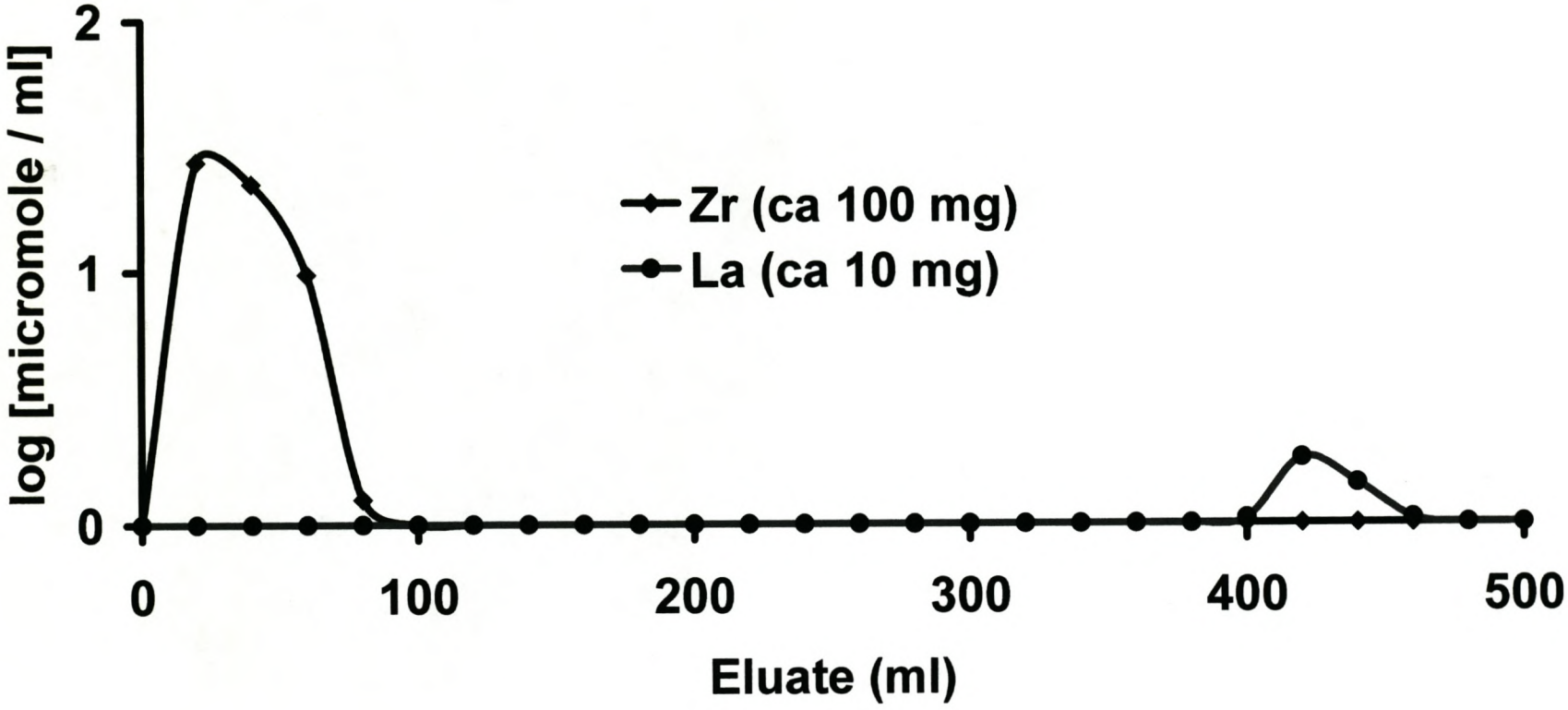

Figure 4.2 Elution curve for Al(III)-La(III) on a AG50W-X8 resin column (10 ml) in 0.05 M oxalic acid – 1.00 M sulphuric acid.

[sorption step and eluting step of Al with 0.05 M oxalic acid – 1.00 M sulphuric acid (0 - 400 ml mark on the x-axis of the curve), La eluted with 4.0 M HNO_3 (400 - 500 ml mark on the x-axis of the curve)].

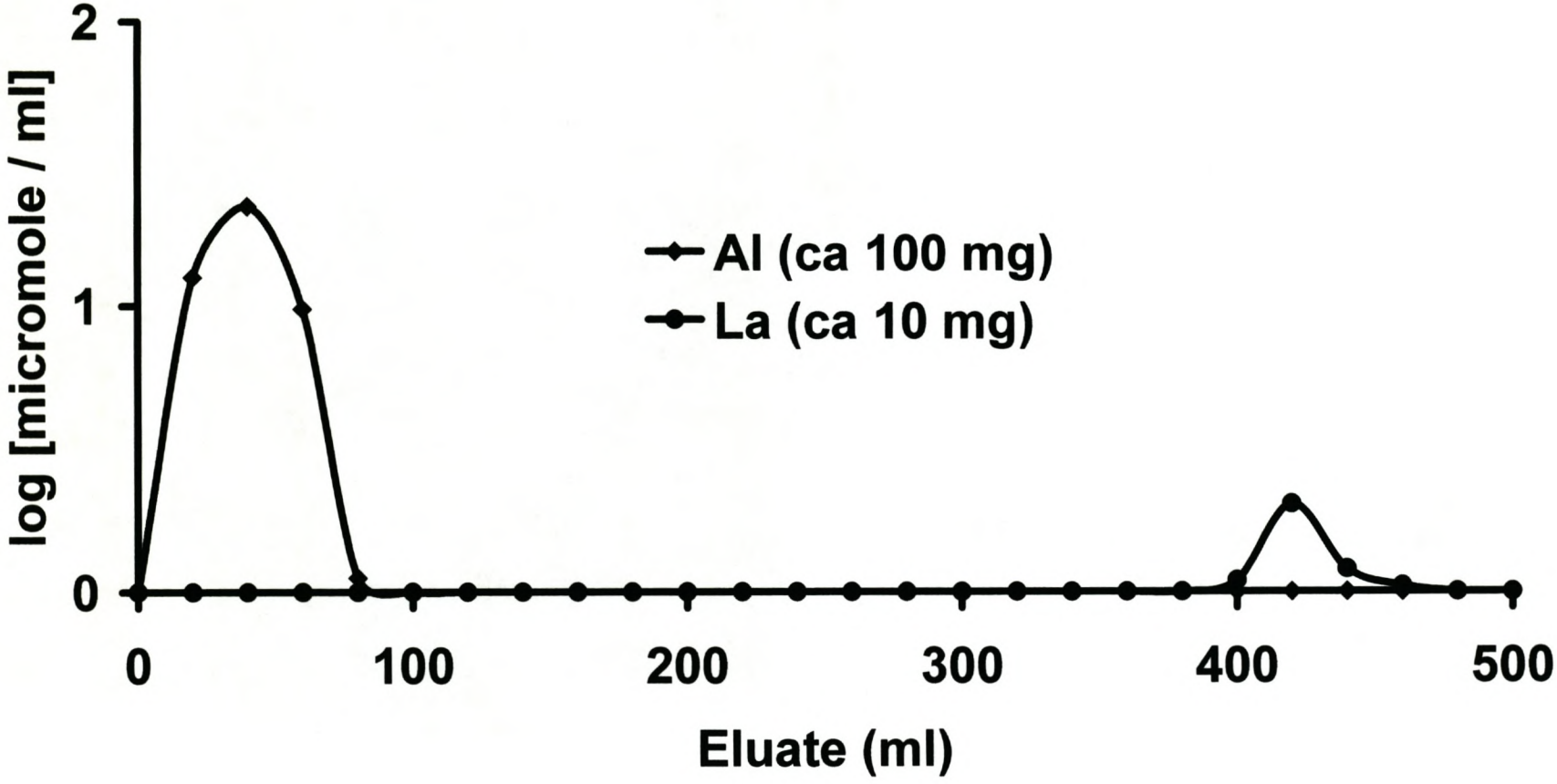

Figure 4.3 Elution curve for Ga(III)-Zn(II) on a AG50W-X8 resin column (15 ml) in 0.05 M oxalic acid – 0.005 M sulphuric acid. [sorption step and eluting step of Ga with 0.05 M oxalic acid – 0.005 M sulphuric acid (0 - 500 ml mark on the x-axis of the curve), Zn eluted with 1.0 M HNO_3 (500 - 600 ml mark on the x-axis of the curve)].

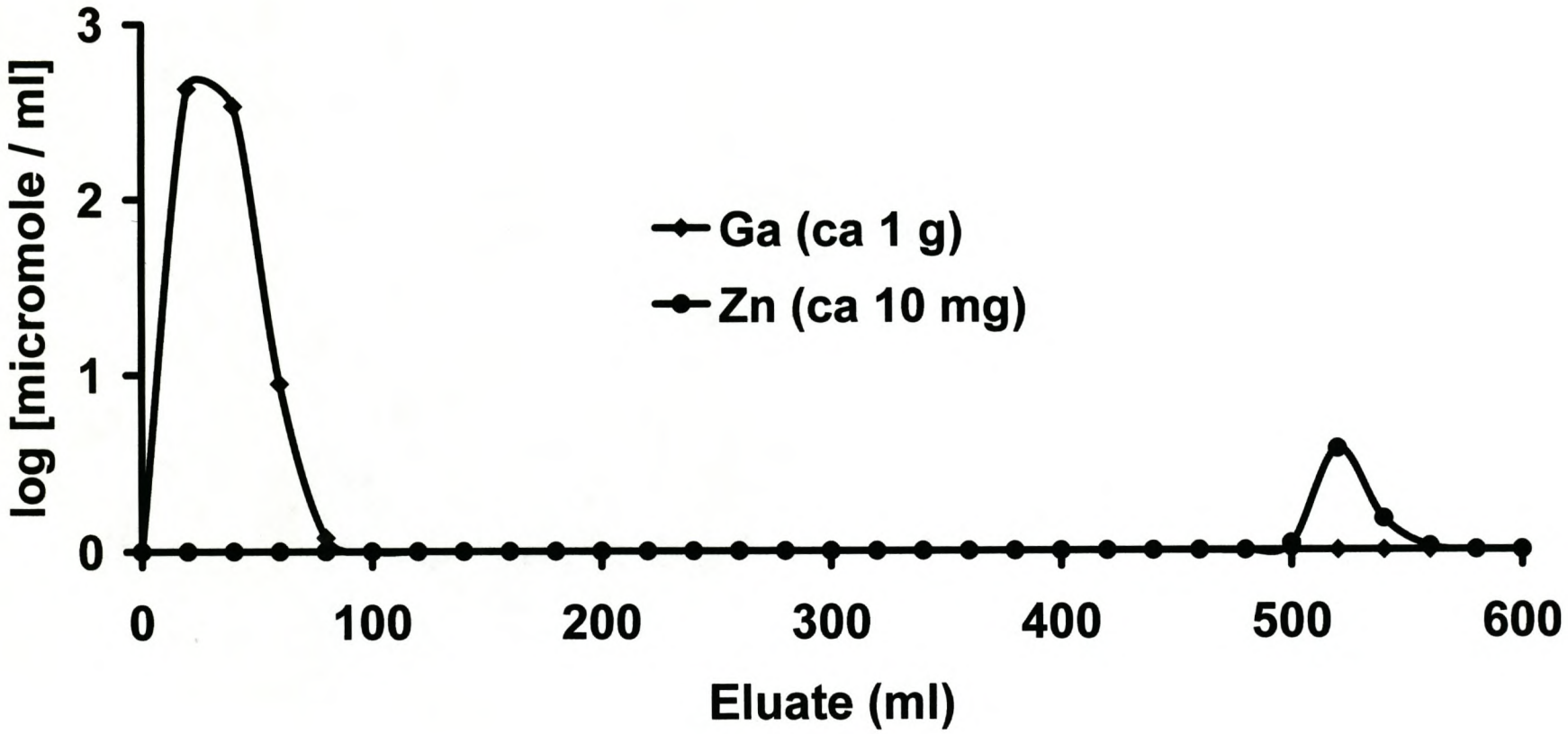

Figure 4.4 Elution curve for As(V)-Zn(II) on a AG50W-X8 resin column (10 ml) in 0.05 M oxalic acid – 0.005 M sulphuric acid. [sorption step and eluting step of As with 0.05 M oxalic acid – 0.005 M sulphuric acid (0 - 400 ml mark on the x-axis of the curve), Zn eluted with 1.0 M HNO_3 (400 - 500 ml mark on the x-axis of the curve)].

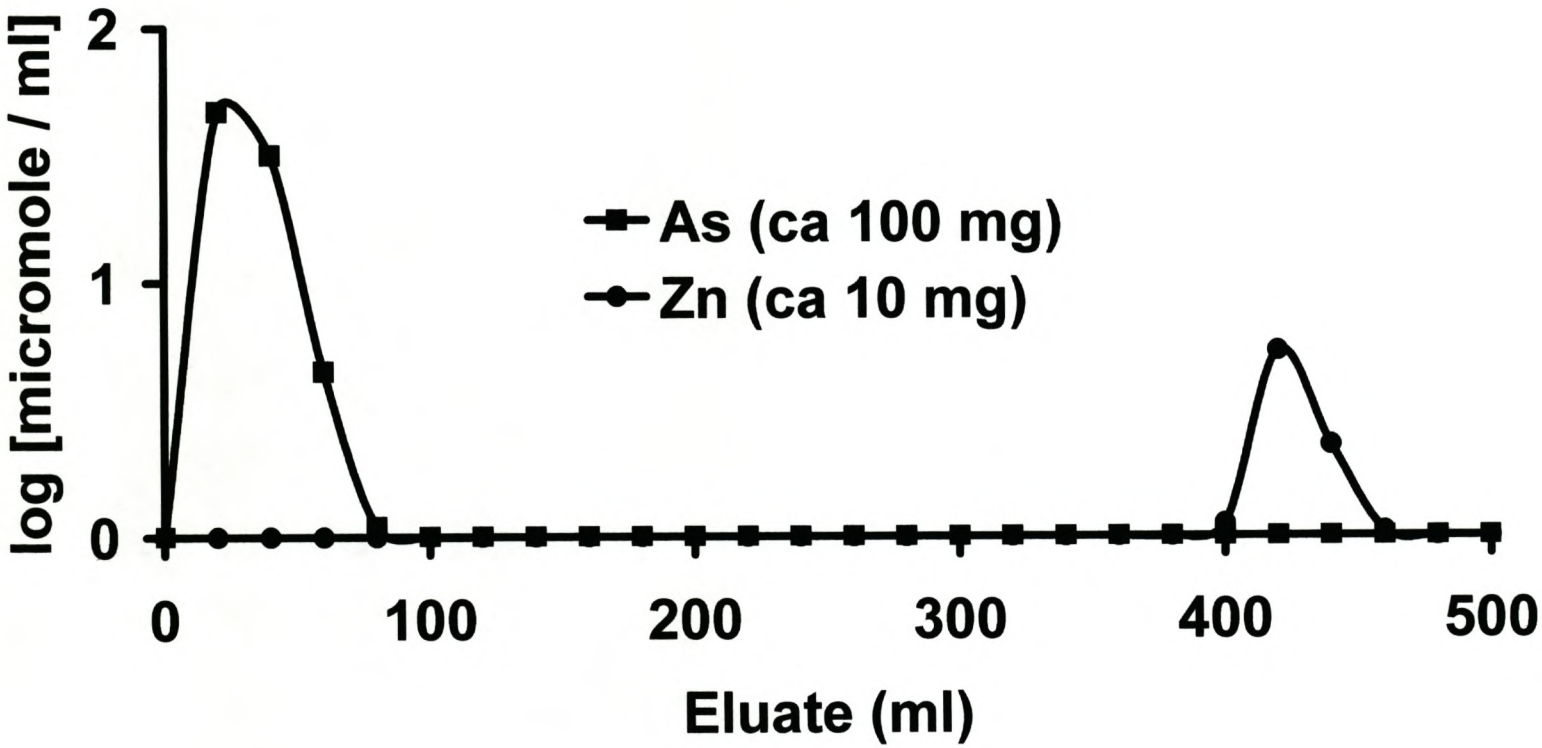

Figure 4.5 Elution curve for Cu(II)-Ce(IV) on a AG50W-X8 resin column (10 ml) in 0.05 M oxalic acid – 0.005 M sulphuric acid. [sorption step and eluting step of Cu with 0.05 M oxalic acid – 0.005 M sulphuric acid (0 - 400 ml mark on the x-axis of the curve), Ce eluted with 2.0 M HNO_3 (400 - 500 ml mark on the x-axis of the curve)].

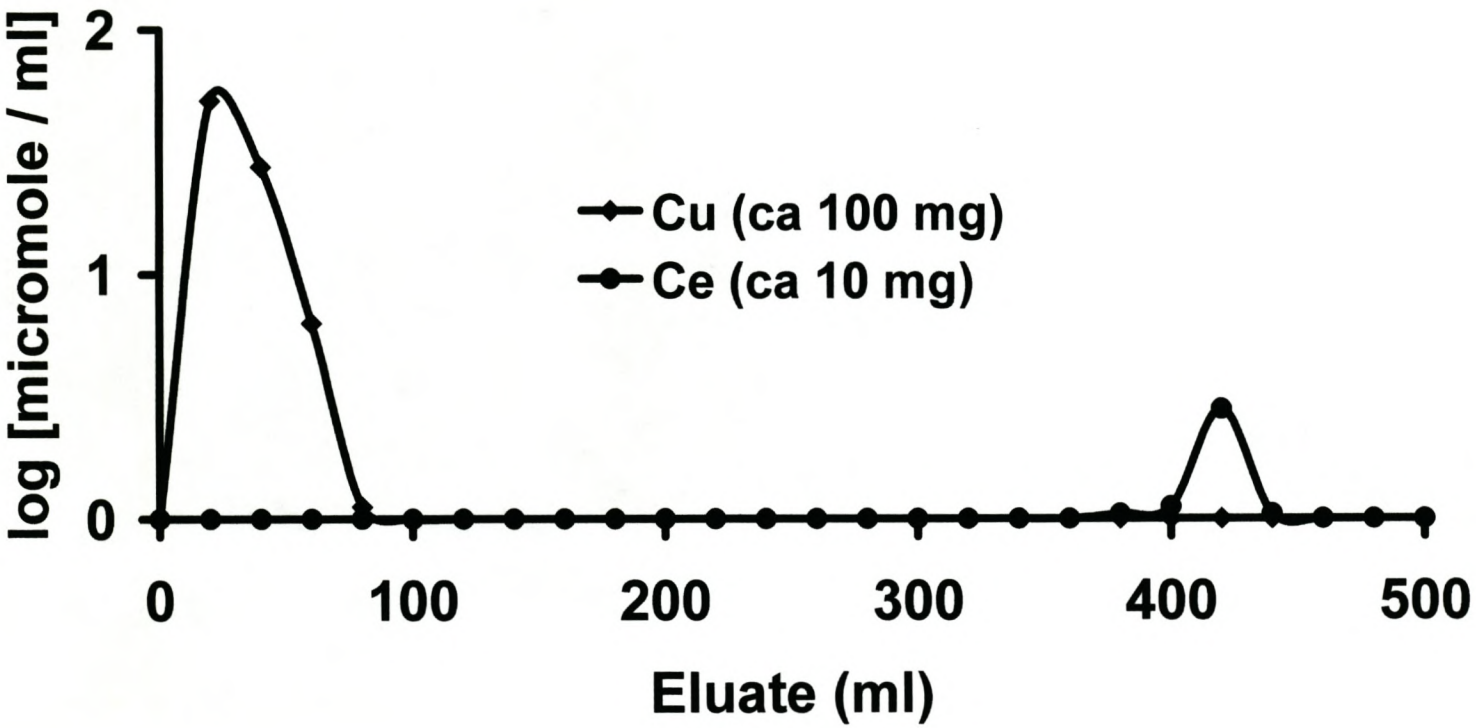

Figure 4.6 Elution curve for Ga(III)-Ce(IV) on a AG50W-X8 resin column (10 ml) in 0.05 M oxalic acid – 0.005 M sulphuric acid. [sorption step and eluting step of Ga with 0.05 M oxalic acid – 0.005 M sulphuric acid (0 - 400 ml mark on the x-axis of the curve), Ce eluted with 2.0 M HNO_3 (400 - 500 ml mark on the x-axis of the curve)].

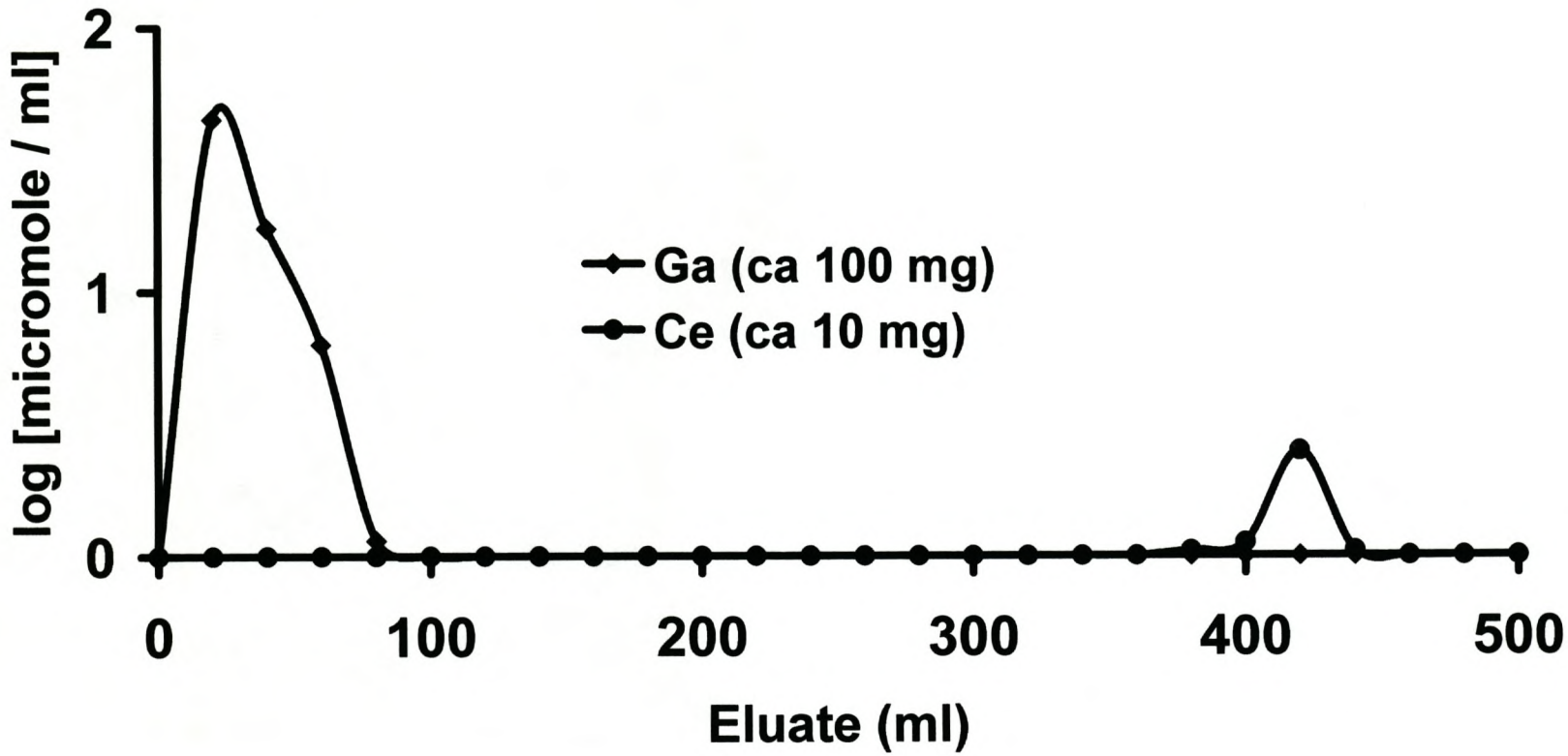

Figure 4.7 Elution curve for Ge(IV)-Ce(III) on a AG50W-X8 resin column (15 ml) in 0.05 M oxalic acid – 0.005 M sulphuric acid. [sorption step and eluting step of Ge with 0.05 M oxalic acid – 0.005 M sulphuric acid (0 - 500 ml mark on the x-axis of the curve), Ce eluted with 2.0 M HNO_3 (500 - 600 ml mark on the x-axis of the curve)].

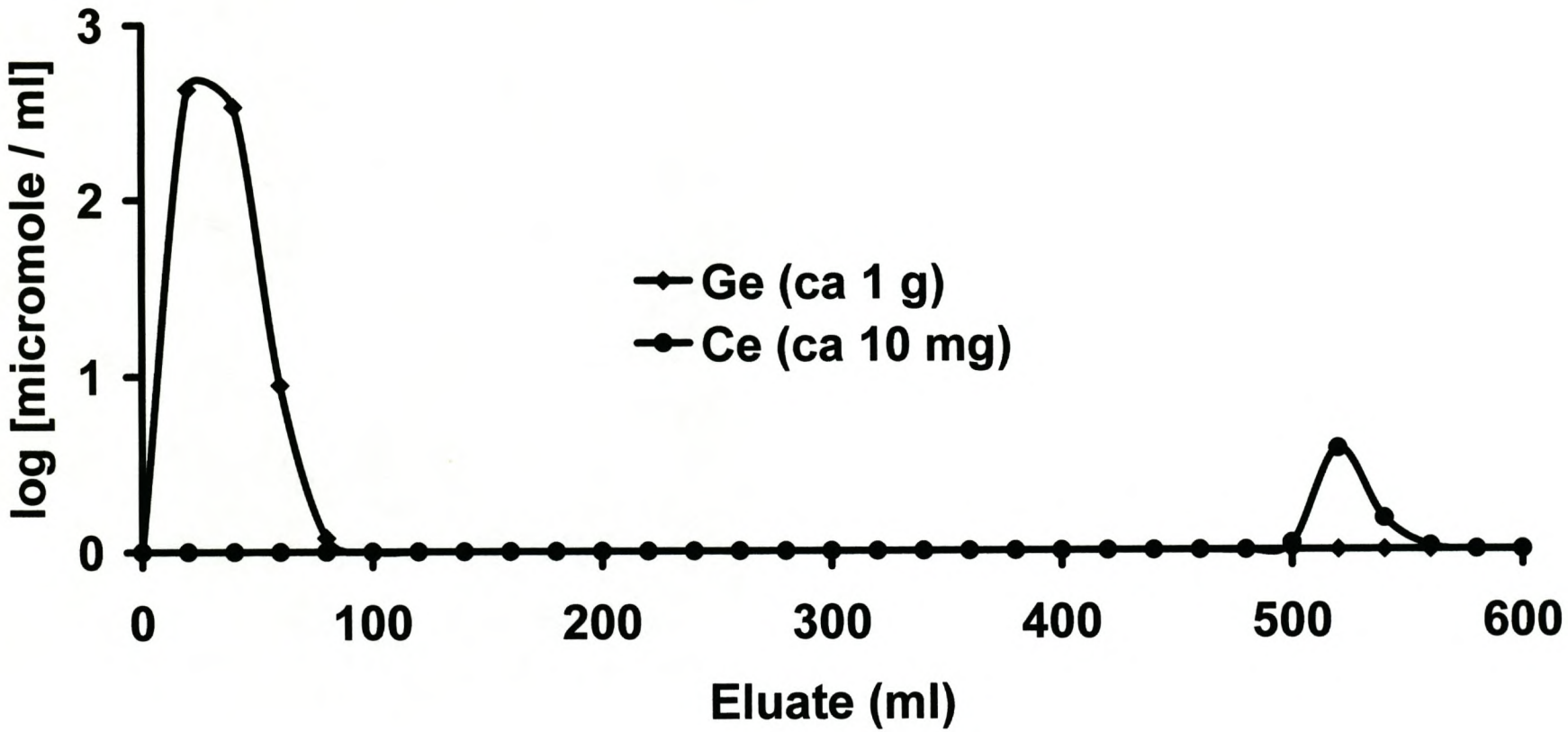

Figure 4.8 Elution curve for Mo(VI)-Y(III) on a AG50W-X8 resin column (10 ml) in 0.25 M oxalic acid – 0.005 M sulphuric acid. [sorption step and eluting step of Mo with 0.25 M oxalic acid –0.005 M sulphuric acid (0 - 400 ml mark on the x-axis of the curve), Y eluted with 2.0 M HNO_3 (400 - 500 ml mark on the x-axis of the curve)].

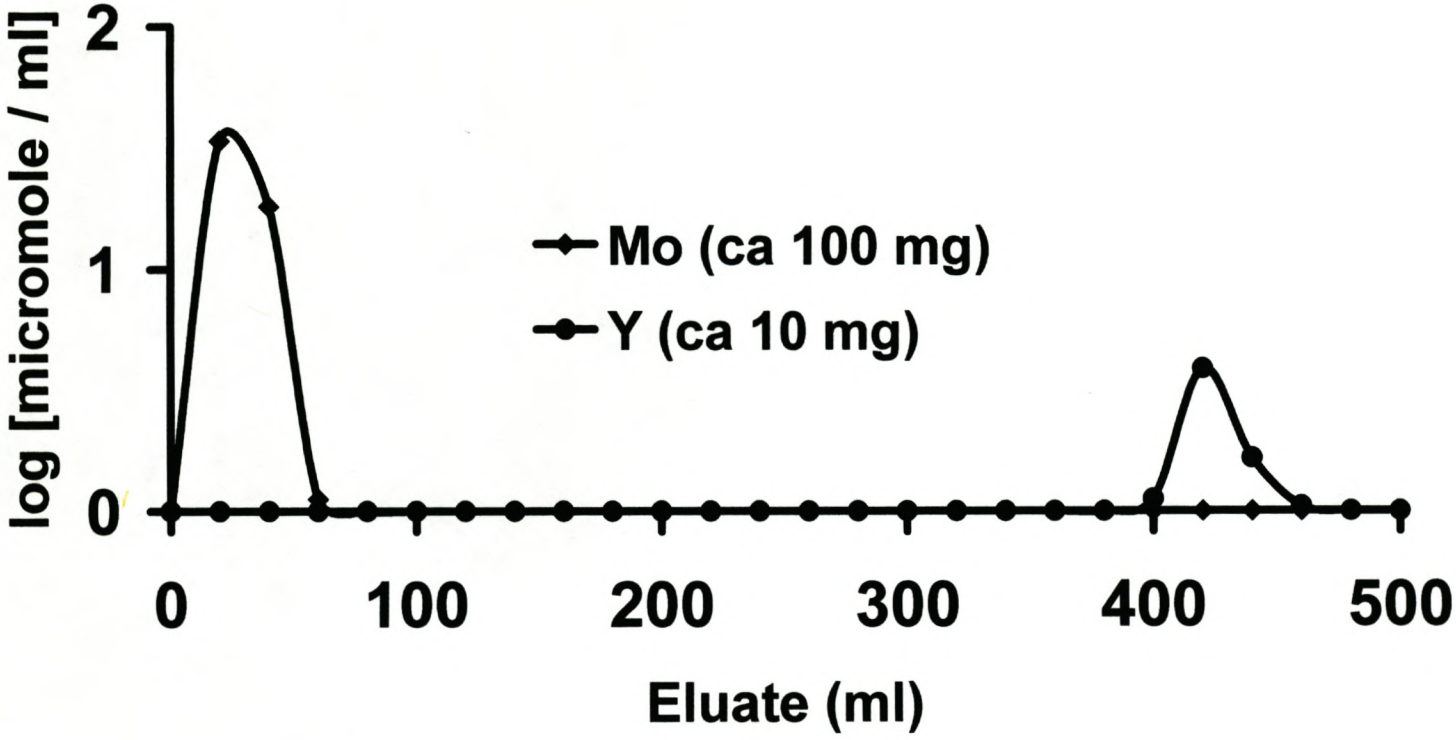

Figure 4.9 Elution curve for Nb(V)-Y(III) on a AG50W-X8 resin column (10 ml) in 0.25 M oxalic acid – 0.005 M sulphuric acid. [sorption step and eluting step of Nb with 0.25 M oxalic acid – 0.005 M sulphuric acid (0 - 400 ml mark on the x-axis of the curve), Y eluted with 2.0 M HNO_3 (400 - 500 ml mark on the x-axis of the curve)].

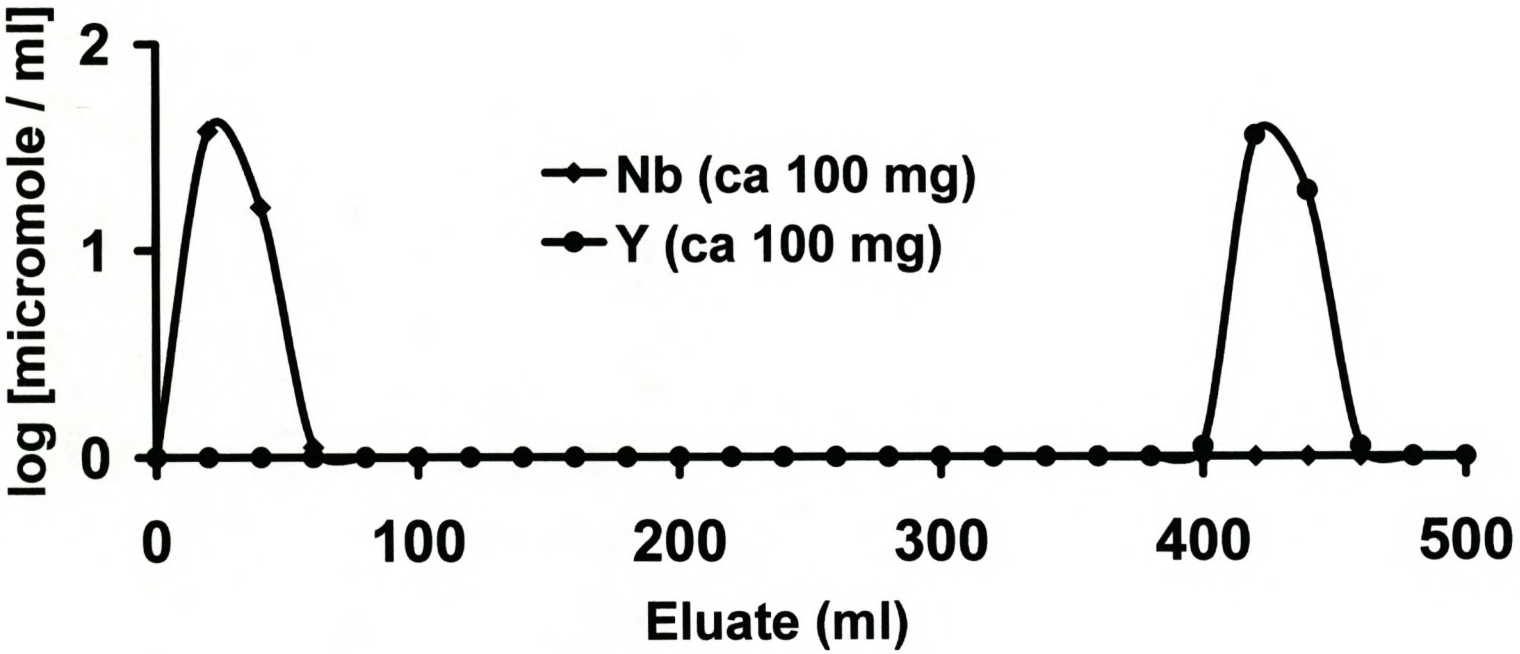

Figure 4.10 Elution curve for Ga(III)-Co(II) on a AG50W-X8 resin column (15 ml) in 0.25 M oxalic acid – 0.005 M sulphuric acid. [sorption step and eluting step of Ga with 0.25 M oxalic acid – 0.005 M sulphuric acid (0 - 500 ml mark on the x-axis of the curve), Co eluted with 2.0 M HNO_3 (500 - 600 ml mark on the x-axis of the curve)].

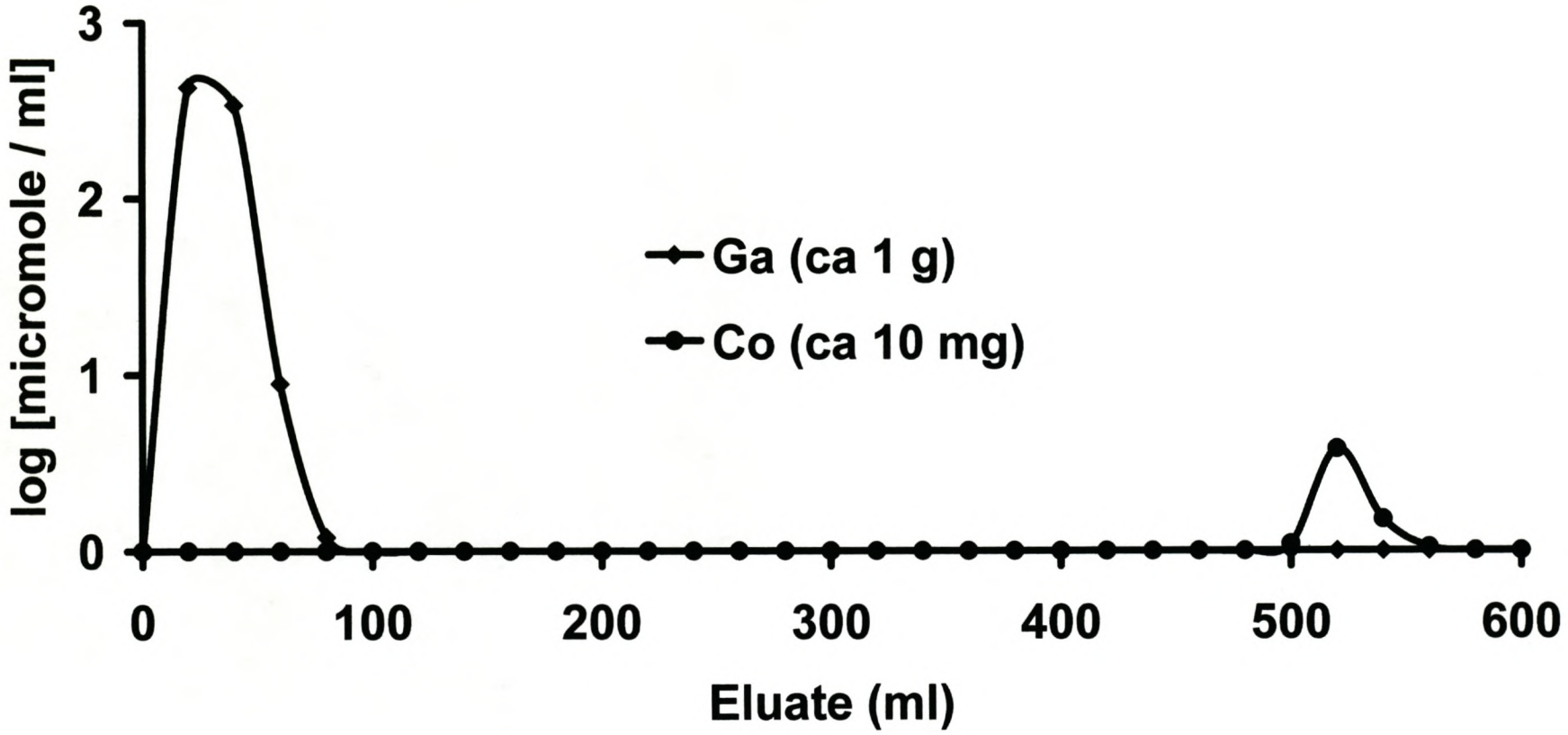

Figure 4.11 Elution curve for As(V)-Co(II) on a AG50W-X8 resin column (10 ml) in 0.25 M oxalic acid – 0.005 M sulphuric acid. [sorption step and eluting step of As with 0.25 M oxalic acid – 0.005 M sulphuric acid (0 - 400 ml mark on the x-axis of the curve), Co eluted with 2.0 M HNO_3 (400 - 500 ml mark on the x-axis of the curve)].

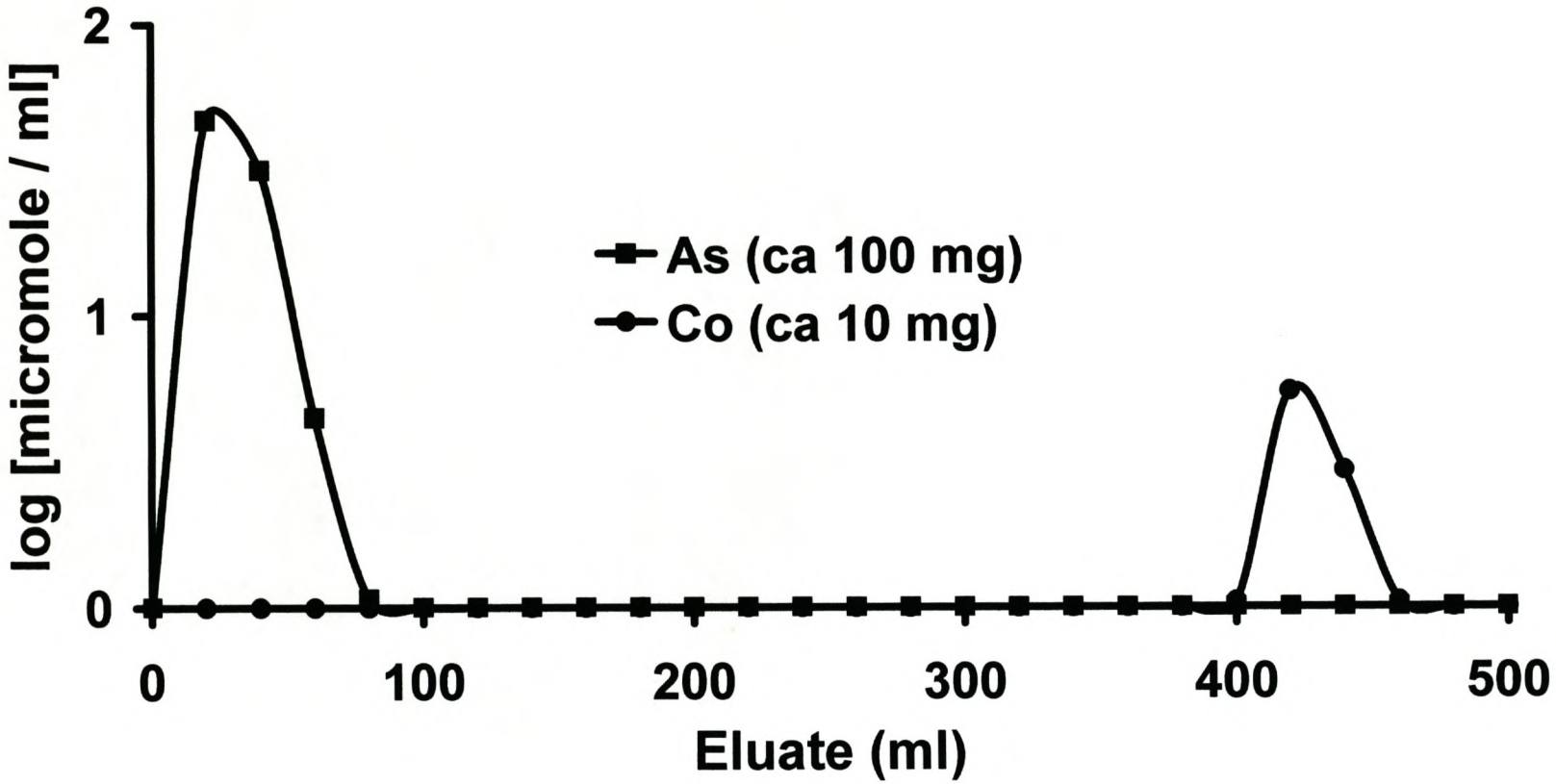

Figure 4.12 Elution curve for Fe(III)-Mn(II) on a AG50W-X8 resin column (10 ml) in 0.25 M oxalic acid – 0.05 M sulphuric acid.

[sorption step and eluting step of Fe with 0.25 M oxalic acid – 0.05 M sulphuric acid (0 - 400 ml mark on the x-axis of the curve), Mn eluted with 2.0 M HNO_3 (400 - 500 ml mark on the x-axis of the curve)].

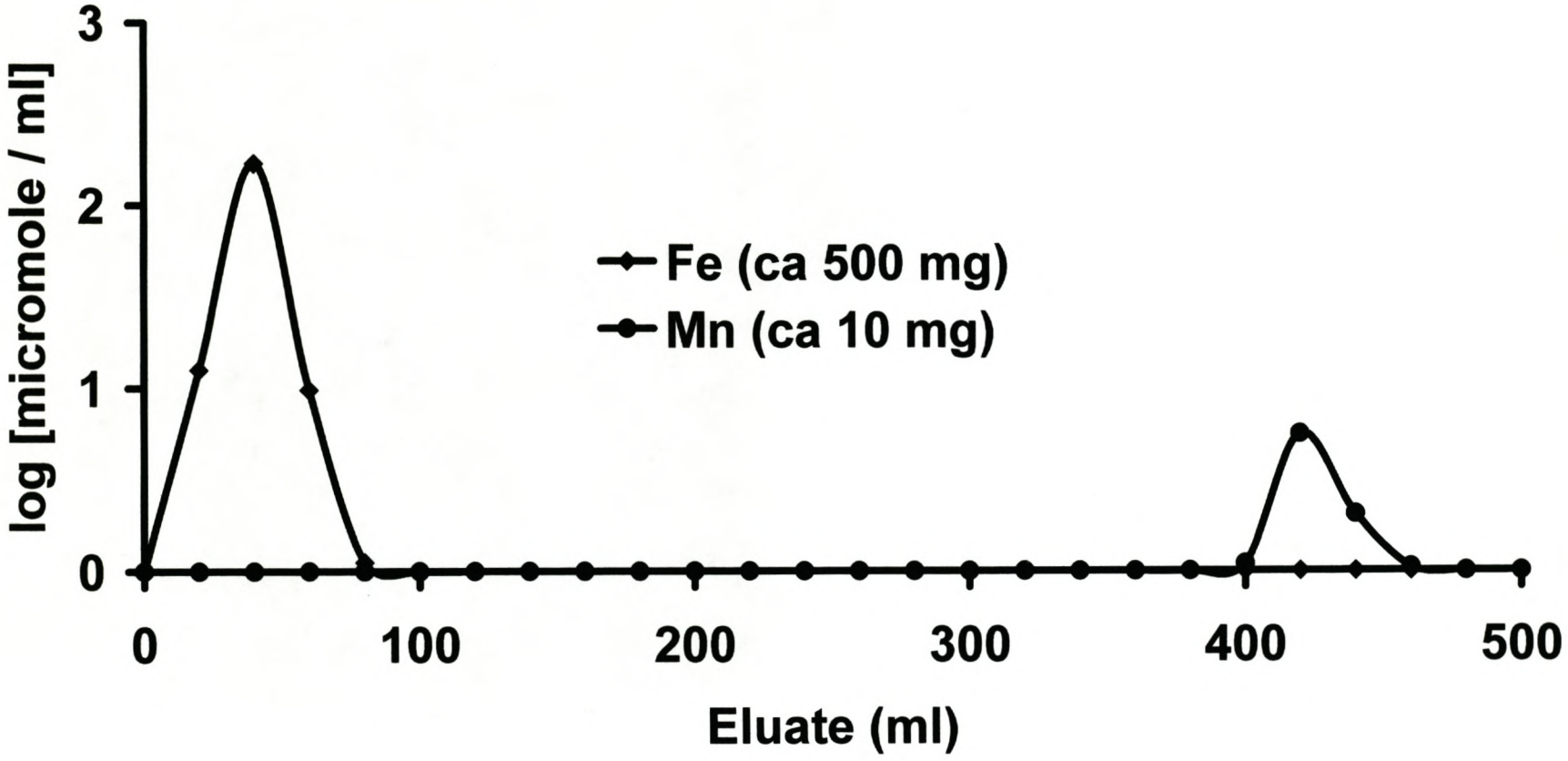

Figure 4.13 Elution curve for Fe(III)-Ga(III)-Zn(II) on a AG50W-X8 resin column (10 ml) in 0.25 M oxalic acid – 0.10 M sulphuric acid. [sorption step and eluting step of Fe and Ga with 0.25 M oxalic acid – 0.10 M sulphuric acid (0 - 500 ml mark on the x-axis of the curve), Zn eluted with 2.0 M HNO_3 (500 - 600 ml mark on the x-axis of the curve)].

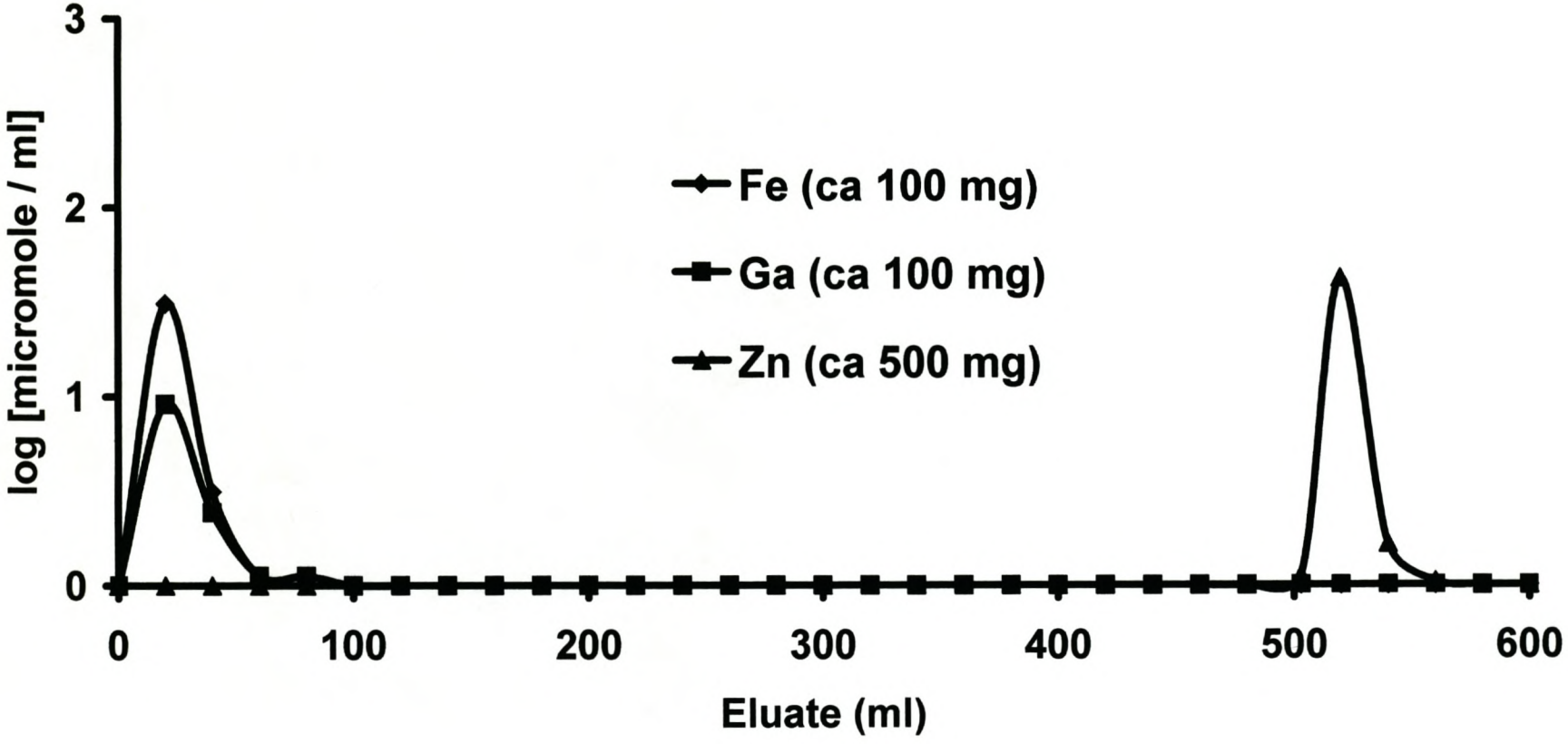

Figure 4.14 Elution curve for Zr(IV)-Ta(V)-Yb(III) on a AG50W-X8 resin column (10 ml) in 0.25 M oxalic acid – 0.25 M sulphuric acid. [sorption step and eluting step of Zr and Ta with 0.25 M oxalic acid – 0.25 M sulphuric acid (0 - 500 ml mark on the x-axis of the curve), Yb eluted with 2.0 M HNO_3 (500 - 600 ml mark on the x-axis of the curve)].

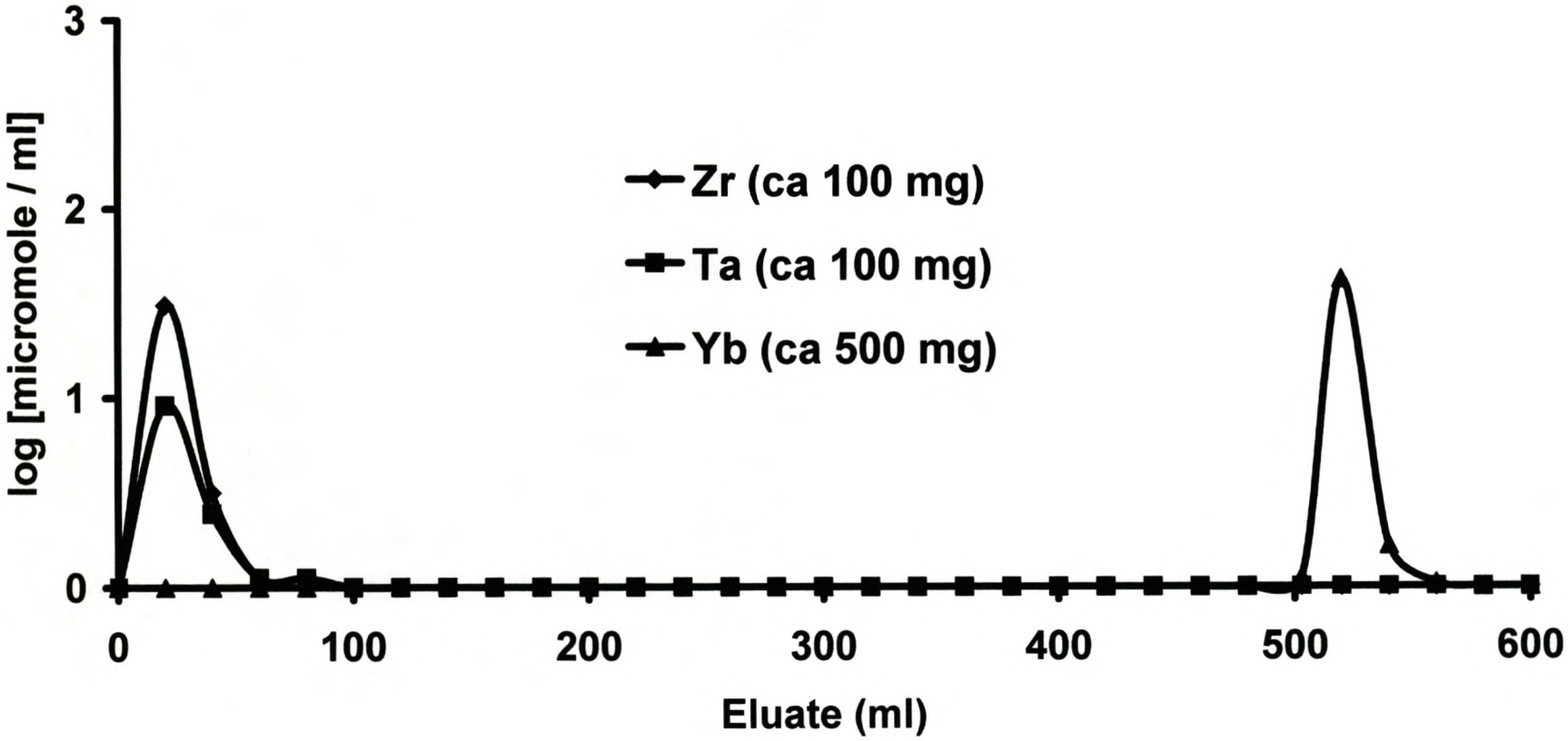

4.4 REFERENCES

1. Nozaki T., Takeuchi K., Yamauchi T. and Nomura T., *Jpn. Analyst*, 27, 454, 1978.
2. Strelow F.W.E. and van der Walt T.N., *S. Afr. J. Chem.*, 37, 149, 1984.
3. Draganic I.C., Draganic C.D. and Dizdar Z.I., *Bull. Inst. Nucl. Sci. Boris Kidrich (Belgrade)*, 55, 37, 1954.
4. Orlandini K.A., *Inorg. Nucl. Chem. Lett.*, 5, 325, 1969.
5. Hamaguchi H., Kuroda R., Sugisita R., Onuma N. and Shimizu T., *Anal. Chim. Acta*, 28, 61, 1963.
6. Suzuki Y., Int. J. *Appl. Radiat. Isot.*, 15, 599, 1964.
7. Nozaki T., Hiraiwa C. H. and Koshiba K., *Bull. Chem. Soc. Jpn.,* 42, 245, 1969.
8. van der Walt T.N. and Strelow F.W.E., *Anal. Chem.,* 57, 2889, 1985.
9. Paunescu N., *J. Radioanal. Nucl. Chem. Lett.*, 104, 209, 1986.
10. Ding X. and Mou S., *J. Chromatogr.*, 920, 101, 2001.
11. Ji-Ying Ji. and Blesa M.A., *Inorg. Chem.,* 37, 3159, 1998.
12. Blesa M.A., *Inorg. Chem.,* 36, 6423, 1997.
13. Sharma S.D. and Sharma S.C., *J. Chromatogr.*, 841, 263, 1999.
14. Greenwood N.N. and Earnshaw A., *Chemistry of the elements,* 1st edition, Pergamon Press, New York, 1984, pp. 1060.
15. Cotton F.A. and Wilkinson G., *Advanced inorganic chemistry,* 4th edition, John Wiley & Sons, New York, 1980, pp. 65.
16. Mellor J.W., *A comprehensive treatise on inorganic and theoretical chemistry,* Vol. XI, Longmans, Green & Co., New York, 1924, pp. 435.

17. Cotton F.A. and Wilkinson G., *Advanced inorganic chemistry,* 4th edition, John Wiley & Sons, New York, 1980, pp.757.

18. Mellor J.W., *A comprehensive treatise on inorganic and theoretical chemistry,* Vol. V, Longmans, Green & Co., New York, 1924, pp. 491.

19. Mellor J.W., *A comprehensive treatise on inorganic and theoretical chemistry,* Vol. VII, Longmans, Green & Co., New York, 1924, pp. 93.

20. Cotton F.A. and Wilkinson G., *Advanced inorganic chemistry,* 4th edition, John Wiley & Sons, New York, 1980, pp. 699.

21. Cotton F.A. and Wilkinson G., *Advanced inorganic chemistry,* 4th edition, John Wiley & Sons, New York, 1980, pp. 721.

22. Mellor J.W., *A comprehensive treatise on inorganic and theoretical chemistry,* Vol. XI, Longmans, Green & Co., New York, 1924, pp. 656.

23. Mellor J.W., *A comprehensive treatise on inorganic and theoretical chemistry,* Vol. XI, Longmans, Green & Co., New York, 1924, pp. 861.

24. Mellor J.W., *A comprehensive treatise on inorganic and theoretical chemistry,* Vol. VII, Longmans, Green & Co., New York, 1924, pp. 478.

25. Mellor J.W., *A comprehensive treatise on inorganic and theoretical chemistry,* Vol. IX, Longmans, Green & Co., New York, 1924, pp. 581.

26. Mellor J.W., *A comprehensive treatise on inorganic and theoretical chemistry,* Vol. XI, Longmans, Green & Co., New York, 1924, pp. 117.

27. Mellor J.W., *A comprehensive treatise on inorganic and theoretical chemistry,* Vol. V, Longmans, Green & Co., New York, 1924, pp. 543.

28. Cotton F.A. and Wilkinson G., *Advanced inorganic chemistry,* 4th edition, John Wiley & Sons, New York, 1980, pp. 999.

29. Mellor J.W., *A comprehensive treatise on inorganic and theoretical chemistry,* Vol. V, Longmans, Green & Co., New York, 1924, pp. 574.

CHAPTER 5

SORPTION BEHAVIOUR OF SELECTED ELEMENTS ON AN ANION EXCHANGER

5.1 INTRODUCTION

A systematic study of the anion exchange distribution coefficients of 12 elements [using radioactive tracer amounts of Mo(VI), In(III), Sc(III), Lu(III), Cu(II), Hg(II), Ce(III), Zn(II), Co(II), Mn(II) and As(III)] with the Dowex® 1-X8 resin in pure oxalic acid solutions, was presented by De Corte et al. [1] The oxalic acid concentrations were varied from 0.001 M to 0.98 M. Strelow et al. [2] presented a systematic study of the anion exchange distribution coefficients of 36 elements (1 mmole) with the Bio-Rad® AG1-X8 resin in an oxalic acid – hydrochloric acid mixture. Two oxalic acid concentrations (0.05 M and 0.25 M) were selected, and the hydrochloric acid concentration was varied from 0.01 M to 4.00 M. Strelow et al. [2] also presented a systematic study of the anion exchange distribution coefficients of 29 elements (1.0 mmole) with the Bio Rad® AG1-X8 resin in an oxalic acid – nitric acid mixture. Again, two oxalic acid concentrations (0.05 M and 0.25 M) were selected, and the nitric acid concentration was varied from 0.01 M to 4.00 M.

Hydrochloric acid is an attractive choice for the mineral acid, because it is volatile and, in addition, the chloride anion is not very strongly adsorbed and therefore does not compete very strongly for resin sites. Unfortunately, some bivalent elements such as Zn, Cd and Hg form stable chloride complexes when oxalate complex formation is suppressed. Nitric acid is also volatile and has only a very slight tendency toward complex formation in dilute aqueous solution. It can therefore be used for separation of the chloride complex-forming elements.

The nitrate anion is adsorbed considerably more strongly than the chloride, and should therefore be very useful in separating the more strongly adsorbed elements. Under similar conditions, the sulphate anion is more strongly adsorbed than the chloride and nitrate anions and should offer a variety of other separation possibilities. Various applications of anion exchange separations in oxalic acid or oxalic acid – mineral acid mixtures have been reported [3-12].

This Chapter focuses on the sorption behaviour of 32 metal ions [Al(III), As(V), Ce(III), Ce(IV), Co(II), Cr(II), Cu(II), Fe(III), Ga(III), Ge(IV), In(III), La(III), Mn(II), Mo(VI), Nb(V), Ni(II), Pr(III), Sb(V), Sc(III), Se(IV), Sn(IV), Ta(V), Tb(III), Te(IV), Ti(IV), V(V), W(VI), Y(III), Yb(III), Zn(II) and Zr(IV)] on an anion exchanger. The equilibrium distribution coefficients of these selected metal ions were investigated on an anion exchange resin (Bio-Rad® AG1X-8) in 0.05 M and 0.25 M oxalic acid at various concentrations of sulphuric acid (0.005 M, 0.05 M, 0.10 M, 0.25 M, 0.50 M, 1.00 M, 1.50 M and 2.00 M). The oxalic acid in the appropriate mixture with a strong mineral acid (sulphuric acid) could be used to control the rate of sorption of the selected metal ions. Using the findings from the above, two component and three component elemental separations on an anion exchange resin were also investigated.

5.2 RESULTS OF ANIONIC EQUILIBRIUM DISTRIBUTION COEFFICIENT

As is evident from Table 5.1 and Table 5.2, the group 5 metal ions [As(V) and Sb(V)] that were studied, showed absolutely no sorption in any of the chosen oxalic acid – sulphuric acid combinations. Similar behaviour was encountered with the cation exchanger, as shown in Chapter 4.

Table 5.1 Anion exchange distribution coefficients in 0.05 M oxalic acid, at various concentrations of H_2SO_4

	Molarity H_2SO_4							
Metal ion	0.005	0.05	0.10	0.25	0.50	1.00	1.50	2.00
Al(III)	1635	375	160	32.0	9.8	<0.5	<0.5	<0.5
As(V)[b]	<0.5	<0.5	<0.5	<0.5	<0.5	<0.5	<0.5	<0.5
Cd(II)[b]	65	35.1	15.1	10.2	5.1	<0.5	<0.5	<0.5
Ce(III)[b]	$>10^4$	6500	4066	1730	850	210	<0.5	<0.5
Ce(IV)[a, b]	9900	3775	1235	365	315	150	<0.5	<0.5
Ce(IV)[b]	1649	980	539	198	95	55	<0.5	<0.5
Co(II)	568	238	88	10.1	<0.5	<0.5	<0.5	<0.5
Cr(III)	655	385	145	65	35.2	14.5	5.5	<0.5
Cu(II)[b]	253	77	45.5	28.5	15.4	2.2	<0.5	<0.5
Fe(III)[a]	4680	1640	713	141	53	<0.5	<0.5	<0.5
Ga(III)	3500	1000	140	30.1	6.2	<0.5	<0.5	<o.5
Ge(IV)	7430	2710	1150	425	120	34.1	5.4	<0.5
In(III)	690	390	195	100	55	25.5	10.5	<0.5
La(III)[b]	445	315	215	90	40.5	15.5	7.5	<0.5
Mn(II)[b]	<0.5	<0.5	<0.5	<0.5	<0.5	<0.5	<0.5	<0.5
Mo(VI)[a]	$>10^4$	8485	3900	2100	1310	680	385	282
Nb(V)	$>10^4$	5970	3775	1520	625	240	121	76
Ni(II)[b]	<0.5	<0.5	<0.5	<0.5	<0.5	<0.5	<0.5	<0.5
Pr(III)[b]	prec	prec	prec	prec	prec	prec	prec	prec
Sb(V)[b]	<0.5	<0.5	<0.5	<0.5	<0.5	<0.5	<0.5	<0.5
Sc(III)	395	255	155	75	31.4	5.6	<0.5	<0.5
Se(IV)[b]	3850	3550	3250	2350	1290	1010	810	665
Sn(IV)	8000	5300	4020	2160	1145	325	185	120
Ta(V)[a]	9722	3178	1710	880	480	225	88	25.4
Tb(III)[b]	prec	prec	prec	prec	prec	prec	prec	prec
Te(IV)	5600	4550	3500	2150	1365	1165	955	750
Ti(IV)[a]	125	89	68	32.1	15.2	10.0	3.1	<0.5
V(V)	$>10^4$	6100	3550	1550	855	350	155	95
W(VI)[a.b]	9030	4820	2425	890	300	135	44.8	26.8
Y(III)[b]	555	345	195	55	15.5	6.5	<0.5	<0.5
Yb(III)[b]	750	605	475	250	75	25.1	5.1	<0.5
Zn(II)[b]	790	327	160	85	25.5	9.5	<0.5	<0.5
Zr(IV)[a]	$>10^4$	9790	2290	390	140	53	47.1	33.3

[a] 1 ml of 30% H_2O_2 present
[b] 0.1 mmol of metal ion
prec = precipitate

Table 5.2 Anion exchange distribution coefficients in 0.25 M oxalic acid, at various concentrations of H_2SO_4

	Molarity H_2SO_4							
Metal ion	0.005	0.05	0.10	0.25	0.50	1.00	1.50	2.00
Al(III)	1185	552	200	95	23.2	8.2	<0.5	<0.5
As(V)[b]	<0.5	<0.5	<0.5	<0.5	<0.5	<0.5	<0.5	<0.5
Cd(II)[b]	45.5	25.1	10.2	5.5	<0.5	<0.5	<0.5	<0.5
Ce(III)[b]	3500	1966	890	350	110	55	10.5	<0.5
Ce(IV)[a, b]	9000	3715	1580	930	550	85	35.5	<0.5
Ce(IV)[b]	1910	1550	1200	550	85	35	<0.5	<0.5
Co(II)	829	280	112	45.2	12.1	<0.5	<0.5	<0.5
Cr(III)	775	395	165	85	45.5	19.5	9.5	<0.5
Cu(II)[b]	71	36.9	21.1	14.4	10.1	5.1	<0.5	<0.5
Fe(III)[a]	6900	3160	1055	302	99	5.9	<0.5	<0.5
Ga(III)	9700	6100	1150	140	42.1	10.1	3.5	<0.5
Ge(IV)	$>10^4$	6410	3035	1215	520	175	104	45
In(III)	725	453	295	167	70	10.1	<0.5	<0.5
La(III)[b]	555	410	305	195	90	25	9.5	<0.5
Mn(II)[b]	<0.5	<0.5	<0.5	<0.5	<0.5	<0.5	<0.5	<0.5
Mo(VI)[a]	$>10^4$	$>10^4$	8320	3840	1700	660	415	305
Nb(V)	6270	4360	3000	1480	740	296	175	111
Ni(II)[b]	<0.5	<0.5	<0.5	<0.5	<0.5	<0.5	<0.5	<0.5
Pr(III)[b]	prec	prec	prec	prec	prec	prec	prec	prec
Sb(V)[b]	<0.5	<0.5	<0.5	<0.5	<0.5	<0.5	<0.5	<0.5
Sc(III)	455	310	205	95	45.5	19.5	8.5	<0.5
Se(IV)[b]	5350	4750	4140	3150	2250	1350	1030	850
Sn(IV)	4390	3600	2950	1970	1170	600	415	250
Ta(V)[a]	5325	2500	1810	820	420	220	110	45.5
Tb(III)[b]	prec	prec	prec	prec	prec	prec	prec	prec
Te(IV)	6100	5250	3900	2550	1555	1300	1050	855
Ti(IV)[a]	158	116	75	55	33.1	14.5	5.2	<0.5
V(V)	$>10^4$	7250	4100	1750	995	450	175	125
W(VI)[a,b]	9370	4800	2430	870	310	145	65	35.8
Y(III)[b]	395	195	110	49.5	25.1	2.5	<0.5	<0.5
Yb(III)[b]	495	430	365	194	29.5	5.5	<0.5	<0.5
Zn(II)[b]	2190	1320	745	280	55	15.3	4.2	<0.5
Zr(IV)[a]	$>10^4$	7480	3130	690	208	50	31.1	26.6

[a] 1 ml of 30% H_2O_2 present
[b] 0.1 mmol of metal ion
prec = precipitate

Group 3 metal ions [Al(III), Ga(III) and In(III)] showed relatively better sorption than group 5 metal ions in both oxalate concentrations in the lower sulphuric acid range (0.005 M – 0.25 M). Group 4 metal ions [Ge(IV) and Sn(IV)] and group 6 metal ions [Se(IV) and Te(IV)] were sorbed relatively more strongly compared to group 3 [Al(III), Ga(III) and In(III)] and group 5 [As(V) and Sb(V)] metal ions in both oxalate concentrations across the chosen sulphuric acid range.

The transition metal ions [Sc(III), Ti(IV), V(V), Cr(III), Mn(II), Fe(III), Co(II), Cu(II), Zn(II), Y(III), Zr(IV), Nb(V), Mo(VI), Cd(II), La(III), Ta(V) and W(VI)] that were studied did not show any significant trend. However, the divalent metal ions [Mn(II), Co(II), Ni(II), Cu(II), Zn(II) and Cd(II)] and the trivalent metal ions [Sc(III), Cr(III), Y(III) and Fe(III)] showed sorption behaviour of a more or less similar order, with the exception of Mn(II) and Ni(II), which showed no sorption, and Fe(III), which had very pronounced sorption of all the divalent and trivalent metal ions in the transition series. The tetravalent metal ions [Zr(IV) and Ti(IV)], the pentavalent metal ions [Nb(V), Ta(V) and V(V)] and the hexavalent metal ions [Mo(VI) and W(VI)] showed relatively similar sorption in both oxalate concentrations across the sulphuric acid range, and it was relatively higher than that of the divalent and trivalent metal ions. The only exception was Ti(IV), which showed relatively weaker sorption. In addition, all the sorbed metal ions showed a decrease in sorption as the concentration of sulphuric acid increased across the chosen range. Generally, these sorbed metal ions showed an increase in sorption in 0.25 M oxalic acid compared to 0.05 M oxalic acid, with the exception of Al(III), Cd(II), Ce(III), Ce(IV), Cu(II), La(III), Mn(II), Ni(II), Sb(V), W(VI) and Yb(III).

The various distribution diagrams of Al(III), Cd(II), Co(II) and Zn(II), which were previously discussed in Chapter 4, were used in an attempt to explain the sorption behaviour of the above sorbed metal ions. The distribution diagrams (Appendix, Figures 8.1 to 8.5) highlight the fact that many of the dominant complexes are negatively charged, and this would play an active role in the nature of sorption of the respective metal ions on an anion exchanger. For example, for the metal ion Al(III), increased sorption is evident in the lower sulphuric acid range (0.005 M – 0.10 M) on the anion exchanger compared to the cation exchanger, and this could be attributed to the strong dominance of the negatively charged $[Al(oxalate)_3]^{3-}$ and $[Al(oxalate)_2]^{-}$ complexes (Appendix, Figure 8.1), which would favour electrostatic sorption on the quaternary ammonium group of the anion exchanger. However, for the metal ions Cd(II), Co(II) and Zn(II), relatively weaker sorption is evident across the chosen sulphuric acid range on the anion exchanger compared to the cation exchanger, even though, according to the respective distribution diagrams (Appendix, Figures 8.2-8.5), the $[Cd(oxalate)_2]^{2-}$ and $[Cd(SO_4)]^{2-}$ complexes for Cd(II), the $[Zn(oxalate)_2]^{2-}$ and $[ZnSO_4]$ complexes for Zn(II) and the $[Co(oxalate)_2]^{2-}$ and $CoSO_4$ complexes for Co(II) are the dominant complexes across the chosen sulphuric acid range. The lower sorption could again be attributed to a set of complex factors such as the ionic strength and hydration energies of the metal complexes (metal-oxalate or the metal-sulphate) and complex charge during the sorption of the metal complex with the quaternary ammonium group of the anion exchanger. Similarly, as with the cation exchanger, the distribution coefficients on the anion exchanger decreased as the concentration of the sulphuric acid increased across the chosen range, and this could be attributed to the increasingly competing SO_4^{2-} anion on the exchange sites of the resin [13] and the influence of the H^+ (of the H_2SO_4) on the dissociation of the oxalic acid.

It could be concluded again that the speciation modelling systems used in the above study were not conclusive in explaining the sorption behaviour of the above metal ions on the studied anion exchanger, because of the non-correlation between the dominant species in solution and the dominant species on the resin column.

Metal ions, for example Cr(III), Sn(IV), V(V) and Mo(VI), showed pronounced sorption on the anion exchanger compared to the cation exchanger (no sorption). Again, the complexes $[Cr_2(SO_4)_3.nH_2O]$ for the metal ion Cr(III) [14], $Sn(SO_4)_2$ for the metal ion Sn(IV) [15], $[VO_2(SO_4)_2]^{3-}$ for the metal ion V(V) [16], and $[Mo_2O(SO_4)_2.nH_2O]$ or $[MoO_2(SO_4)]$ for the metal ion Mo(VI) [17] are regarded as the dominant complexes, as explained in Chapter 4. These complexes are strongly associated with anions that are involved in the sorption of the respective metal ions with the anion exchanger. Again, varying sorption could be attributed to a set of complex factors such as the ionic strength and hydration energies of the metal complexes (metal-oxalate or the metal-sulphate) and complex charge. Lanthanides [Ce(III), Pr(III), Tb(III) and Yb(III)] were problematic in maintaining stable oxalate complexes, as mentioned in Chapter 4. Only Ce(IV), Ce(III) and Yb(III) in minimal amounts (0.1 mmole) remained in solution during the equilibration studies. Pr(III) and Tb(III) formed oxalate precipitates [$Pr_2(oxalate)_3$ and $Tb_2(oxalate)_3$ respectively] during the equilibration studies [18].

Table 5.1 and Table 5.2 also show that a variety of elemental separations is possible. In both oxalate concentrations, the relatively more strongly sorbed metal ions Mo(VI), Se(IV), Sn(IV), Te(IV) and V(V) could easily be separated from all the other studied metal ions in 2.00 M sulphuric acid, with the exception of Nb(V), Pr(III), Ta(V), Tb(III), W(VI) and Zr(IV). The metal ions [As(V), Mn(II), Ni(II) and Sb(V)] that showed absolutely no sorption in any of the

oxalic acid – sulphuric acid combinations, could easily be separated from the other studied metal ions in the lower sulphuric acid range (0.005 M – 0.10 M). Various other separations are possible under a variety of conditions, provided the separation factor between the two metal ions to be separated, is large enough.

An important feature of the oxalic acid - sulphuric acid system on an anion exchanger was the enhanced sorption of Sn(IV) compared to its sorption in the oxalic acid - nitric acid system [2]. In the oxalic acid - sulphuric acid system, the distribution coefficients of the metal ions varied from 8060 to 120 across the sulphuric acid range (0.005 M – 2.00 M) in 0.05 M oxalic acid, whereas in the oxalic acid - nitric acid system, the distribution coefficients varied from 60 to 21 across the nitric acid range (0.01 M - 0.50 M) in 0.05 M oxalic acid. When the nitric acid concentration was extended from 1.00 M to 4.00 M, precipitation occurred [2]. Another feature of the oxalic acid - sulphuric acid system was the enhanced sorption of Zn(II) and Co(II) compared to both the oxalic acid - hydrochloric acid and the oxalic acid - nitric acid [2]. The distribution coefficients varied between 790 and 160 for Zn(II) and between 568 and 88 for Co(II) across the sulphuric acid range (0.005 M – 0.10 M) in 0.05 M oxalic acid, whereas the distribution coefficients for both metal ions were <30 in both systems (0.01 M – 4.00 M hydrochloric acid / 0.05 M oxalic acid and 0.01 M – 4.00 M nitric acid / 0.05 M oxalic acid). The difference in sorption of the above could again be attributed to the double negatively charged sulphate anion compared to the singly charged nitrate and chloride anions.

5.3 RESULTS OF ELUTION CURVES

The distribution coefficients in Tables 5.1 and 5.2 indicated numerous possibilities for separations. Some were selected for further investigation and a few of these were selected for typical multi-element elution curves using synthetic mixtures to demonstrate the versatility of the system. A series of 10 ml and 13 ml resin columns was prepared as described in Chapter 3.

5.3.1 Elution Curve of As(V)-Zr(IV)

A two component separation was possible in the 0.05 M oxalic acid – 0.005 M sulphuric acid mixture for As(V) [$K_d < 0.5$] and Zr(IV) [$K_d > 10^4$], because of a high separation factor of ~10^5. A 10 ml resin column was equilibrated with 50 ml of 0.05 M oxalic acid – 0.005 M sulphuric acid. A solution containing 100 mg As(V) and 10 mg Zr(IV) in 50 ml of 0.05 M oxalic acid – 0.005 M sulphuric acid, was prepared and passed through the resin column. The elements were washed onto the resin with small portions of the solution of the same composition, and the As(V) was eluted with a total volume of 350 ml of solution (including washings). Zr(IV) was then eluted with 2.00 M nitric acid (100 ml). The flow rate was 4.0 ± 0.4 ml/min throughout, and fractions (20 ml in volume) were collected from the beginning of the sorption step. The fractions were treated and analysed as described above. The experimental curve is shown in Figure 5.1 and, as illustrated, complete separation was possible between As(V) and Zr(IV), with only trace amounts of As(V) [20 μg] detected in the Zr(IV) eluate. No breakthrough of Zr(IV) was apparent in the sorption and eluting steps.

5.3.2 Elution Curve of Co(II)-Fe(III)

A two component separation was possible in the 0.05 M oxalic acid – 0.25 M sulphuric acid mixture for Co(II) [K_d = 10.1] and Fe(III) [K_d = 141], because of a separation factor of 15. A 10 ml resin column was equilibrated with 50 ml of 0.05 M oxalic acid – 0.25 M sulphuric acid. A solution containing 100 mg Co(II) and 10 mg Fe(III) in 50 ml of 0.05 M oxalic acid – 0.25 M sulphuric acid, was prepared and passed through the resin column. The elements were washed onto the resin with small portions of the solution of the same composition, and the Co(II) was eluted with a total volume of 350 ml of solution (including washings). Fe(III) was then eluted with 1.00 M nitric acid (100 ml). The flow rate was 4.0 ± 0.4 ml/min throughout, and fractions (20 ml in volume) were collected from the beginning of the sorption step. The fractions were treated and analysed as described above. The experimental curve is shown in Figure 5.2 and, as illustrated, complete separation was possible between Co(II) and Fe(III), with only trace amounts of Co(II) [25 μg] detected in the Fe(III) eluate. No breakthrough of Fe(III) was apparent in the sorption and eluting steps.

5.3.3 Elution Curve of Ni(II)-As(V)-Se(IV)

A three component separation was possible in the 0.05 M oxalic acid – 1.00 M sulphuric acid mixture for Ni(II) [$K_d < 0.5$], As(V) [$K_d < 0.5$] and Se(IV)[K_d = 1010], because of a separation factor of ~2000 for both Ni(II)-Se(IV) and As(V)-Se(IV). A 10 ml resin column was equilibrated with 50 ml of 0.05 M oxalic acid – 1.00 M sulphuric acid. A solution containing 100 mg Ni(II), 100 mg As(V) and 10 mg Se(IV) in 50 ml of 0.05M oxalic acid – 1.00 M sulphuric acid, was prepared and passed through the resin column. The elements were washed

onto the resin with small portions of the solution of the same composition, and the Ni(II) and As(V) were eluted with a total volume of 350 ml of solution (including washings). Se(IV) was then eluted with 2.00 M nitric acid (100 ml). The flow rate was 4.0 ± 0.4 ml/min. throughout, and fractions (20 ml in volume) were collected from the beginning of the sorption step. The fractions were treated and analysed as described above. The experimental curve is shown in Figure 5.3 and, as illustrated, complete separation was possible between Ni(II)/As(V) and Se(IV), with only trace amounts of Ni(II) [20 μg] and As(V) [25 μg] detected in the Se(IV) eluate. No breakthrough of Se(IV) was apparent in the sorption and eluting steps.

5.3.4 Elution Curve of Ni(II)-Co(II)

A two component separation was possible in the 0.25 M oxalic acid – 0.005 M sulphuric acid mixture for Ni(II) [$K_d < 0.5$] and Co(II) [$K_d < 829$], because of a separation factor of ~2000. A 10 ml resin column was equilibrated with 50 ml of 0.25 M oxalic acid – 0.005 M sulphuric acid. A solution containing 1 g Ni(II) and 10 mg Co(II) in 50 ml of 0.25 M oxalic acid – 0.005 M sulphuric acid, was prepared and passed through the resin column. The elements were washed onto the resin with small portions of the solution of the same composition, and the Ni(II) was eluted with a total volume of 350 ml of solution (including washings). Co(II) was then eluted with 1.00 M nitric acid (100 ml). The flow rate was 4.0 ± 0.4 ml/min throughout, and fractions (20 ml in volume) were collected from the beginning of the sorption step. The fractions were treated and analysed as described above. The experimental curve is shown in Figure 5.4 and, as illustrated, complete separation was possible between Ni(II) and Co(II), with only trace amounts of Ni(II) [15 μg] detected in the Co(II) eluate. No breakthrough of Co(II) was apparent in the sorption and eluting steps.

5.3.5 Elution Curve of Ni(II)-Fe(III)

A two component separation was possible in the 0.25 M oxalic acid – 0.05 M sulphuric acid mixture for Ni(II) [$K_d < 0.5$] and Fe(II) [$K_d = 3160$], because of a separation factor of ~6000. A 10 ml resin column was equilibrated with 50 ml of 0.25 M oxalic acid – 0.05 M sulphuric acid. A solution containing 1 g Ni(II) and 10 mg Fe(II) in 50 ml of 0.25 M oxalic acid – 0.05 M sulphuric acid, was prepared and passed through the resin column. The elements were washed onto the resin with small portions of the solution of the same composition, and the Ni(II) was eluted with a total volume of 350 ml of solution (including washings). Fe(II) was then eluted with 1.00 M nitric acid (100 ml). The flow rate was 4.0 ± 0.4 ml/min throughout, and fractions (20 ml in volume) were collected from the beginning of the sorption step. The fractions were treated and analysed as described above. The experimental curve is shown in Figure 5.5 and, as illustrated, complete separation was possible between Ni(II) and Fe(III), with only trace amounts of Ni(II) [10 μg] detected in the Fe(III) eluate. No breakthrough of Fe(III) was apparent in the sorption and eluting steps.

5.3.6 Elution Curve of Al(III)-Zn(II)-Ge(IV)

A three component separation is possible in the 0.25 M oxalic acid – 1.00 M sulphuric acid mixture for Al(III) [$K_d = 8.2$], Zn(II) [$K_d = 15.3$] and Ge(IV) [$K_d = 175$], because of a separation factor of ~21 and ~11 for Al(III)-Ge(IV) and Zn(II)-Ge(IV) respectively. A 10 ml resin column was equilibrated with 50 ml of 0.25 M oxalic acid – 1.00 M sulphuric acid. A solution containing 100 mg Al(III), 100 mg Zn(II) and 10 mg Ge(IV) in 50 ml of 0.25 M oxalic acid – 1.00 M sulphuric acid, was prepared and passed through the resin column. The elements

were washed onto the resin with small portions of the solution of the same composition, and the Al(III) and Zn(II) were eluted with a total volume of 350 ml of solution (including washings). Ge(IV) was then eluted with 1.00 M nitric acid (100 ml). The flow rate was 4.0 ± 0.4 ml/min throughout, and fractions (20 ml in volume) were collected from the beginning of the sorption step. The fractions were treated and analysed as described above. The experimental curve is shown in Figure 5.6 and, as illustrated, complete separation was possible between Al(III)/Zn(II) and Ge(IV), with only trace amounts of Al(III) [15 μg] and Zn(II) [10 μg] detected in the Ge(IV) eluate. No breakthrough of Ge(IV) was apparent in the sorption and eluting steps.

5.3.7 Elution Curve of As(V)-Cu(II)-Ge(IV)

A three component separation is possible in the 0.25 M oxalic acid – 1.00 M sulphuric acid mixture for As(V) [$K_d < 0.5$], Cu(II) [$K_d = 5.1$] and Ge(IV) [$K_d = 175$], because of a separation factor of ~350 and ~25 for As(V)-Ge(IV) and Cu(II)-Ge(IV) respectively. A 10 ml resin column was equilibrated with 50 ml of 0.25 M oxalic acid – 1.00 M sulphuric acid. A solution containing 100 mg As(V), 100 mg Cu(II) and 10 mg Ge(IV) in 50 ml of 0.25 M oxalic acid – 1.00 M sulphuric acid, was prepared and passed through the resin column. The elements were washed onto the resin with small portions of the solution of the same composition, and the As(V) and Cu(II) were eluted with a total volume of 350 ml of solution (including washings). Ge(IV) was then eluted with 1.00 M nitric acid (100 ml). The flow rate was 4.0 ± 0.4 ml/min throughout, and fractions (20 ml in volume) were collected from the beginning of the sorption step. The fractions were treated and analysed as described above. The experimental curve is shown in Figure 5.7 and, as illustrated, complete separation was possible between As(V)/Cu(II)

and Ge(IV), with only trace amounts of As(V) [10 μg] and Cu(II) [10 μg] detected in the Ge(IV) eluate. No breakthrough of Ge(IV) was apparent in the sorption and eluting steps.

5.3.8 Elution Curve of Ga(III)-Ge(IV) in 0.05 M oxalic acid – 0.25 M sulphuric acid

A two component separation was investigated in the 0.05 M oxalic acid – 0.25 M sulphuric acid mixture for Ga(III) [K_d = 30.1] and Ge(IV) [K_d = 425], with a separation factor of ~14. A 13 ml resin column was equilibrated with 50 ml of 0.05 M oxalic acid – 0.25 M sulphuric acid. A solution containing 5 g Ga(III) and 10 mg Ge(IV) in 50 ml of 0.05 M oxalic acid – 0.25 M sulphuric acid, was prepared and passed through the resin column. The elements were washed onto the resin with small portions of the solution of the same composition, and the Ga(III) was eluted with a total volume of 450 ml of solution (including washings). Ge(IV) was then eluted with 1.00 M nitric acid (100 ml). The flow rate was 4.0 ± 0.4 ml/min throughout, and fractions (20 ml in volume) were collected from the beginning of the sorption step. The fractions were treated and analysed as described above. The experimental curve is shown in Figure 5.8. No breakthrough of Ge(IV) was apparent in the sorption and eluting steps. However, relatively high trace amounts of Ga(III) [190 μg] were detected in the Ge(IV) eluate. This was due to tailing of Ga(III) [relatively high K_d] in the eluting step, which did not improve even when the volume of the eluting step was increased. Further work was undertaken to determine the optimum conditions for the elemental separation of Ga(III) from Ge(IV), using the same concentrations for both Ga (5 g) and Ge (10 mg), but varying the oxalic acid – sulphuric acid concentrations. This is described in sections 5.3.9 to 5.3.13, and the elution curves are shown in Figures 5.3.9 to 5.3.13.

5.3.9 Elution Curve of Ga(III)-Ge(IV) in 0.05 M oxalic acid – 0.50 M sulphuric acid

A two component separation was investigated in the 0.05 M oxalic acid – 0.50 M sulphuric acid mixture for Ga(III) [K_d = 6.2] and Ge(IV) [K_d = 120], with a separation factor of ~20. A 13 ml resin column was equilibrated with 50 ml of 0.05 M oxalic acid – 0.50 M sulphuric acid. A solution containing 5 g Ga(III) and 10 mg Ge(IV) in 50 ml of 0.05 M oxalic acid – 0.50 M sulphuric acid, was prepared and passed through the resin column. The elements were washed onto the resin with small portions of the solution of the same composition, and the Ga(III) was eluted with a total volume of 450 ml of solution (including washings). Ge(IV) was then eluted with 1.00 M nitric acid (100 ml). The flow rate was 4.0 ± 0.4 ml/min throughout, and fractions (20 ml in volume) were collected from the beginning of the sorption step. The fractions were treated and analysed as described above. The experimental curve is shown in Figure 5.9. Breakthrough of Ge(IV) was apparent in the sorption and eluting steps, and trace amounts of Ga(III) [105 µg] were detected in the Ge(IV) eluate.

5.3.10 Elution Curve of Ga(III)-Ge(IV) in 0.05 M oxalic acid – 1.00 M sulphuric acid

A two component separation was investigated in the 0.05 M oxalic acid – 1.00 M sulphuric acid mixture for Ga(III) [K_d < 0.5] and Ge(IV) [K_d = 34.1], with a separation factor of ~70. A 13 ml resin column was equilibrated with 50 ml of 0.05 M oxalic acid – 1.00 M sulphuric acid. A solution containing 5 g Ga(III) and 10 mg Ge(IV) in 50 ml of 0.05 M oxalic acid – 1.00 M sulphuric acid, was prepared and passed through the resin column. The elements were washed onto the resin with small portions of the solution of the same composition, and the Ga(III) was eluted with a total volume of 450 ml of solution (including washings). Ge(IV) was then eluted

with 1.00 M nitric acid (100 ml). The flow rate was 4.0 ± 0.4 ml/min throughout, and fractions (20 ml in volume) were collected from the beginning of the sorption step. The fractions were treated and analysed as described above. The experimental curve is shown in Figure 5.10. Breakthrough of Ge(IV) in the sorption and eluting steps was relatively more pronounced compared to the previous elution curve, but the trace amount of Ga(III) [85 μg] detected in the Ge(IV) was at an acceptable level.

5.3.11 Elution Curve of Ga(III)-Ge(IV) in 0.25 M oxalic acid – 0.50 M sulphuric acid

A two component separation was investigated in the 0.25 M oxalic acid – 0.50 M sulphuric acid mixture for Ga(III) [K_d = 42.1] and Ge(IV) [K_d = 520], with a separation factor of ~12. A 13 ml resin column was equilibrated with 50 ml of 0.25 M oxalic acid – 0.50 M sulphuric acid. A solution containing 5 g Ga(III) and 10 mg Ge(IV) in 50 ml of 0.25 M oxalic acid – 0.50 M sulphuric acid, was prepared and passed through the resin column. The elements were washed onto the resin with small portions of the solution of the same composition, and the Ga(III) was eluted with a total volume of 450 ml of solution (including washings). Ge(IV) was then eluted with 1.00 M nitric acid (100 ml). The flow rate was 4.0 ± 0.4 ml/min throughout, and fractions (20 ml in volume) were collected from the beginning of the sorption step. The fractions were treated and analysed as described above. The experimental curve is shown in Figure 5.11. Again, no breakthrough of Ge(IV) in the sorption and eluting steps was evident, but the amount of Ga(III) [195 μg] detected in the Ge(IV) was significantly higher due to excessive tailing of Ga(III).

5.3.12 Elution Curve of Ga(III)-Ge(IV) in 0.25 M oxalic acid – 1.00 M sulphuric acid

A two component separation was investigated in the 0.25 M oxalic acid – 1.00 M sulphuric acid mixture for Ga(III) [K_d = 10.1] and Ge(IV) [K_d = 175], with a separation factor of ~17. A 13 ml resin column was equilibrated with 50 ml of 0.25 M oxalic acid – 1.00 M sulphuric acid. A solution containing 5 g Ga(III) and 10 mg Ge(IV) in 50 ml of 0.25 M oxalic acid – 1.00 M sulphuric acid was prepared and passed through the resin column. The elements were washed onto the resin with small portions of the solution of the same composition, and the Ga(III) was eluted with a total volume of 450 ml of solution (including washings). Ge(IV) was then eluted with 1.00 M nitric acid (100 ml). The flow rate was 4.0 ± 0.4 ml/min throughout, and fractions (20 ml in volume) were collected from the beginning of the sorption step. The fractions were treated and analysed as described above. The experimental curve is shown in Figure 5.12. No breakthrough of Ge(IV) in the sorption and eluting steps was evident, and the amount of Ga(III) [75 μg] detected in the Ge(IV) was at an acceptable level.

5.3.13 Elution Curve of Ga(III)-Ge(IV) in 0.25 M oxalic acid – 1.00 M sulphuric acid

In this elution curve, the optimum resin column size was investigated. The same conditions as described in section 5.3.12 were used, but in this case a 10 ml resin column was used. The experimental curve is shown in Figure 5.13. The amount of Ga(III) [35 μg] detected in the Ge(IV) was found to be the best (lowest), for all the elemental separations of Ga(III) from Ge(IV) studied. However, breakthrough of Ge(IV) in the sorption and eluting steps was evident. This would not be ideal for radioisotopic separations. Elution curves 5.3.8 to 5.3.13 showed variable behaviour. In determining the optimum conditions for the elemental

separation of Ga(III) from Ge(IV), the separation factor ($\alpha^{Ge}_{Ga} = D_{Ge}/D_{Ga}$) for Ge(IV) and Ga(III) at varying oxalic acid – sulphuric acid concentrations had to be considered, as shown in Table 5.3.

Table 5.3 Equilibrium distribution coefficients and separation factor for Ge(IV) and Ga(III) in varying oxalic acid – sulphuric acid concentration.

H_2SO_4(M)	0.005	0.05	0.10	0.25	0.50	1.00	1.50	2.00
0.05 M oxalic acid								
Ge(IV)	7430	2710	1150	425	120	34.1	5.4	<0.5
Ga(III)	3500	1000	140	30.1	6.2	<0.5	<0.5	<0.5
α^{Ge}_{Ga}	2.1	2.7	8.2	14.1	19.4	68.2	10.8	1.0
0.25 M oxalic acid								
Ge(IV)	$>10^4$	6410	3035	1215	520	175	104	45
Ga(III)	9700	6100	1150	140	42.1	10.1	3.5	<0.5
α^{Ge}_{Ga}	1.3	1.1	2.6	8.7	12.4	17.3	29.7	90

The separation factor is optimal in the 1.00 M sulphuric acid containing 0.05 M oxalic acid or the 2.00 M sulphuric acid containing 0.25 M oxalic acid. However, at these sulphuric acid concentrations, the distribution coefficients are relatively low and separation of Ge from Ga is not feasible. From observation of the distribution coefficients, the best option seems to be to use either 0.5 M sulphuric acid containing 0.05 M oxalic acid or 1.00 M sulphuric acid containing 0.25 M oxalic acid as the sorption medium and eluent for Ga. The latter mixture was chosen as the most suitable sorption medium and eluent for Ga, because the distribution coefficient for Ge is higher. This was experimentally confirmed by elution curves 5.3.8 to 5.3.13 with 5 g Ga and 10 mg Ge, which are summarised in Table 5.4.

A summary of the other elution curves is also shown in Table 5. 4. As indicated in the Table, the elution curves 5.3.1 to 5.3.7 behaved similarly: no significant tailing was evident during any of the eluting steps; there was no breakthrough of the primary element during the sorption and eluting steps; and low levels of contaminants were detected in the final product eluate. Although the separation factor was fairly low at times, an acceptable elemental separation was still possible and could easily be adapted for radiochemical separations, as will be shown in Chapter 6.

Table 5.4 Summary of results of various elution curves on the anion exchange resin (AG1-X8).

Elution curve number	Elution curve	% Breakthrough of metals in sorption step	% Breakthrough of metals in eluting step	Total contaminant in the retained metal eluate
1	As(V)-Zr(IV)	As(97.5%)-Zr(0%)	As(2.9%)-Zr(0%)	20 µg As(V)
2	Co(II)-Fe(III)	Co(94.9%)-Fe(0%)	Co(5.5%)-Fe(0%)	25 µg Co(II)
3	Ni(II)-As(V)-Se(IV)	Ni(97.2%)-As(97.9%)-Se(0%)	Ni(2.9%)-As(2.1%)-Se(0%)	20 µg Ni(II), 25 µg As(V)
4	Ni(II)-Co(II)	Ni(96.5%)-Co(0%)	Ni(3.4%)-Co(0%)	15 µg Ni(II)
5	Ni(II)-Fe(III)	Ni(97.2%)-Fe(0%)	Ni(2.9%)-Fe(0%)	10 µg Ni(II)
6	Al(III)-Zn(II)-Ge(IV)	Al(95.9%)-Zn(95.5%)-Ge(0%)	Al(4.4%)- Zn(4.7%)-Ge(0%)	15 µg Al(III), 10 µg Zn(II)
7	As(V)-Cu(II)-Ge(IV)	As(98.3)-Cu(97.1%)-Ge(0%)	As(1.9)-Cu(2.5%)-Ge(0%)	10 µg As(V), 10 µg Cu(II)
8	Ga(III)-Ge(IV)	Ga(93.1%)–Ge(0%)	Ga(6.7%)–Ge(0%)	190 µg Ga(III)
9	Ga(III)-Ge(IV)	Ga(96.2%)–Ge(1.5%)	Ga(3.9%)–Ge(0.01%)	105 µg Ga(III)
10	Ga(III)-Ge(IV)	Ga(98.4%)–Ge(5.9%)	Ga(1.9%)–Ge(0.9%)	85 µg Ga(III)
11	Ga(III)-Ge(IV)	Ga(92.3%)–Ge(0%)	Ga(7.9%)–Ge(0%)	195 µg Ga(III)
12	Ga(III)-Ge(IV)	Ga(95.1%)–Ge(0%)	Ga(2.7%)–Ge(0%)	75 µg Ga(III)
13	Ga(III)-Ge(IV)	Ga(97.1%)–Ge(0.9%)	Ga(2.7%)–Ge(0.01%)	35 µg Ga(III)

Figure 5.1 Elution curve for As(V)-Zr(IV) on a AG1-X8 resin column (10 ml) in 0.05 M oxalic acid – 0.005 M sulphuric acid. [sorption step and eluting step of As with 0.05 M oxalic acid – 0.005 M sulphuric acid (0 - 400 ml mark on the x-axis of the curve), Zr eluted with 2.0 M HNO_3 (400 - 500 ml mark on the x-axis of the curve)].

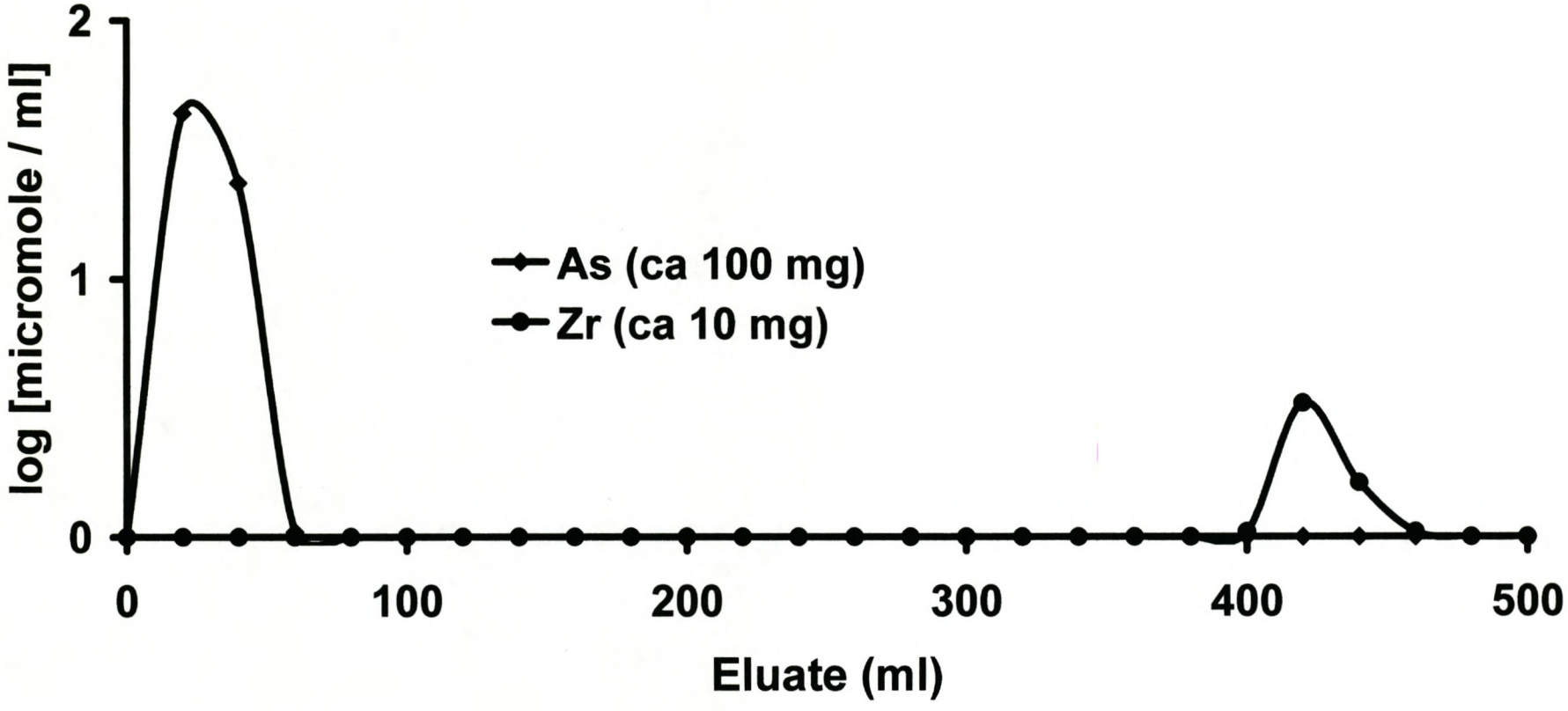

Figure 5.2 Elution curve for Co(II)-Fe(III) on a AG1-X8 resin column (10 ml) in 0.05 M oxalic acid – 0.25 M sulphuric acid. [sorption step and eluting step of Co with 0.05 M oxalic acid – 0.25 M sulphuric acid (0 - 400 ml mark on the x-axis of the curve), Fe eluted with 1.0 M HNO_3 (400 - 500 ml mark on the x-axis of the curve)].

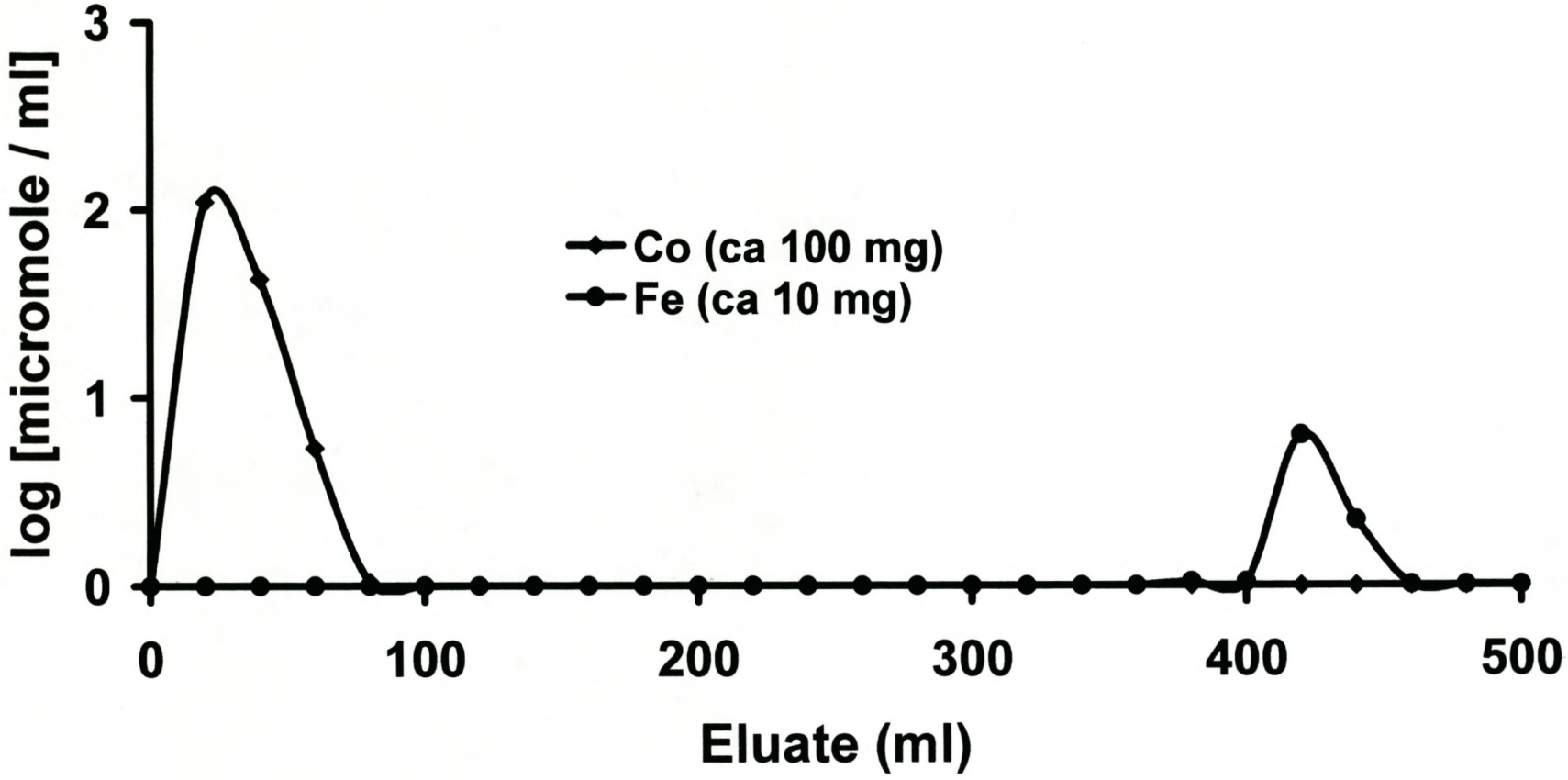

Figure 5.3 Elution curve for Ni(II)-As(V)-Se(IV) on a AG1-X8 resin column (10 ml) in 0.05 M oxalic acid–1.00 M sulphuric acid. [sorption step and eluting step of Ni and As with 0.05 M oxalic acid – 1.00 M sulphuric acid (0 - 400 ml mark on the x-axis of the curve), Se eluted with 2.0 M HNO_3 (400 - 500 ml mark on the x-axis of the curve)].

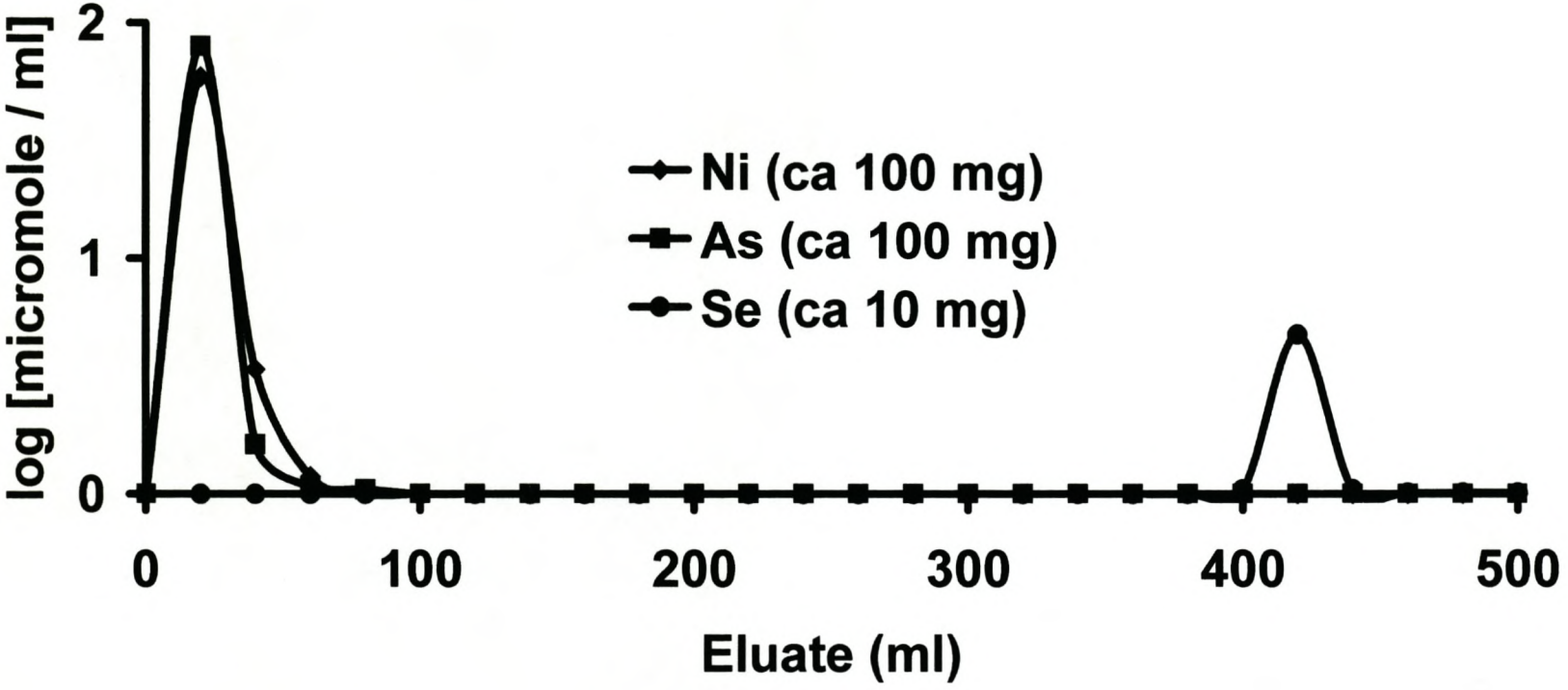

Figure 5.4 Elution curve for Ni(II)-Co(II) on a AG1-X8 resin column (10 ml) in 0.25 M oxalic acid – 0.005 M sulphuric acid. [sorption step and eluting step of Ni with 0.25 M oxalic acid – 0.005 M sulphuric acid (0 - 400 ml mark on the x-axis of the curve), Co eluted with 1.0 M HNO_3 (400 - 500 ml mark on the x-axis of the curve)].

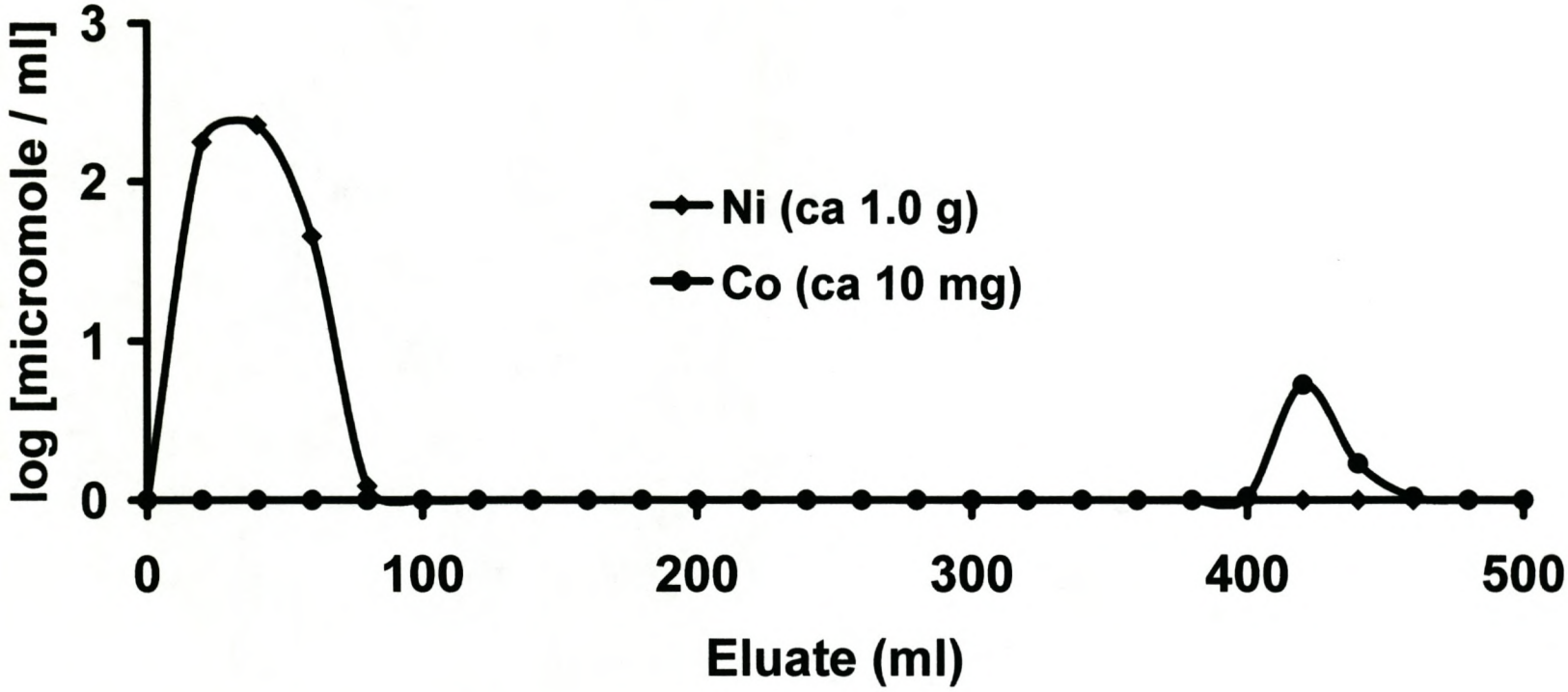

Figure 5.5 Elution curve for Ni(II)-Fe(III) on a AG1-X8 resin column (10 ml) in 0.25 M oxalic acid – 0.05 M sulphuric acid. [sorption step and eluting step of Ni with 0.25 M oxalic acid – 0.05 M sulphuric acid (0 - 400 ml mark on the x-axis of the curve), Fe eluted with 1.0 M HNO_3 (400 - 500 ml mark on the x-axis of the curve)].

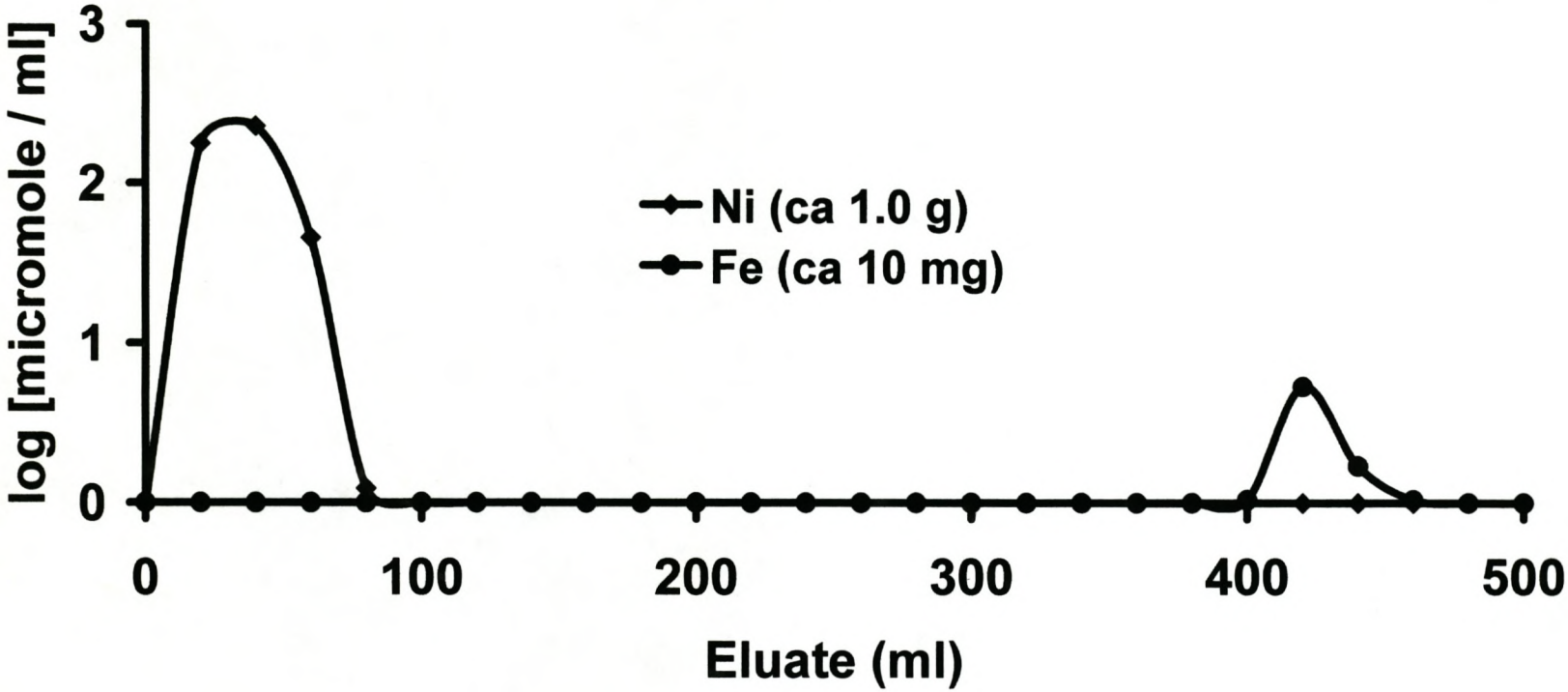

Figure 5.6 Elution curve for Al(III)-Zn(II)-Ge(IV) on a AG1-X8 resin column (10 ml) in 0.25 M oxalic acid–1.00 M sulphuric acid. [sorption step and eluting step of Al and Zn with 0.25 M oxalic acid – 1.00 M sulphuric acid (0 - 400 ml mark on the x-axis of the curve), Ge eluted with 1.0 M HNO_3 (400 - 500 ml mark on the x-axis of the curve)].

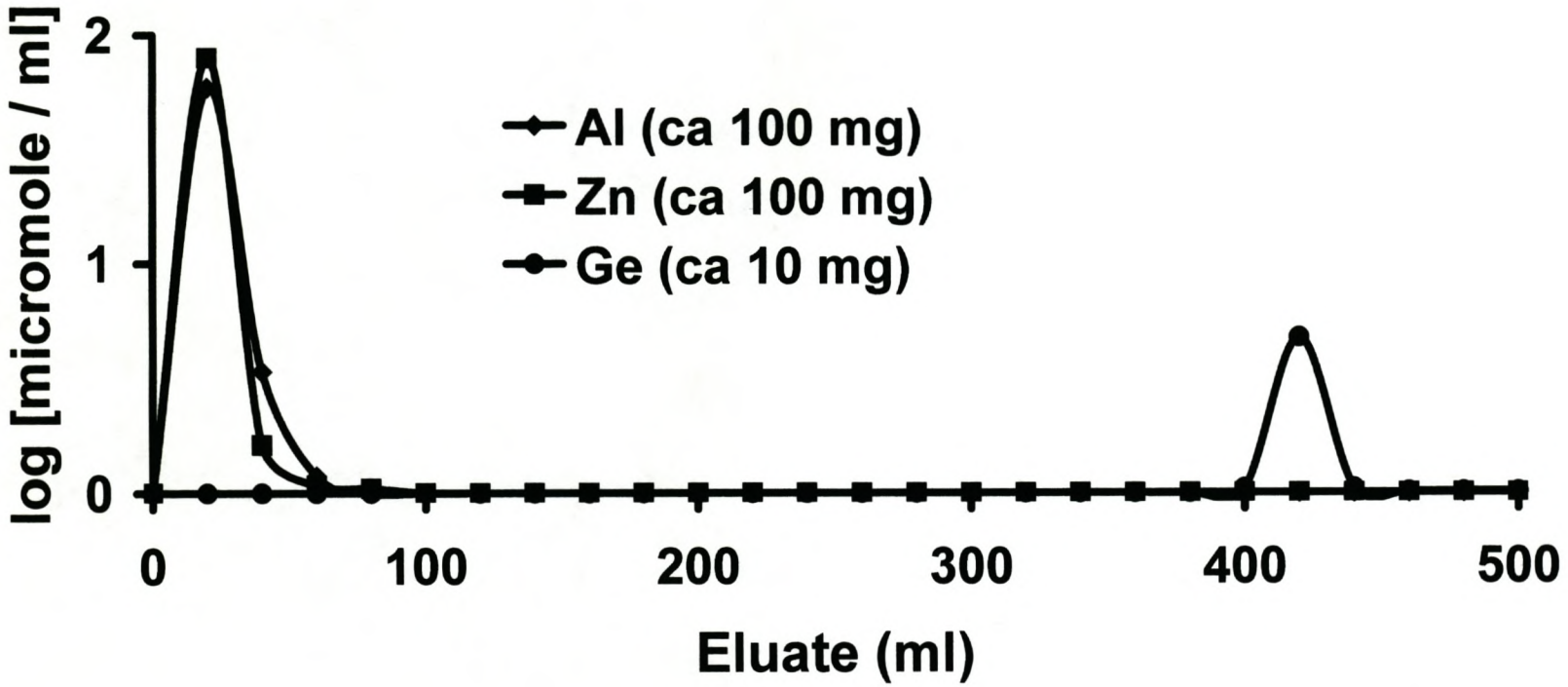

Figure 5.7 Elution curve for As(V)-Cu(II)-Ge(IV) on a AG1-X8 resin column (10 ml) in 0.25 M oxalic acid – 1.00 M sulphuric acid. [sorption step and eluting step of As and Cu with 0.25 M oxalic acid – 1.00 M sulphuric acid (0 - 400 ml mark on the x-axis of the curve), Ge eluted with 1.0 M HNO_3 (400 - 500 ml mark on the x-axis of the curve)].

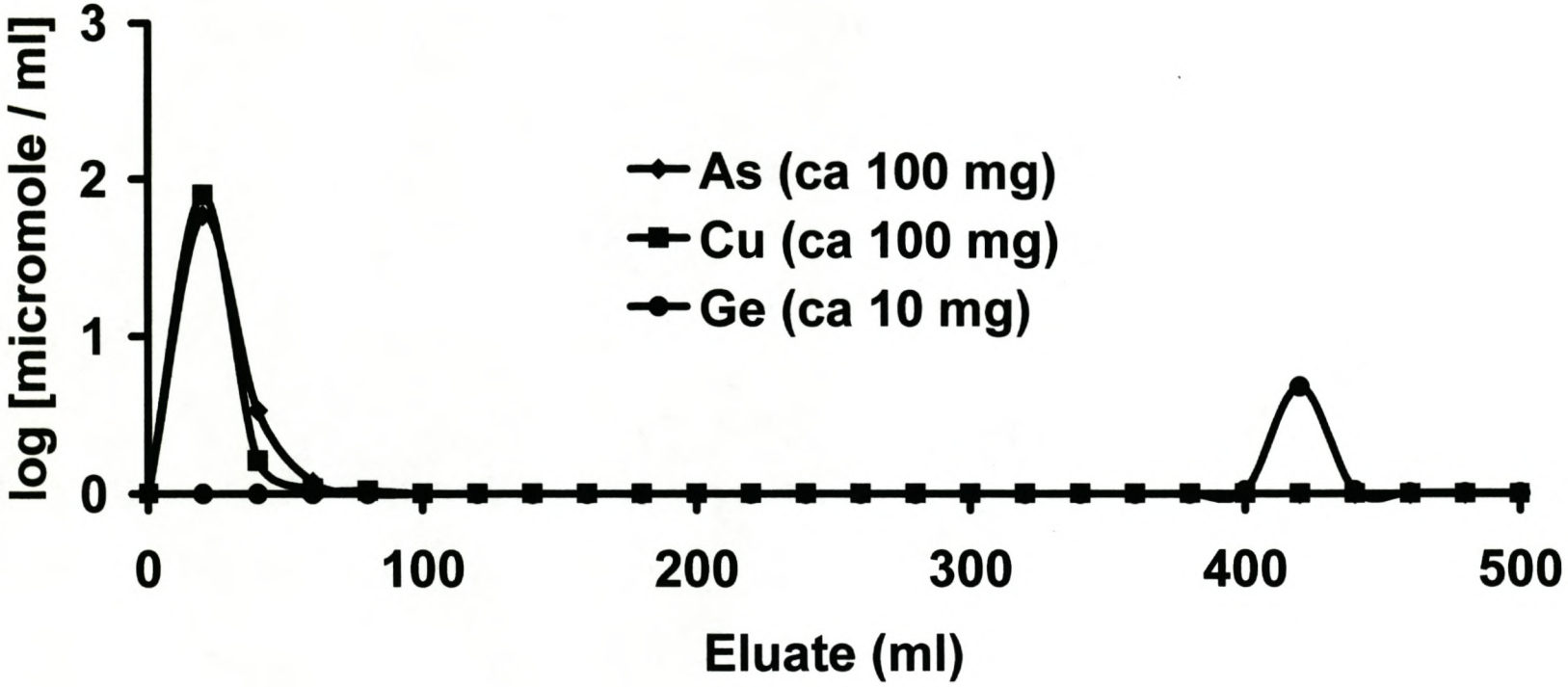

Figure 5.8 Elution curve for Ga(III)-Ge(IV) on a AG1-X8 resin column (13 ml) in 0.05 M oxalic acid – 0.25 M sulphuric acid. [sorption step and eluting step of Ga with 0.05 M oxalic acid – 0.25 M sulphuric acid (0 - 500 ml mark on the x-axis of the curve), Ge eluted with 1.0 M HNO_3 (500 - 600 ml mark on the x-axis of the curve)].

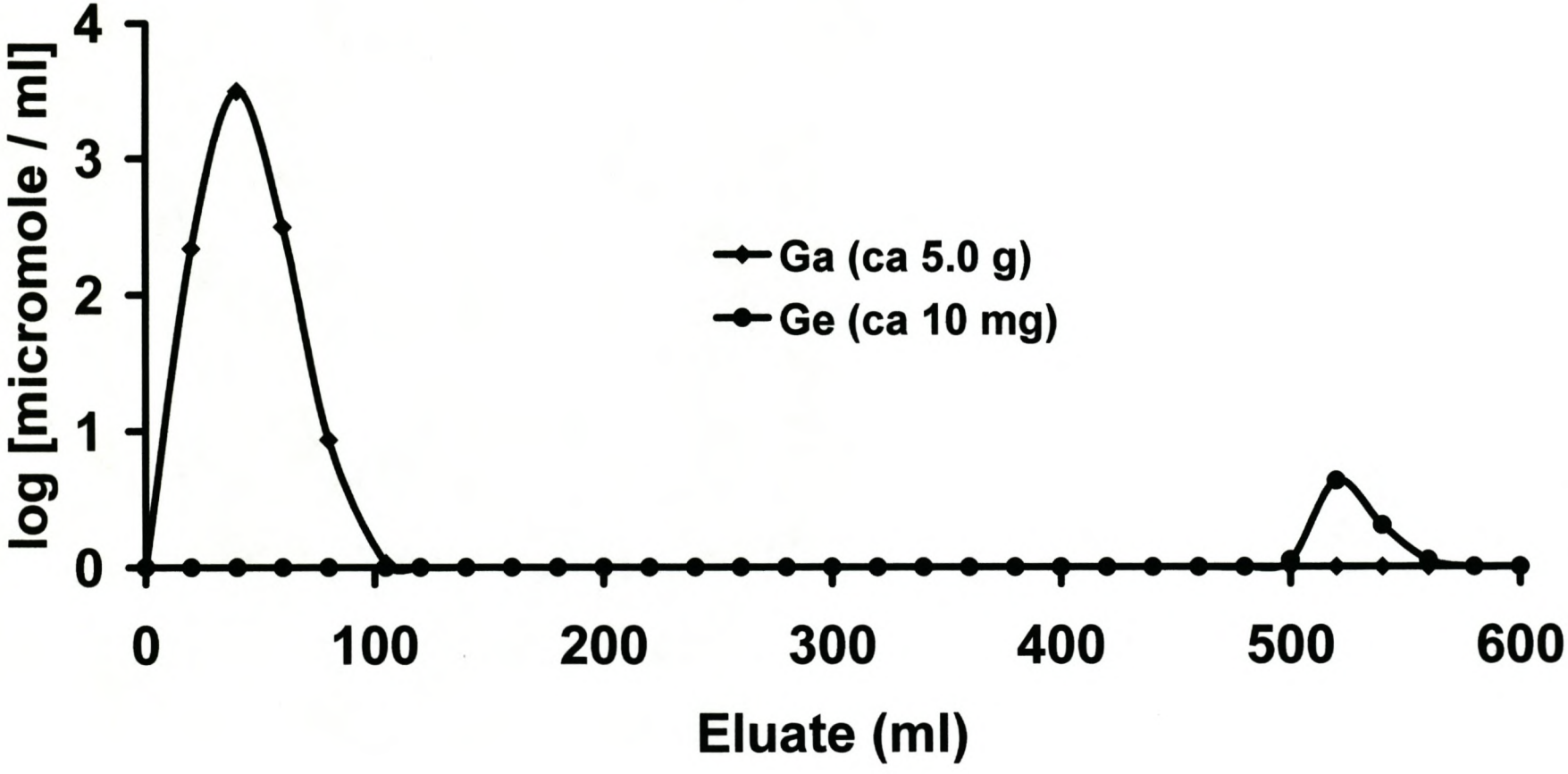

Figure 5.9 Elution curve for Ga(III)-Ge(IV) on a AG1-X8 resin column (13 ml) in 0.05 M oxalic acid – 0.50 M sulphuric acid. [sorption step and eluting step of Ga with 0.05 M oxalic acid – 0.50 M sulphuric acid (0 - 500 ml mark on the x-axis of the curve), Ge eluted with 1.0 M HNO_3 (500 - 600 ml mark on the x-axis of the curve)].

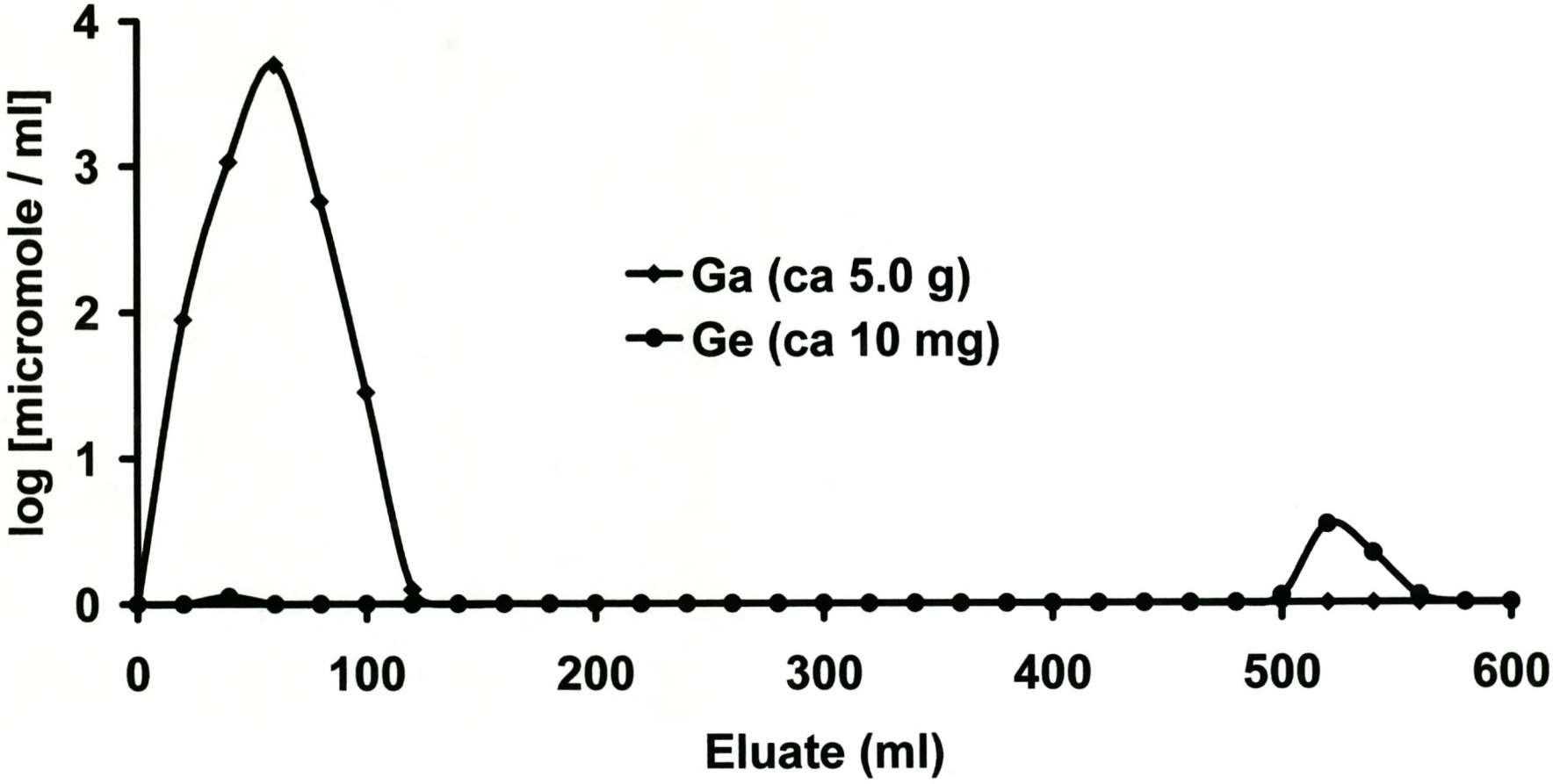

Figure 5.10 Elution curve for Ga(III)-Ge(IV) on a AG1-X8 resin column (13 ml) in 0.05 M oxalic acid – 1.00 M sulphuric acid. [sorption step and eluting step of Ga with 0.05 M oxalic acid – 1.00 M sulphuric acid (0 - 500 ml mark on the x-axis of the curve), Ge eluted with 1.0 M HNO_3 (500 - 600 ml mark on the x-axis of the curve)].

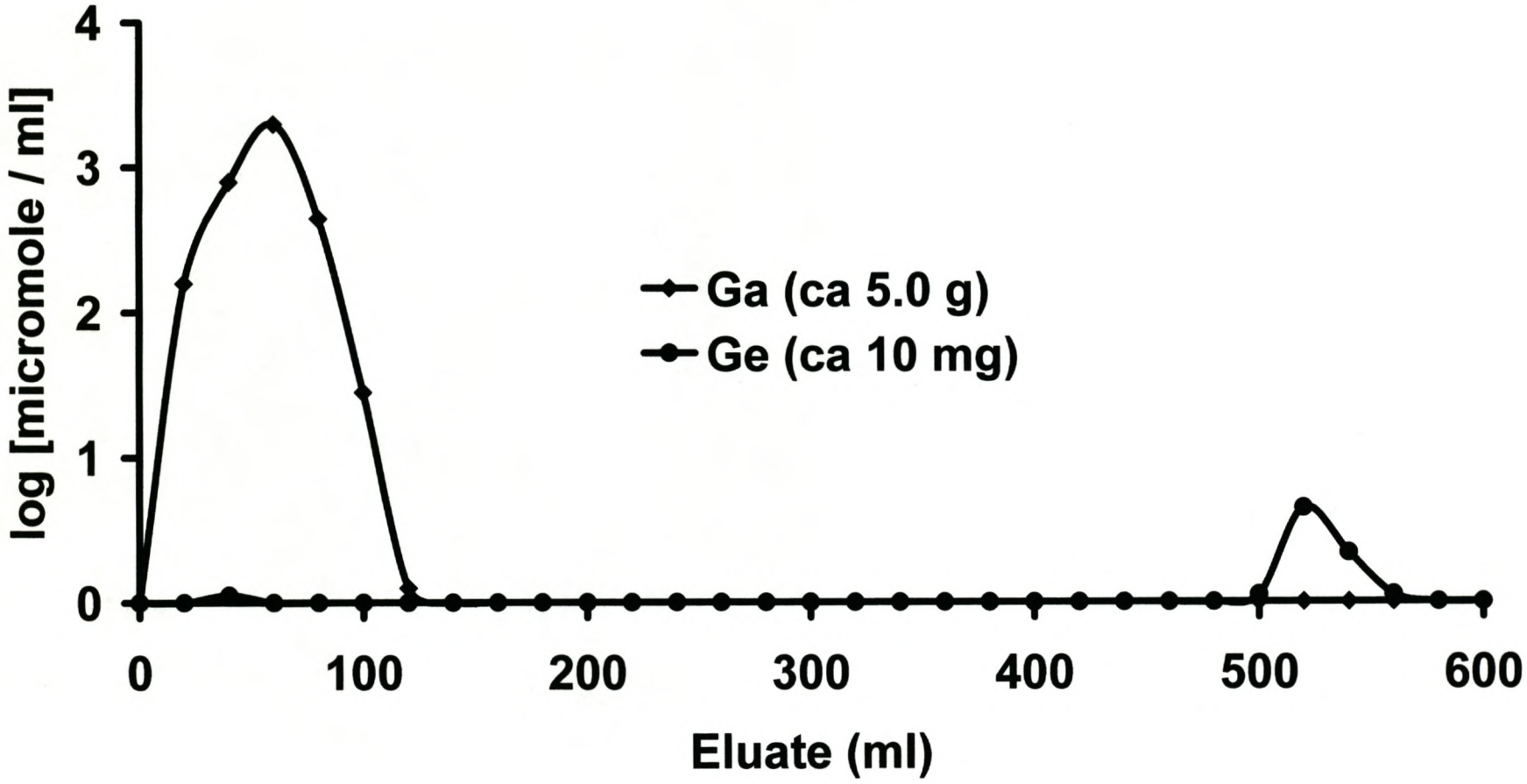

Figure 5.11 Elution curve for Ga(III)-Ge(IV) on a AG1-X8 resin column (13 ml) in 0.25 M oxalic acid – 0.50 M sulphuric acid. [sorption step and eluting step of Ga with 0.25 M oxalic acid – 0.50 M sulphuric acid (0 - 500 ml mark on the x-axis of the curve), Ge eluted with 1.0 M HNO_3 (500 - 600 ml mark on the x-axis of the curve)].

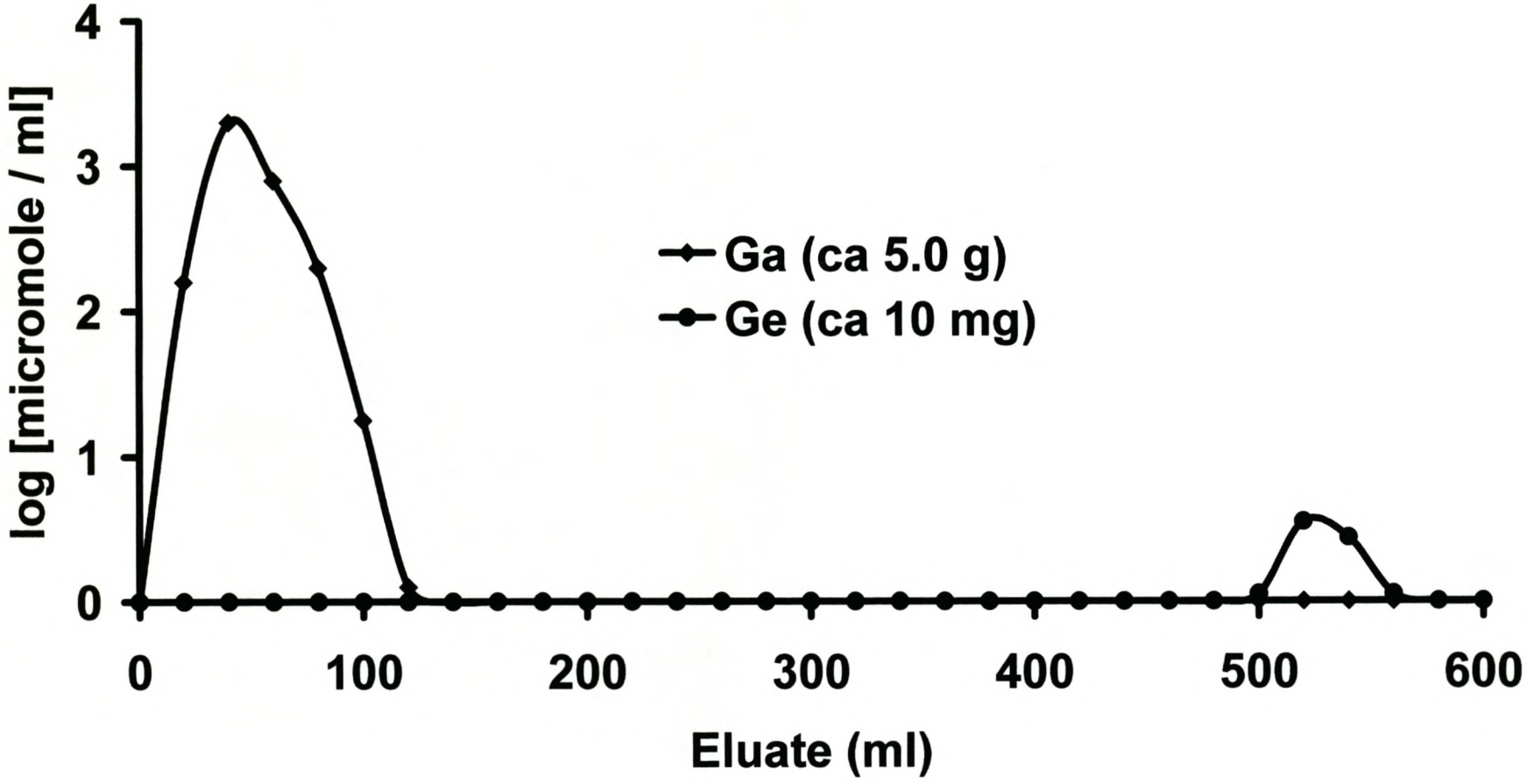

Figure 5.12 Elution curve for Ga(III)-Ge(IV) on a AG1-X8 resin column (13 ml) in 0.25 M oxalic acid – 1.00 M sulphuric acid. [sorption step and eluting step of Ga with 0.25 M oxalic acid – 1.00 M sulphuric acid (0 - 500 ml mark on the x-axis of the curve), Ge eluted with 1.0 M HNO_3 (500 - 600 ml mark on the x-axis of the curve)].

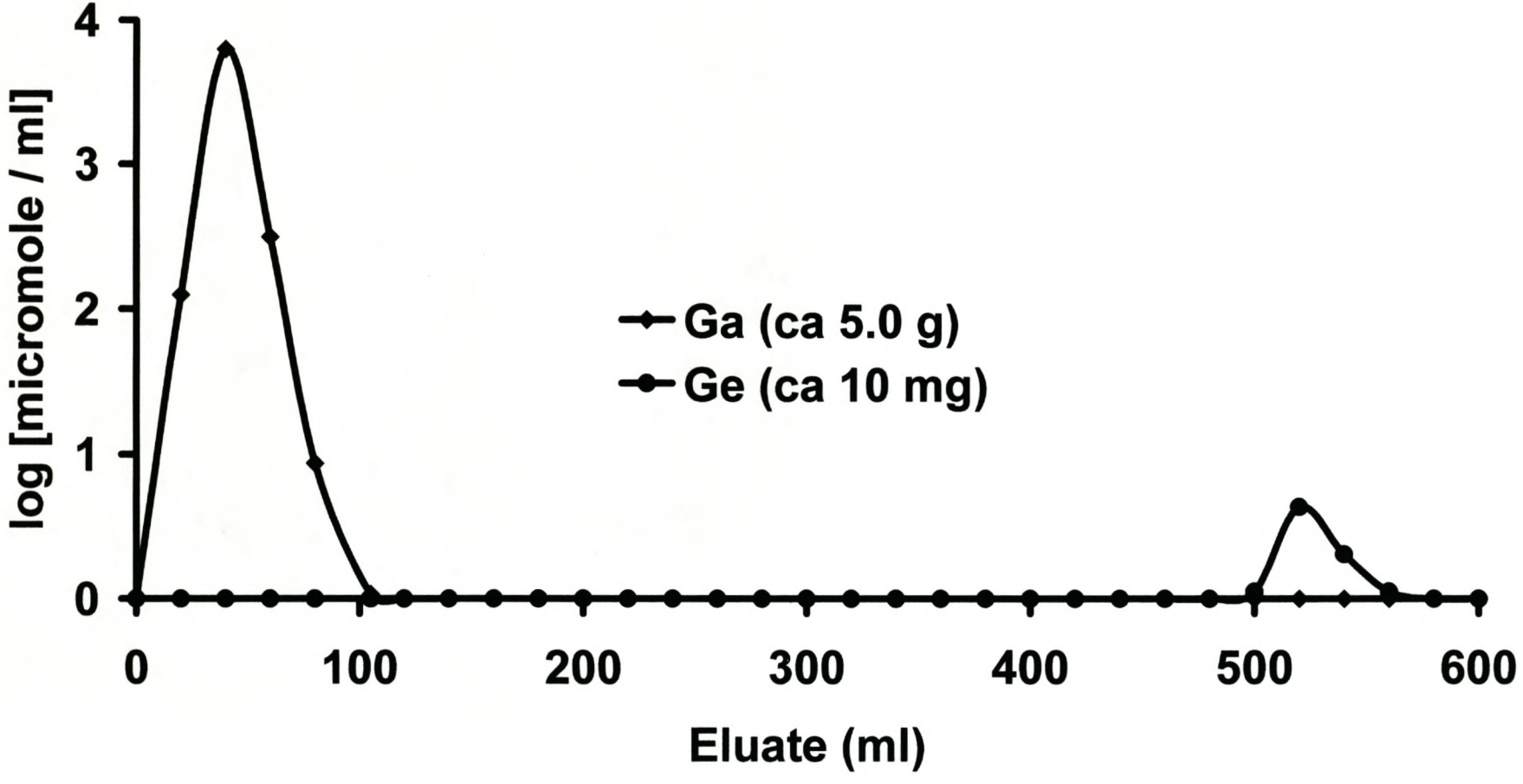

Figure 5.13 Elution curve for Ga(III)-Ge(IV) on a AG1-X8 resin column (10 ml) in 0.25 M oxalic acid – 1.00 M sulphuric acid. [sorption step and eluting step of Ga with 0.25 M oxalic acid – 1.00 M sulphuric acid (0 - 500 ml mark on the x-axis of the curve), Ge eluted with 1.0 M HNO_3 (500 - 600 ml mark on the x-axis of the curve)].

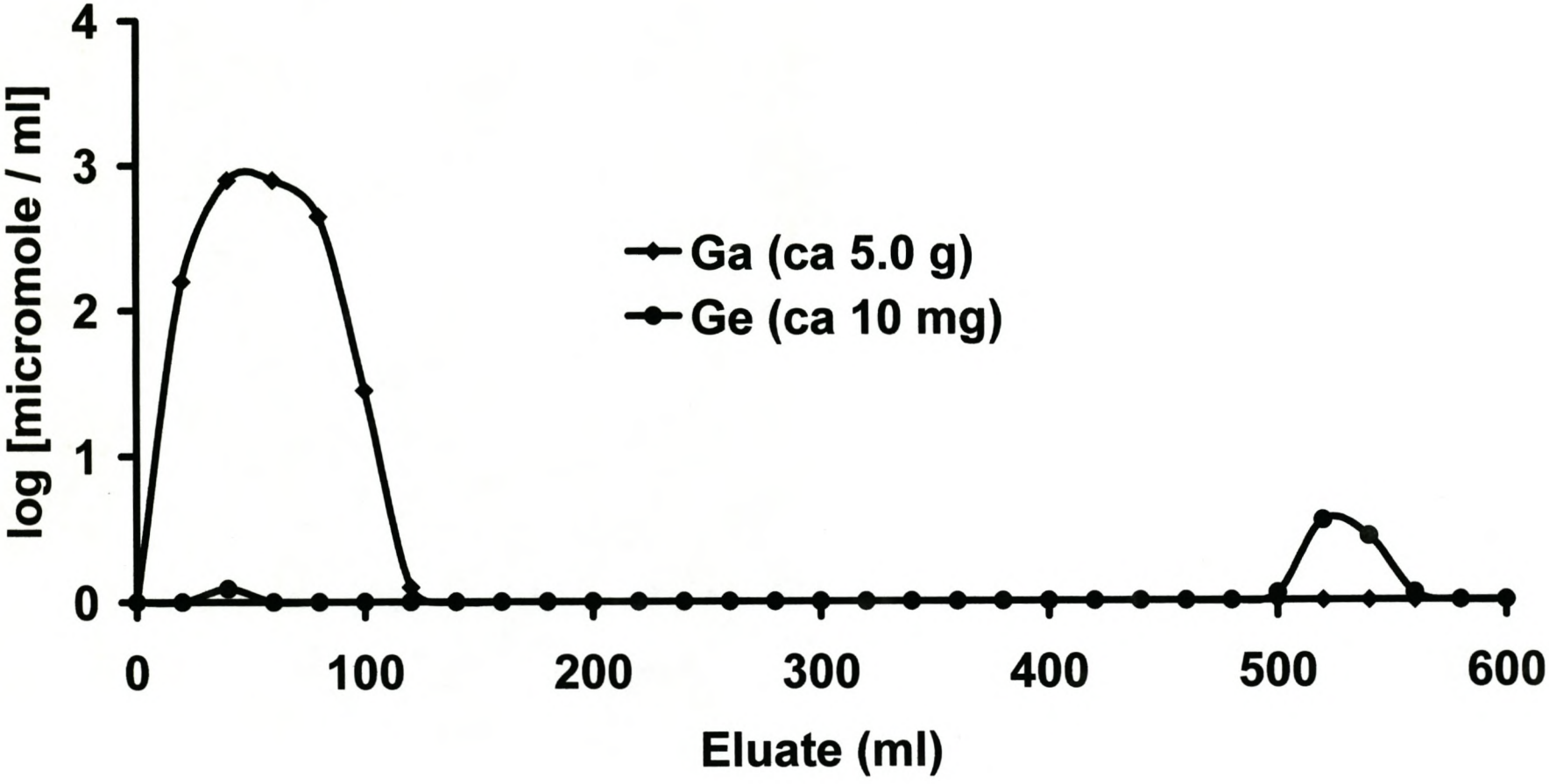

5.4 RESULTS OF QUANTITATIVE SEPARATION OF MIXTURES

A series of 13 ml AG1-X8 resin columns was prepared as described previously. Appropriate volumes of standard solutions of Ge(IV) [10 µg, 100 µg, 1000 µg] and one other element [Al(III), As(V), Co(II), Cu(II), Ga(III), In(III), La(III), Ni(II), Zn(II), Y(III) and Yb(III), ca 0.01 g, 0.1 g or 0.5 g] were accurately measured out in triplicate, mixed and adjusted to a volume of about 50 ml containing a 0.25 M oxalic acid – 1.00 M sulphuric acid mixture. Three equivalent aliquots of each solution were measured out and kept separately as standards for comparison with solutions obtained after separation, using similar dilutions or volumes for the final determination of the elements in the standards and separated solutions. The mixed solutions were passed through the equilibrated resin columns and washed onto the resin with small portions of 0.25 M oxalic acid – 1.00 M sulphuric acid mixture, 250 ml in total. When separating 0.5 g of Ga(III) from Ge(IV), a total volume of 400 ml of 0.25 M oxalic acid – 1.00 M sulphuric acid mixture was used. The Ge(IV) was eluted with 100 ml 1.00 M nitric acid. The different fractions were collected from the beginning of the sorption step, the excess acid was evaporated on a water bath, the residue was diluted with water to an appropriate volume, and the amounts of each element in all fractions were determined by the analytical techniques described previously. The results shown in Table 5.5 are a clear indication that separation of Ge(IV) from other metal ions [Al(III), As(V), Co(II), Cu(II), Ga(III), In(III), La(III), Ni(II), Zn(II), Y(III) and Yb(III)] can be conducted quantitatively without difficulty.

Table 5.5 Results of quantitative separation of mixtures on the anion exchange resin.

Other Element	Amount taken		Amount found[a]		Amount of other element found in Ge(IV) fraction, μg
	Ge(IV) [μg]	Other element [g]	Ge(IV) [μg]	Other element [g]	
Al(III)	100	0.5002	99.8 ± 0.5	0.5004 ± 0.0002	1.0–3.0
As(V)	100	0.5003	99.7 ± 0.4	0.5001 ± 0.0005	2.5–3.5
Co(II)	10	0.0101	9.6 ± 0.6	0.0099 ± 0.0003	0.5–0.7
Cu(II)	10	0.0103	9.8 ± 0.5	0.0101 ± 0.0003	0.6–0.9
Ga(III)	1000	0.5002	999.1 ± 0.9	0.5001 ± 0.0003	5.5–6.1
In(III)	1000	0.1002	1000.5 ± 0.3	0.0999 ± 0.0006	4.3–4.9
La(III)	100	0.1003	99.6 ± 0.5	0.0998 ± 0.0004	1.8–2.1
Ni(II)	10	0.1004	9.9 ± 0.5	0.0999 ± 0.0005	1.1–1.3
Y(III)	10	0.1004	9.9 ± 0.3	0.0999 ± 0.0004	1.6–1.9
Yb(III)	10	0.1001	10.2 ± 0.3	0.1004 ± 0.0002	0.9–1.3
Zn(II)	10	0.1001	10.2 ± 0.5	0.1004 ± 0.0002	0.9–1.4

[a]Results are the means of triplicate runs.

5.5 REFERENCES

1. De Corte F., Van Den Winkel P., Speecke A. and Hoste J., *Anal. Chim. Acta.*, 42, 67, 1968.
2. Strelow F.W.E., Weinert C.H.S.W. and Eloff C., *Anal. Chem.*, 44, 2352, 1972.
3. Walter R.I., *J. Inorg. Nucl. Chem.*, 6, 58. 1958.
4. Abdel-Rassoul A.A. and Mohammad S., *Z. Anorg. Allg. Chem. (Leipzig)*, 330, 96, 1964.
5. Yajima S., Shikata E. and Yamaguchi C., *Jpn Analyst,* 7, 721, 1958.
6. Klerkx L., *Bull. Soc. R. Sci. Liege (Belgium),* 33, 199, 1964.
7. Bandi W.R., Buyok E.G., Lewis L.L. and Melnik L.M., *Anal. Chem.,* 33, 1275, 1961.
8. Herman M., *Ind. Chim. Belg,* 23, 123, 1958.
9. Ding X. and Mou S., *J. Chromatogr.*, 920, 101, 2001.
10. Ji-Ying Ji. and Blesa M.A., *Inorg. Chem.,* 37, 3159, 1998.
11. Blesa M.A., *Inorg. Chem.,* 36, 6423, 1997.
12. Sharma S.D. and Sharma S.C., *J. Chromatogr.*, 841, 263, 1999.
13. Cotton F.A. and Wilkinson G., *Advanced inorganic chemistry,* 4th edition, John Wiley & Sons, New York, 1980, pp. 65.
14. Mellor J.W., *A comprehensive treatise on inorganic and theoretical chemistry,* Vol. XI, Longmans, Green & Co., New York, 1924, pp. 435.
15. Cotton F.A. and Wilkinson G., *Advanced inorganic chemistry,* 4th edition, John Wiley & Sons, New York, 1980, pp. 721.

16. Mellor J.W., *A comprehensive treatise on inorganic and theoretical chemistry,* Vol. XI, Longmans, Green & Co., New York, 1924, pp. 656.

17. Mellor J.W., *A comprehensive treatise on inorganic and theoretical chemistry,* Vol. VII, Longmans, Green & Co., New York, 1924, pp. 478.

18. Mellor J.W., *A comprehensive treatise on inorganic and theoretical chemistry,* Vol. V, Longmans, Green & Co., New York, 1924, pp. 543.

CHAPTER 6

SELECTIVE SEPARATIONS OF RADIOISOTOPES BY ION EXCHANGE CHROMATOGRAPHY

In this Chapter it is shown how the findings of Chapters 4 and 5 can be adapted for radioisotopic separations. Firstly, the findings of the systematic study of exchange behaviour of Ge(IV) and Ga(III) in the varying oxalic acid – sulphuric acid mixtures are used to develop a separation involving ^{68}Ge from Ga_2O target material. A method based on acid dissolution of the target and anion exchange chromatography on an anion exchange resin (AG1-X8) is developed. Secondly, other radioisotopic separations are proposed using the findings on the exchange behaviour of the other elements.

6.1 CYCLOTRON PRODUCTION OF ^{68}Ge WITH A Ga_2O TARGET

6.1.1 Introduction

^{68}Ge ($t_{½}$=288 d) decays by electron capture to ^{68}Ga ($t_{½}$=68 m), which disintegrates mainly by positron emission (90.5%) [1]. Its daughter [^{68}Ga, which emits β^+– and γ–rays (1077 keV)] lasts several months and is obtained by the use of ^{68}Ge in equilibrium with its daughter, ^{68}Ga, in a ^{68}Ge / ^{68}Ga generator system [2]. ^{68}Ge has many uses: for instance, it has been used as a positron source in positron annihilation studies in nuclear physics and for metal radiography in industry [3]. However, ^{68}Ge is used mainly in a ^{68}Ge / ^{68}Ga generator for positron emission tomography (PET) in nuclear medicine [4,5]. The

availability of ^{68}Ga from the generator, for radiopharmaceutical purposes, has increased the demand for ^{68}Ge [6].

Various nuclear reactions leading to ^{68}Ge production are possible by either the ^{66}Zn (α, 2n) ^{68}Ge (^{66}Zn abundance: 27.8%) or by the ^{69}Ga (p, 2n) ^{68}Ge (^{69}Ge abundance: 60%) reaction. The former reaction has a yield of 1–2 $\mu Ci.\mu Ah^{-1}$ while the latter reaction has a yield of 20 $\mu Ci.\mu Ah^{-1}$ [7]. For medical cyclotrons, the second reaction is often used because of higher yields and because the chemical processing involves only two elements (germanium and gallium) in the separation, whereas the zinc target involves a third element (zinc), which introduces additional radionuclidic impurities.

Target matrices include the following: Ga metal (natural or enriched, melting point: 39 ^{0}C) [8,9], Ga_2O_3 (melting point: 1900 ^{0}C) [10], Ga_4Ni (melting point: 900 ^{0}C) [11] and RbBr (melting point: 682 ^{0}C) [12]. The Ga_4Ni and RbBr targets were avoided, because, again, additional components (Ni and Rb respectively) were added to the system. The natural Ga metal (low melting point) and the isotopically enriched Ga metal (expensive material) were also not considered, because an aluminium canister cannot be used to encapsulate the Ga metal. Ga_2O_3 prohibited the use of high particle beam currents.

After bombardment of the target, ^{68}Ge may be separated from the target material by various methods. Grant et al. [12] reported on the dissolution of a RbBr target in a 6 M HCl solution followed by quantitative distillation of ^{68}Ge from a 6 M HCl solution. Gleason [8] reported on the distillation of ^{68}Ge from a ^{69}Ga target using CCl_4. Pao et al.

[7] reported on the dissolution of Ga_2O_3 in 16 M HNO_3 solution under reflux followed by ion exchange chromatography of ^{68}Ge on a hydrous zirconium oxide medium. Loc'h et al. [11] reported on the dissolution of Ga_4Ni in cold HNO_3 solution, followed by the recovery of ^{68}Ge by liquid-liquid extraction in a 9 M HCl–CCl_4 system. Borong and Yinsong [10] reported on the dissolution of Ga_2O_3 in a concentrated H_2SO_4 solution, followed by liquid–liquid extraction of ^{68}Ge in H_2SO_4–HCl and H_2SO_4–KI systems. Kopecky et al. [13] reported on the extraction of ^{68}Ge into CCl_4 from concentrated HCl solution using an α–particle irradiated Zn target.

At the iThemba LABS, as mentioned previously, the routine production of radioisotopes is carried out by means of a high energy proton (66 MeV) beam which has high beam currents (>65 μAh) available. For large-scale production, large targets (3–10 g) are normally used. At the iThemba LABS, an in-house Ga_2O target was developed. A gallium suboxide target with empirical formula Ga_2O has been developed by mixing 4.0 mole Ga with 1.0 mole Ga_2O_3. Ga_2O is similar to the indium suboxide (In_2O), which is used for the production of ^{111}In. No systematic information on the distribution coefficients of Ge(IV) and Ga(III) in the oxalic acid – sulphuric acid mixture was found in the literature. We used the relevant data in Chapter 5 to investigate and develop a separation of ^{68}Ge from the Ga_2O target.

6.1.2 Experimental

6.1.2.1 Reagents and apparatus

The grade of reagents, metals and anion exchange resin together with the analytical intrumentation and techniques were the same as described in Chapter 3.

6.1.2.2 Target preparation and irradiation

Gallium oxide (1.874 g) and gallium metal (2.789 g) were heated at 60 ^{0}C until the gallium metal had melted. The mixture was then heated at 700 ^{0}C for a further 15 minutes and mixed well (the process was repeated several times). The Ga_2O was cooled to room temperature, ground to a fine powder, and again heated to 700 ^{0}C and again cooled. The Ga_2O target (ca 4.5 g) was prepared by unaxial pressing of the above mixture at a pressure of 523 MPa under vacuum by means of a suitable punch and die (machined from a high carbon and high chromium tool set). The disc (20 mm diameter and 1 mm thick) was encapsulated in an aluminium canister, which was sealed by a cold welding process. The targets were bombarded with a proton beam (energy window: 2-34 MeV; current: 65 μA) for 10–15 minutes.

6.1.2.3 Chemical processing

Initial column separations were done using the inactive Ga_2O target. The target was gently heated and stirred in 5.0 M H_2SO_4 solution (50 ml). After complete dissolution, the solution was heated to dryness (8 h). The residue was then dissolved in deionised water (25 ml) and again evaporated to dryness. The resultant residue was dissolved in 10.0 M H_2SO_4 solution (10 ml), followed by addition of 0.5 M oxalic acid (50 ml) and deionised water (40 ml) in succession. The sorption solution was spiked with the ^{67}Ga and ^{69}Ge radiotracer (0.1 ml). The solution was pumped with a peristaltic pump at a rate of 3 ± 0.5 $ml.min^{-1}$ onto a preconditioned AG1–X8 (13ml) resin column as described above. The gallium (and ^{67}Ga) was eluted with 0.25 M oxalic acid – 1.00 M sulphuric acid (450 ml) followed by deionised water (50 ml). The ^{69}Ge radionuclide was then eluted with 5.0 M HNO_3 (100 ml). The ^{69}Ge eluate was evaporated to dryness and finally dissolved in deionised water (10 ml).

6.1.2.4 Proton-irradiated Ga_2O target

The bombarded Ga_2O disc was recovered from the aluminium canister after a decay period (10 d) and processed using chemical steps similar to those described above (schematic diagram, Figure 6.1).

6.1.3 Results and Discussion

The optimum conditions (0.25 M oxalic acid – 1.00 M sulphuric acid mixture) for the elemental separation of Ga(III) from Ge(IV) as described in Chapter 5, were chosen and adapted for the chemical processing of the inactive Ga_2O target (spiked with ^{67}Ga and ^{69}Ge radiotracer) and the proton-irradiated Ga_2O target.

Various dissolution methods of the target material (inactive Ga_2O) were investigated. Dissolution with concentrated and diluted HNO_3 solutions (15 M and 5 M respectively) was avoided, because it required refluxing. Dissolution with concentrated HCl solution (10 M) was also avoided because of vaporization of $GeCl_4$ at 83 ^0C. Complete dissolution of the target material was possible with a 5 M H_2SO_4 solution, but this was a lengthy (8 h) process. The results of the column separation of both the inactive target with radiotracers and that of the proton-irradiated target are presented in Table 6.1. The proton-irradiated target was processed after a decay period (10 d), when only the long-lived Ga and Ge radionuclides were present. During the separation, ^{67}Ga and ^{69}Ge radionuclides were again used to follow the efficiency of the separation, because β^+– and γ–rays were present for ^{68}Ge. The findings of the initial work (Chapter 5) were very similar to the results obtained with the inactive target with the radiotracers as well as with the proton-irradiated targets.

The Ga radionuclides were very easily eluted during the sorption (>94%) and the eluting (>4%) steps. The final Ge radionuclide product was recovered from the resin column with high yield (>95%). The final ^{68}Ge product had an acceptable level of inactive

Ga(III) present (<100 μg). The ^{68}Ge was detected by assaying the ^{68}Ga in the final ^{68}Ge product. This was performed at calibration time (15 days after the end of bombardment), when all the original ^{68}Ga had decayed, and the remaining ^{68}Ga was due to the ^{68}Ge / ^{68}Ga parent-daughter equilibrium. No ^{69}Ge (1107 keV) or other radionuclidic impurities were detected at calibration time. The ^{68}Ge had a radionuclidic purity of >99.99% at calibration time.

The irradiation yield (15.1 μCi / μAh^{-1}) was of similar order to the theoretical yield (20 μCi / μAh^{-1}) [7]. Losses could be attributed to volatilisation of the Ge radionuclides during the dissolution of the target. This could, however, be minimised if a closed system existed.

Table 6.1 Results of various column separations on the anion exchange resin (AG1-X8).

Elution curve number	% Breakthrough of metals (inactive or active) in sorption step	% Breakthrough of metals (inactive or active) in eluting step	Total contaminant in the retained metal eluate
1[a]	Ga(95.1%)–Ge(0%)	Ga(4.9%)–Ge(0%)	90 μg Ga(III)
2[a]	Ga(96.1%)–Ge(0%)	Ga(3.7%)–Ge(0%)	75 μg Ga(III)
3[a]	Ga(95.1%)–Ge(0%)	Ga(4.9%)–Ge(0%)	85 μg Ga(III)
4[b]	Ga(95.1%)–Ge(0%)	Ga(4.7%)–Ge(0%)	90 μg Ga(III)
5[b]	Ga(96.1%)–Ge(0%)	Ga(4.1%)–Ge(0%)	80 μg Ga(III)
6[b]	Ga(95.1%)–Ge0%)	Ga(4.9%)–Ge(0%)	90 μg Ga(III)

[a]inactive Ga_2O target with radiotracer ^{67}Ga and ^{69}Ge
[b]proton–irradiated Ga_2O target

Figure 6.1 Schematic diagram for the separation of high purity ^{68}Ge from a proton–irradiated Ga_2O.

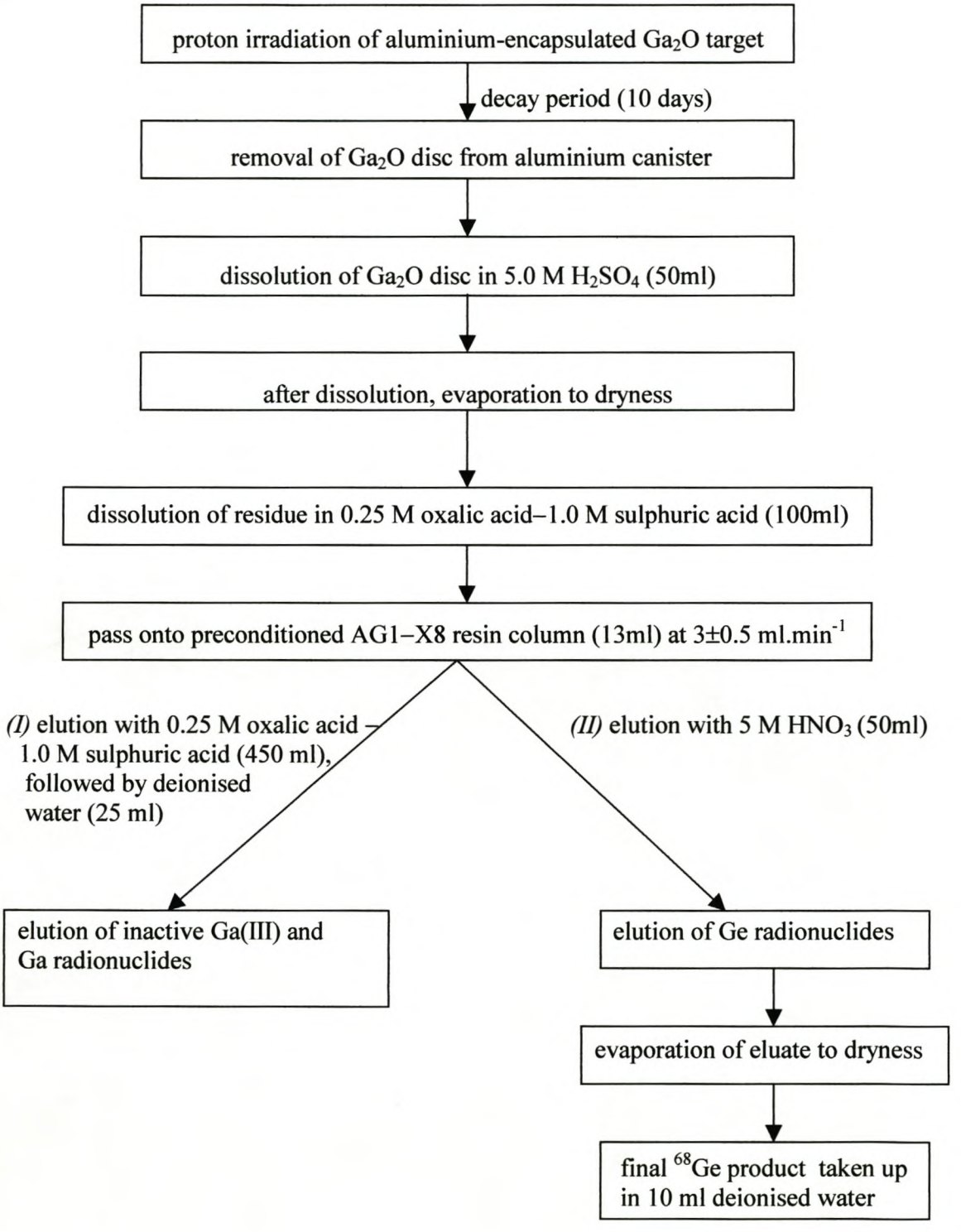

6.2 OTHER PROPOSED APPLICATIONS

In this section it will be shown how the elution curves described in Chapters 4 and 5 can be adapted for selective radiochemical separations. The following are only suggested procedures that can be used in each specific instance.

6.2.1 ^{75}As (p, 4n) ^{72}Se

In the above nuclear process [14, 15], the radioisotope of interest, ^{72}Se, needs to be separated from the As target material. The elution curve involving these elements (As and Se) in the 0.25 M oxalic acid – 0.005 M sulphuric acid on the AG1-X8 resin column can easily be adapted for a possible radiochemical separation. The ^{72}Se would be firmly retained on the resin column while the As target material and its related radioisotopes eluted under conditions related to this elution curve (5.3.3).

6.2.2 ^{58}Ni (p, 2n) $^{57}Cu \rightarrow {}^{56}Ni \rightarrow {}^{56}Co$

In the above nuclear process [16], the radioisotope of interest, ^{56}Co, needs to be separated from the Ni target material. The elution curve involving these elements (Ni and Co) in the 0.25 M oxalic acid – 0.005 M sulphuric acid on the AG1-X8 resin column can easily be adapted for a possible radiochemical separation. The ^{56}Co would be retained on the resin column while the Ni target material and its related radioisotopes are eluted from the column under conditions related to this elution curve (5.3.4).

6.2.3 ^{58}Ni (p, 4n) ^{55}Cu → ^{55}Ni → ^{55}Co → ^{55}Fe

In the above nuclear process [17], the radioisotope of interest, ^{55}Fe, needs to be separated from the Ni target material. The elution curve involving these elements (Ni and Fe) in the 0.25 M oxalic acid – 0.05 M sulphuric acid on the AG1-X8 resin column can easily be adapted for a possible radiochemical separation. The ^{55}Fe would be firmly retained on the resin column while the Ni target material and its related radioisotopes are eluted from the column under conditions related to this elution curve (5.3.5).

6.2.4 As (p, spall) ^{68}Ge

In the above nuclear process [18, 19], the radioisotope of interest, ^{68}Ge, needs to be separated from the As target material. The elution curve involving these elements (As and Ge) in the 0.25 M oxalic acid – 1.00 M sulphuric acid on the AG1-X8 resin column can easily be adapted for a possible radiochemical separation. The ^{68}Ge would be firmly retained on the resin column while the As target material and its related radioisotopes are eluted from the column under conditions related to this elution curve (5.3.7).

6.2.5 ^{67}Zn (^{3}He, 2n) ^{68}Ge

In the above nuclear process [20], the radioisotope of interest, ^{68}Ge, needs to be separated from the Zn target material. The elution curve involving these elements (Zn and Ge) in the 0.25 M oxalic acid – 1.00 M sulphuric acid on the AG1-X8 resin column could easily

be adapted for a possible radiochemical separation. The ^{68}Ge would be firmly retained on the resin column while the Zn target material and its related radioisotopes are eluted from the column under conditions related to this elution curve (5.3.6).

6.2.6 ^{59}Co (d, 2p7n) ^{52}Fe

In the above nuclear process [21], the radioisotope of interest, ^{52}Fe, needs to be separated from the Co target material. The elution curve involving these elements (Co and Fe) in the 0.05 M oxalic acid – 0.25 M sulphuric acid on the AG1-X8 resin column could easily be adapted for a possible radiochemical separation. The ^{52}Fe would be firmly retained on the resin column while the Co target material and its related radioisotopes are eluted from the column under conditions related to this elution curve (5.3.2).

6.2.7 As (p, spall) ^{62}Zn

In the above nuclear process [22, 23], the radioisotope of interest, ^{62}Zn, needs to be separated from the As target material. The elution curve involving these elements (As and Zr) in the 0.05 M oxalic acid – 0.00 5 M sulphuric acid on the AG50W-X8 resin column could easily be adapted for a possible radiochemical separation involving As and Zn. The ^{62}Zn (similar equilibrium distribution coefficient as Zr) would be firmly retained on the resin column while the As target material and its related radioisotopes are easily eluted from the column under conditions related to the elution curve 5.3.2.

6.2.8 ^{89}Y (α, n) ^{92m}Nb

In the above nuclear process [24, 25], the radioisotope of interest, ^{92m}Nb, needs to be separated from the Y target material. The elution curve involving these elements (Y and Nb) in the 0.25 M oxalic acid – 0.005 M sulphuric acid on the AG50W-X8 resin column could easily be adapted for a possible radiochemical separation. In this case, the dissolution media of the target is split into four equal volumes and passed through the resin columns individually. The ^{92m}Nb should flow through the column with minimal retention, while, the target material and its related radioisotopes should be held on the resin column. If traces of ^{89}Y and its related radioisotopes are found in the ^{92m}Nb eluate, then this same eluate is again passed through a new resin column. All the ^{92m}Nb eluate fractions should then be collectively evaporated and taken up in a minimal volume of an appropriate solution for further work.

6.2.9 ^{66}Zn (p, n) ^{66}Ga

A similar process to the above is required for the radioisotope of interest, ^{66}Ga, to be separated from the Zn target material [26, 27]. The elution curve involving these elements (Zn and Ga) in the 0.05 M oxalic acid – 0.005 M sulphuric acid on the AG50W-X8 resin column could easily be adapted for a possible radiochemical separation. In this case, the dissolution media of the target is again split into four equal volumes and passed through the resin columns individually. The ^{66}Ga should flow through the column with minimal retention, while the target material and its related radioisotopes should be held

on the resin column. If traces of ^{66}Zn and its related radioisotopes are found in the ^{66}Ga eluate, then the process is repeated as above. All the ^{66}Ga eluate fractions should then be collectively evaporated and taken up in a minimal volume of an appropriate solution for futher work.

6.2.10 ^{55}Mn (p, 4n) ^{52}Fe

A similar process to the above is required for the radioisotope of interest, ^{52}Fe, to be separated from the Mn target material [28]. The elution curve involving these elements (Mn and Fe) in the 0.25 M oxalic acid – 0.05 M sulphuric acid on the AG50W-X8 resin column could easily be adapted for a possible radiochemical separation. Again, the dissolution media of the target is split into four equal volumes and passed through the resin columns individually. The ^{55}Fe should flow through the column with minimal retention, while, the target material and its related radioisotopes should be held on the resin column. If traces of ^{55}Mn and its related radioisotopes are found in the ^{55}Fe eluate, then the process is repeated as above. All the ^{55}Mn eluate fractions are collectively evaporated and taken up in a minimal volume of an appropriate solution for further work.

In the above elution curves we considered only the separation of the radioisotope of interest from the target material. During bombardment of a target material, however, various other nuclear reactions could occur, which could result in involved radiocontaminants, thus complicating the radiochemical separation. A separation is

possible if there is an acceptable separation factor between the radioisotope of interest and the radiocontaminants.

As was shown with the elution curves involving the cation exchange resins, it is possible to devise a separation if there is a fairly acceptable separation factor between two elements or two radioisotopes.

6.3 REFERENCES

1. Iwata Y., Kawamoto M. and Yoshizawa Y., *Int. J. Appl. Radiat. Isot.,* 31, 1537, 1983.
2. Choppin G.R. and Rydberg J., *Nuclear chemistr: theory and applications*, Pergamon Press, New York, 1985, pp. 35.
3. Hughes E., *Material in Engineering*, 2, 34, 1980.
4. Lambrecht R.M. and Sajjad M., *Radiochim Acta*, 43, 171, 1988.
5. Lambrecht R.M., *Radiochim Acta*, 34, 9, 1988.
6. Qaim S.M., *IAEA-SR-131/5*, Vienna Austria, 13-17 October 1986.
7. Pao P.J., Silvester D.J. and Waters S.L., *J. Radioanal. Chem.*, 64, 267, 1981.
8. Gleason G.I., *Int. J. Appl. Radiat. Isot.,* 8, 90, 1960.
9. Mirzadeh S., Kahn M., Grant P.M. and O'Brien H.A., *Radiochim. Acta*, 28, 47, 1981.
10. Barong B. and Yinsong W., *Nucl. Sci. Tech.,* 3, 202, 1992.
11. Loc'h C., Maziere B., Comar D. and Knipper R, *Int. J. Appl. Radiat. Isot.*, 33, 267, 1982.
12. Grant P.M., Miller D.A., Gilmore J.S. and O'Brien H.A., *Int. J. Appl. Radiat. Isot.*, 33, 415, 1982.
13. Kopecky P., Mudrova B. and Svoboda K., *Int. J. Appl. Rad. Isot.,* 24, 73, 1973.
14. Nozaki T., Itoh Y. and Ogawa K., *Int. J. Appl. Radiat. Isot.,* 30, 595, 1979.
15. Taylor D.M., *Int. J. Appl. Radiat. Isot.,* 52 , 911, 2000.

16. Taylor W.A., Herring A.N., Lopez R.M., Moody D.A., Philips D.R. and Staroski R.C., *Int. J. Appl. Rad. Isot.,* 42, 208, 1991.

17. Reimer P. and Qaim S.M., *Radiochim. Acta*, 80, 113, 1998.

18. Grant P.M., O' Brien H.A. Jr., Bayhurst B.P., Gilmore R.J., Prestwood R.J., Whipple R.E. and Wanek P.M., *J. Labell. Compd. Radiopharm.*, 16, 212, 1979.

19. Naidoo C and van der Walt T.N., *Int. J. Appl. Radiat. Isot.,* 54, 915, 2001.

20. Grutter A., *Int. J. Appl. Radiat. Isot.,* 33, 725, 1982.

21. Horiguchi T., Kumahora H., Inoue H. and Yoshizawa Y., *Int. J. Appl. Radiat. Isot.,* 34, 1531, 1983.

22. Michel R. and Galas M., *Int. J. Appl. Radiat. Isot.,* 24,1325, 1983.

23. Kohler M., Harms A.V. and Alber D., *Int. J. Appl. Radiat. Isot.,* 53, 197, 2000.

24. Pandy U., Muhkerjee A., Chaudhary P.R., Pillai M.R.A. and Venkatesh M., *Int. J. Appl. Radiat. Isot.,* 55, 471, 2001.

25. Lahiri S., Nayak D., Ramaswami A and Manohor S.B., *Int. J. Appl. Radiat. Isot.,* 52, 797, 2000.

26. Nayak D. and Lahiri S., *Int. J. Appl. Radiat. Isot.,* 54, 189, 2001.

27. Gul K., *Int. J. Appl. Radiat. Isot.,* 54, 311, 2001.

28. Stang L.G., *Prog. Nucl. Med.*, 4, 34, 1978.

CHAPTER 7

CONCLUSION

In this Chapter I review how the results in Chapters 4, 5 and 6 have met the objectives of this study and also identify some areas requiring further investigation.

7.1 REVIEW OF THE RESEARCH RESULTS WITH RESPECT TO THE OBJECTIVES OF THIS STUDY

7.1.1 Objective I

The equilibrium distribution coefficients of 32 metal ions [Al(III), As(V), Cd(II), Ce(III), Ce(IV), Co(II), Cr(III), Cu(II), Fe(III), Ga(III), Ge(IV), In(III), La(III), Mn(II), Mo(VI), Nb(V), Ni(II), Pr(III), Sb(V), Sc(III), Se(IV), Sn(IV), Ta(V), Tb(III), Te(IV), Ti(IV), V(V), W(VI), Y(III), Yb(III), Zn(II) and Zr(IV)] on a cation exchanger (Bio-Rad® AG50W-X8) in varying oxalic acid - sulphuric acid mixtures were successfully determined. The equilibrium distribution coefficients of these selected metal ions were determined in both 0.05 M and 0.25 M oxalic acid at various concentrations of sulphuric acid (0.005 M, 0.05 M, 0.10 M, 0.25 M, 0.50 M, 1.00 M, 1.50 M and 2.00 M). Table 4.1 and Table 4.2, in Chapter 4, illustrated that the metal ions Al(III), Cd(II), Ce(III), Ce(IV), Co(II), Cu(II), In(III), La(III), Mn(II), Ni(II), Sc(III), Y(III), Yb(III) and Zn(II) showed some degree of sorption, whereas the other metal ions studied showed no sorption at any of the chosen oxalic acid – sulphuric acid combinations. It was also proved that, for a fixed oxalic acid concentration, all metal ions with a K_d >0.5 showed a decrease in

distribution coefficient with increasing concentration of sulphuric acid. In addition, the distribution coefficients of metal ions >0.5 were generally higher in the 0.05 M oxalate medium compared to the 0.25 M oxalate medium.

In attempting to explain the sorption behaviour of the above metal ions, a speciation modelling program, MINEQL+, was used to develop speciation modelling systems for the metals Al(III), Cd(II), Co(II) and Zn(II) in varying oxalic acid – sulphuric acid combinations [1-10]. The distribution diagrams (Chapter 8) of these metals showed that all the dominant complexes were either negatively charged or neutral, i.e. no cations were present under the specified conditions. It was proposed that sorption involved the sulphonate group of the cation exchanger forming strong ionic bonds with the metal ions. The variable sorption of the sorbed metal ions was attributed to a set of complex factors such as the strength of the metal ion bond with the sulphonate group of the cation exchanger, the influence of the H^+ (of the H_2SO_4) on the dissociation of the oxalic acid, and/or the equilibrium shift of the metal-oxalate complexes to free ions, as explained in Chapter 4. Each of these factors could either suppress or enhance sorption depending on the specific conditions. It was concluded that the speciation modelling system used in the above study was not conclusive in explaining the sorption behaviour of the above metal ions on the studied cation exchanger, because of the non-correlation between the dominant species in solution and the dominant species on the resin column.

It was also highlighted in Chapter 4, in the case of the metal ions that had shown no sorption, that the dominant complexes of the specific metal ions were strongly associated with anions (ion pairs or even molecules) and hence the limitations on cation exchange sorption. In addition, it was shown that Pr(III) and Tb(III) formed oxalate precipitates [$Pr_2(oxalate)_3$ and $Tb_2(oxalate)_3$ respectively] during the equilibration studies. For the sake of completeness, it would be interesting to determine the sorption behaviour of the remaining elements in groups 1 and 2, the halogens and the actinides on a cation exchanger (Bio-Rad® AG50W-X8) in varying oxalic acid - sulphuric acid mixtures.

Two component [Zr(IV)-La(III); Al(III)-La(III); Ga(III)-Zn(II); As(V)-Zn(II); Cu(II)-Ce(IV); Ga(III)-Ce(IV); Ge(IV)-Ce(III); Mo(VI)-Y(III); Nb(V)-Y(III); Ga(III)-Co(II); As(V)-Co(II) and Fe(III)-Mn(II)] and three component [Fe(III)-Ga(III)-Zn(II) and Zr(IV)-Ta(V)-Yb(III)] elemental separations of a specific element from the other element or elements on a 10 ml or 13 ml cation exchange resin in a variety of oxalic acid – sulphuric acid mixtures, were successfully determined. Summaries of the results of the various elution curves are given in Chapter 4 (Table 4.3). As indicated, all the elution curves behaved similarly: no significant tailing was evident during any of the eluting steps; there was no breakthrough of the primary element during the sorption and eluting steps; and low levels of contaminants (<100 μg in total) were detected in the final product eluate. Many more elemental separations could be developed.

7.1.2 Objective II

The equilibrium distribution coefficients of the same 32 metal ions discussed above were determined on an anion exchanger (Bio-Rad® AG1-X8) in varying oxalic acid - sulphuric acid mixtures. Similarly, 0.05 M and 0.25 M oxalic acid at various concentrations of sulphuric acid (0.005 M, 0.05 M, 0.10 M, 0.25 M, 0.50 M, 1.00 M, 1.50 M and 2.00 M) were used. Table 5.1 and Table 5.2 in Chapter 5 illustrated that, for a fixed oxalic acid concentration, all metal ions with a distribution coefficient >0.5 showed a decrease in distribution coefficients with increasing concentration of sulphuric acid. Generally, these sorbed metal ions also showed an increase in sorption in 0.25 M oxalic acid compared to 0.05 M oxalic acid, with the exception of Al(III), Cd(II), Ce(III), Ce(IV), Cu(II), La(III), Mn(II), Ni(II), Sb(V), W(VI) and Yb(III).

Table 5.1 and Table 5.2 also illustrated that the group 5 metal ions [As(V) and Sb(V)] that were studied, showed absolutely no sorption in any of the chosen oxalic acid – sulphuric acid combinations. Similar behaviour was encountered with the cation exchanger, as was shown in Chapter 4. Group 3 metal ions [Al(III), Ga(III) and In(III)] showed relatively better sorption than group 5 metal ions [As(V) and Sb(V)] in both oxalate concentrations in the lower sulphuric acid concentration range (0.005M – 0.25M). Group 4 metal ions [Ge(IV) and Sn(IV)] and group 6 metal ions [Se(IV) and Te(IV)] were relatively more strongly sorbed compared to groups 3 and 5 metal ions studied in both oxalate concentrations across the chosen sulphuric acid range. The transition metal ions [Sc(III), Ti(IV), V(V), Cr(III), Mn(II), Fe(III), Co(II), Cu(II), Zn(II), Y(III), Zr(IV),

Nb(V), Mo(VI), Cd(II), La(III), Ta(V) and W(VI)] that were studied, did not show any significant trend. Tetravalent metal ions, pentavalent metal ions and hexavalent metal ions that were studied showed relatively similar sorption in both oxalate concentrations across the sulphuric acid concentration range, which was relatively higher than for the divalent and trivalent metal ions.

The various distribution diagrams of Al(III), Cd(II), Co(II) and Zn(II) that were discussed in Chapter 4, were used in attempts at explaining the sorption behaviour of the above sorbed metal ions. The distribution diagrams (Appendix, Figures 8.1 to 8.5) showed that many of the dominant complexes were negatively charged, and this played an active role in the nature of sorption of the respective metal ions on an anion exchanger. For example, for the metal ion Al(III), increased sorption was evident in the lower sulphuric acid concentration range (0.005 M – 0.1 M) on the anion exchanger compared to the cation exchanger, and this was attributed to the strong dominance of the negatively charged $[Al(oxalate)_3]^{3-}$ and $[Al(oxalate)_2]^{-}$ complexes (Appendix, Figure 8.1), which would favour electrostatic sorption on the quaternary ammonium group of the anion exchanger. However, for the metal ions Cd(II), Co(II) and Zn(II), relatively weaker sorption was evident across the chosen sulphuric acid concentration range on the anion exchanger compared to the cation exchanger, even though according to the respective distribution diagrams (Appendix, Figures 8.2-8.5), the dominant complexes across the chosen sulphuric acid range were negatively charged. The lower sorption was attributed to a set of complex factors such as the ionic strength and hydration energies of the metal complexes (metal-oxalate or metal-sulphate) and complex charge. Similarly, as with the

cation exchanger, the distribution coefficients on the anion exchanger decreased as the concentration of the sulphuric acid increased across the chosen range, and this was attributed to the increasing suppression of the dissociation of the oxalic acid, which lowered the complexation effect. Again, it was concluded that the speciation modelling system used in the above study was not conclusive in explaining the sorption behaviour of the above metal ions on the studied anion exchanger, because of the non-correlation between the dominant species in solution and the dominant species on the resin column.

Other metal ions studied, for example Cr(III), Sn(IV), V(V) and Mo(VI), showed pronounced sorption on the anion exchanger compared to the cation exchanger (no sorption), and this was attributed to many of the dominant complexes associated with the above metal ions being strongly associated with anions that are involved in the sorption of the respective metal ions with the anion exchanger. Again, varying sorption could be attributed to factors such as the ionic strength and hydration energies of the metal complexes (metal-oxalate or metal-sulphate) and complex charge. Again, for the sake of completeness, it would be interesting to determine the sorption behaviour of the remaining elements in groups 1 and 2, the halogens and the actinides on an anion exchanger (Bio-Rad® AG1-X8) in varying oxalic acid - sulphuric acid mixtures.

Two component [As(V)-Zr(IV); Co(II)-Fe(III); Ni(II)-Co(II) and Ni(II)-Fe(III)] and three component [Ni(II)-As(V)-Se(IV); Al(III)-Zn(II)-Ge(IV) and As(V)-Cu(II)-Ge(IV)] elemental separations of a specific element from the other element(s) on a 10 ml or 13 ml anion exchange resin in a variety of oxalic acid – sulphuric acid mixtures, were also

successfully determined. Summaries of the results of the various elution curves were given in Chapter 5 (Table 5.4). Again, as in the case of the cation exchange resin, the elution curves behaved similarly: no significant tailing was evident during any of the eluting steps; there was no breakthrough of the primary element during the sorption and eluting steps; and low levels of contaminants (<50 μg in total) were detected in the final product eluate. Again, many more elemental separations could be developed. In order to obtain the optimum conditions for a Ga(III)-Ge(IV) elemental separation, six elemental separations involving 5 g Ga and 10 mg Ge with varying oxalic acid-sulphuric acid mixtures and varying column sizes, were determined. The most suitable conditions were the 0.25 M oxalic acid – 1.00 M sulphuric acid mixture and the 13 ml anion exchange resin column. No breakthrough of Ge(IV) in the sorption and eluting steps was evident, and the amount of Ga(III) [<75 μg] detected in the Ge(IV) eluate was found to be at an acceptable level. The other elemental separations had breakthrough of the Ge(IV) in the sorption or eluting steps and/or excessive tailing of Ga(III).

7.1.3 Objective III

Quantitative separation of mixtures [Ge(IV) in combination with Al(III), As(V), Co(II), Cu(II), Ga(III), In(III), La(III), Ni(II), Y(III), Yb(III) and Zn(II)] on an anion exchange resin in 0.25 M oxalic acid – 1.00 M sulphuric acid mixture were also successfully carried out. These separations formed a partial basis to objective IV.

7.1.4 Objective IV

The systematic information on exchange behaviour of Ge(IV) and Ga(III) in the varying oxalic acid – sulphuric acid mixtures described in Chapter 5, were used to develop a successful separation involving ^{68}Ge from the Ga_2O target material. A method based on acid dissolution of the target and chromatography on an anion exchange resin (AG1-X8) was developed. The optimal conditions (0.25 M oxalic acid – 1.00 M sulphuric acid mixture) for the elemental separation of Ga(III) from Ge(IV) were chosen and adapted for the chemical processing of the inactive Ga_2O target (spiked with ^{67}Ga and ^{69}Ge radiotracer) and the proton-bombarded Ga_2O target. The bombarded target was processed after a decay period (10 d), when only the long-lived Ga and Ge radionuclides were present. Dissolution of the target material was accomplished in 5.0 M H_2SO_4. The Ga radionuclides were very easily eluted during the sorption (>94%) and the eluting (>4%) steps. The final Ge radionuclide product was recovered from the resin column with high yield (>95%). The final ^{68}Ge product had acceptable levels of inactive Ga(III) present (< 100 μg). No ^{69}Ge (1107 keV) or other radionuclidic impurities were detected at calibration time. The ^{68}Ge had a radionuclidic purity of >99.99% at calibration time. The irradiation yield (15.1 μCi / μAh^{-1}) was of similar order to the theoretical yield (20 μCi / μAh^{-1}) [11]. The chemical separation involving the large-scale production of ^{68}Ge could easily be adapted for hot-cell facilities and also to develop a ^{68}Ge / ^{68}Ga generator [11-30], but this falls beyond the scope of this study.

It was also successfully shown how some of the experimental elution curves described in Chapters 4 and 5 could easily be adapted for radiochemical separations. However, further investigations involving the radiochemical separation of the radioisotope of interest from the bombarded target in the respective applications (Chapter 6), are required.

7.1.5 Objective V

The MINEQL+ speciation modelling program was used to do a speciation study of the metal ions Al(III), Cd(II), Co(II) and Zn(II) in varying oxalic acid - sulphuric acid mixtures. The speciation data was expressed as distribution diagrams as shown in Chapter 8 (Appendix). Only these metal ions were selected due to the reliability of the thermodynamic data (at the studied conditions) in the speciation program's database. However, as indicated in Chapters 4 and 5, the speciation modelling systems used in this study could not be used to explain conclusively the sorption behaviour of metals under the studied conditions.

7.1.6 Objective VI

Analytical methods such as graphite furnace atomic absorption spectrometry for sub-micro level analysis, were successfully adapted for Ga, Al and Fe, and a summary of the recommended instrumental parameters for these elements was given in Chapter 3 (Table 3.3, Table 3.4 and Table 3.5 respectively). In addition, induced coupled plasma emission

methods for the elements Al, As, Ce, Cd, Co, Cr, Cu, Fe, Ga, Ge, In, La, Mn, Mo, Nb, Ni, Pr, Sb, Sc, Se, Sn, Ta, Tb, Te, Ti, V, W, Y, Yb, Zn, and Zr were also adapted according to the studied matrix (0.5 M HNO_3). A summary of the recommended instrumental parameters for these elements was given in Chapter 3 (Table 3.6).

In conclusion, this study has provided systematic information about the ion exchange behaviour of 32 metal ions in oxalic acid – sulphuric acid mixtures, thus putting additional options at the disposal of the analyst when devising elemental separations. As a result, it was possible to develop an alternative route for the cyclotron production of ^{68}Ge from a Ga_2O target material involving oxalic acid – sulphuric acid as an eluting agent. Presently, the iThemba LABS exports ^{68}Ge (chemical purity >99.99%) in bombarded gallium targets to the Los Alamos National Laboratory (LANL) in the United States of America. LANL recovers the ^{68}Ge by a chemical process. However, it is envisaged that it would be more economically viable for the iThemba LABS to produce its own ^{68}Ge from Ga_2O targets on a large scale for the demanding export market.

7.2 REFERENCES

1. Ball J.W. and Nordstrom D.K., *U.S. Geological Survey Open – File Report,* 91, 189, 1992.
2. Nordstrom D.K., Plummer L.N and Jones B.F., *American Chemical Society Symposium Series, Washington D.C.,* 416, 398, 1990.
3. Parkhurst D.L. and Plummer L.N., *Geochemical models,* Van Nostrand Reinhold, New York, 1993, pp. 199.
4. Parkhurst D.L., *U.S Geological Survey Water-Resources Investigations Report*, 95, 143, 1995.
5. Barak P., *J. Agron. Educ.,* 19, 44, 1990.
6. Plummer L.N., Prestemon E.C. and Parkhurst D.L., *U.S Geological Survey Water-Resources Investigations Report*, 94, 130, 1994.
7. Tao S., Wen Y., Long A., Dawson R., Cao J. and Xu F., *Comp. and Chem.,* 25, 215, 2001.
8. Pesavento M., Alberti G. and Profumo A., *Anal. Chim. Acta.,* 405, 309, 2000.
9. Morel F.M.M., *Principles and applications of aquatic chemistry*, Wiley-Interscience, New York, 1983, pp. 25.
10. Westall J.C., Zachary J.L. and Morel F.M.M., *MINEQL, A computer program for the calculation of chemical equilbrium composition of aqueous system,* Massachusetts Institute of Technology, (MIT), Tech. No. 18, 1976.
11. Pao P.J., Silvester D.J. and Waters S.L., *J. Radioanal. Chem.*, 64, 267, 1981.

12. Yano Y., *In radiopharmaceuticals (editor Subramanian G. et al.), Soc. Nucl. Med.*, New York, 1975, pp. 236.

13. Lieser K.H., *Radiochim. Acta*, 23, 57, 1976.

14. Hnatowich D.J., *Int. J. Appl. Radiat. Isot.*, 28, 169, 1977.

15. Lambrecht R.M. and Marcos N., *Applications of nuclear and radiochemistry,* Pergamon Press, New York, 1982, pp. 57.

16. Lambrecht R.M., *Radiochim. Acta*, 34, 9, 1983.

17. Finn R.D., Molinsky V.J., Hupf H.B. and Kramer H., *Radionuclide Generators for Biomedical Applications*, NAS-NS-3202, USDOE, 1983.

18. Knapp F.F. Jr. and Butler T.A., *Radionuclide Generators, ACS Symposium Series*, Washington D. C., 1984.

19. Clark J.C., *Second European symposium on radiopharmacy and radiopharmaceuticals*, Martinus Nijhoff Publishers, Holland, 1986, pp. 35.

20. Guillaume M. and Brihaye C., *Int. J. Radiat. Appl. Instrum., Part B, Nucl. Med. Biol.*, 13, 89, 1986.

21. Loc'h C., Maziere B. and Comar D., *J. Nucl. Med.*, 21, 171, 1980.

22. Hanrahan T.J., Yano Y., Welch M.J., McElvany K.D. and Moore H.A. Jr., *J. Labelled Comp. Radiopharm.* 19, 1537, 1982.

23. McElvany K.D, Hopkins K.T., Hanrahan T.J., Moore K.D. and Welch M.J., *J. Labelled Comp. Radiopharm.* 19, 1419, 1982.

24. Neirinckx R.O., Davis M.A., *J. Nucl. Med.*, 21, 81, 1980.

25. Malyshev K.V. and Smirnov V.V., *Radiokhimiya*, 17, 137, 1975.

26. Seidel W.E. and Lieser K.H., *Radiochim. Acta*, 19, 196, 1973.

27. Greene M.W. and Tucker W.D., *Int. J. Appl. Radiat. Isot.,* 12, 62, 1961.

28. Kopecky P. and Mudrova B., *Int. J. Appl. Radiat. Isot.,* 25, 263, 1974.

29. Arino H., Skraba W.J. and Kramer H.H., *Int. J. Appl. Radiat. Isot.,* 29, 117, 1978.

30. Neirinckx R.O., Davis M. A., *J. Nucl. Med.,* 20, 1075, 1979.

CHAPTER 8

APPENDIX

8.1 SPECIATION DATA OF STUDIED ELEMENTS

Figure 8.1 Distribution diagram of Al(III) in 0.05 M oxalic acid in varying sulphuric acid concentrations (0.005 M – 2.00 M).

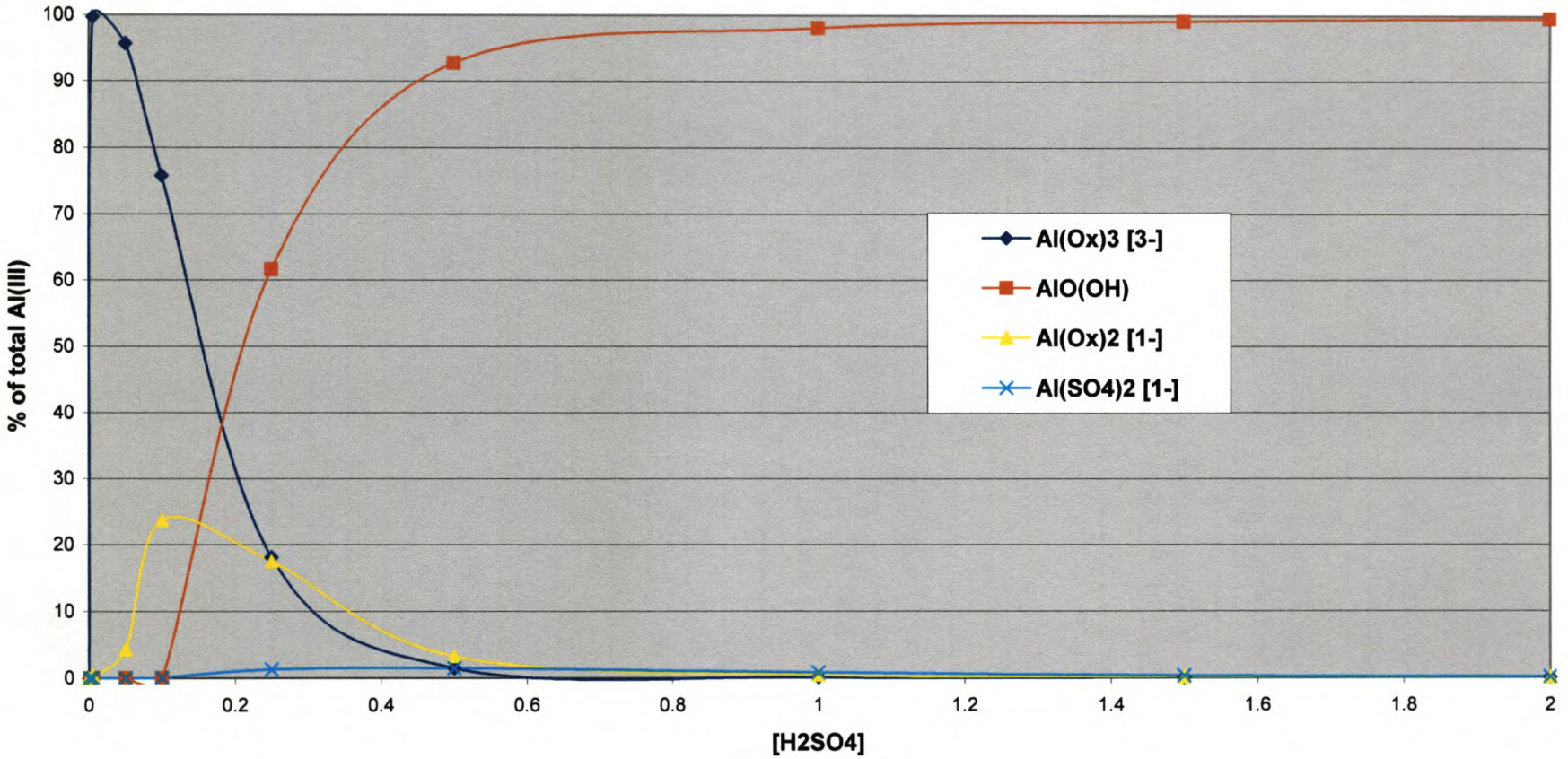

Figure 8.2 Distribution diagram of Zn(II) in 0.05 M oxalic acid in varying sulphuric acid concentrations (0.005 M – 2.00 M).

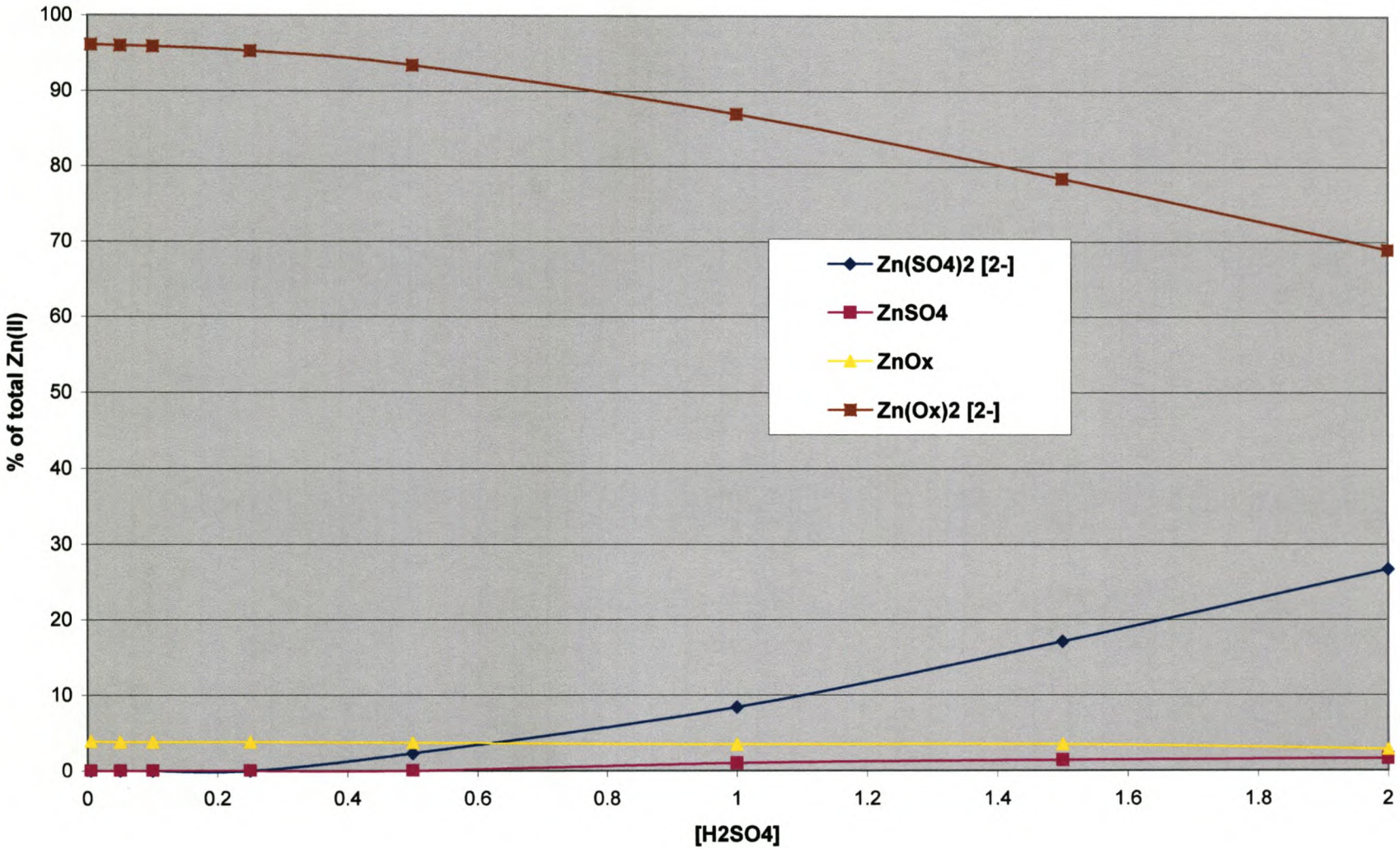

Figure 8.3 Distribution diagram of Co(II) in 0.05 M oxalic acid in varying sulphuric acid concentrations (0.005 M – 2.00 M).

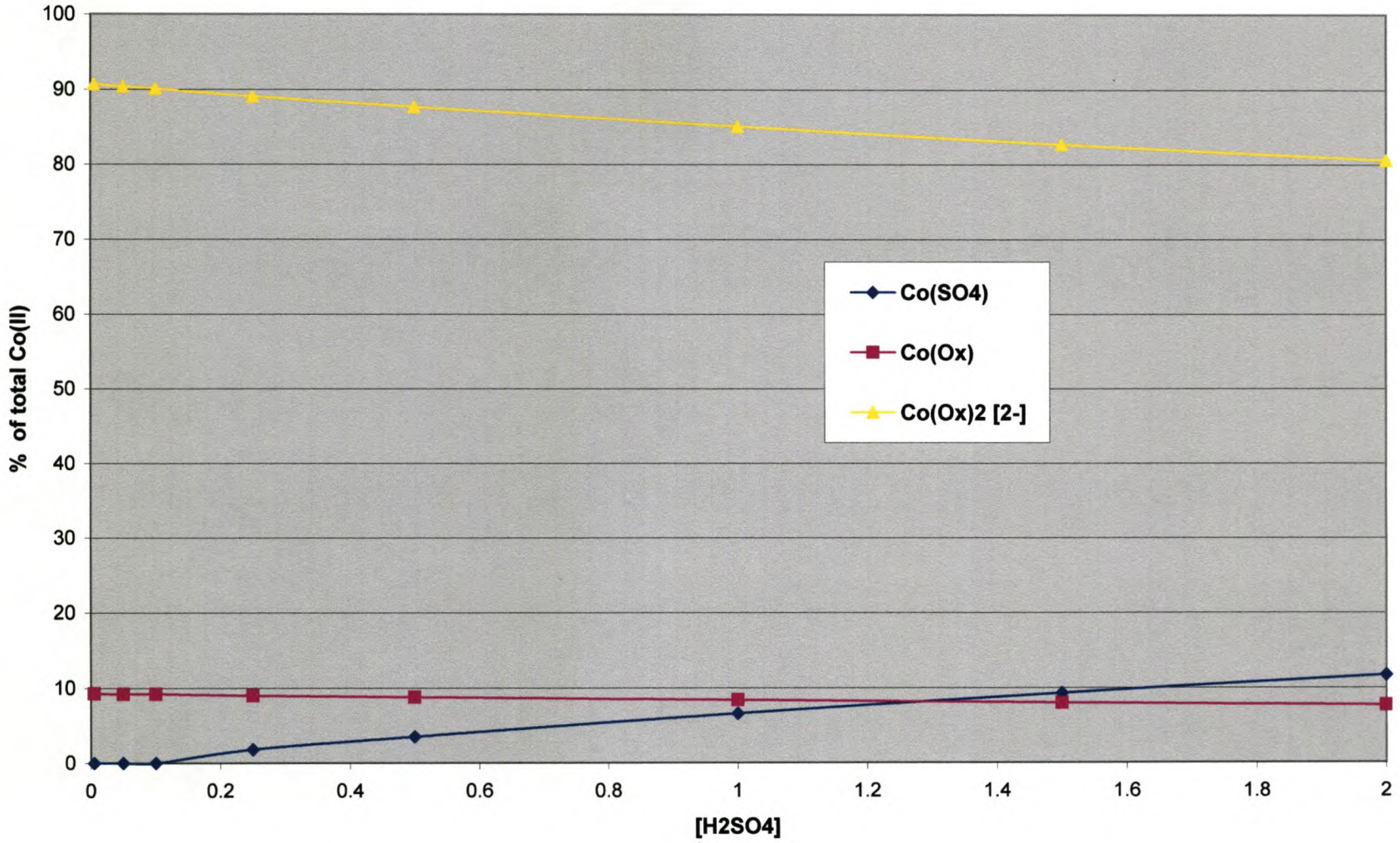

Figure 8.4 Distribution diagram of Cd(II) in 0.05 M oxalic acid in varying sulphuric acid concentration (0.005 M – 2.00 M).

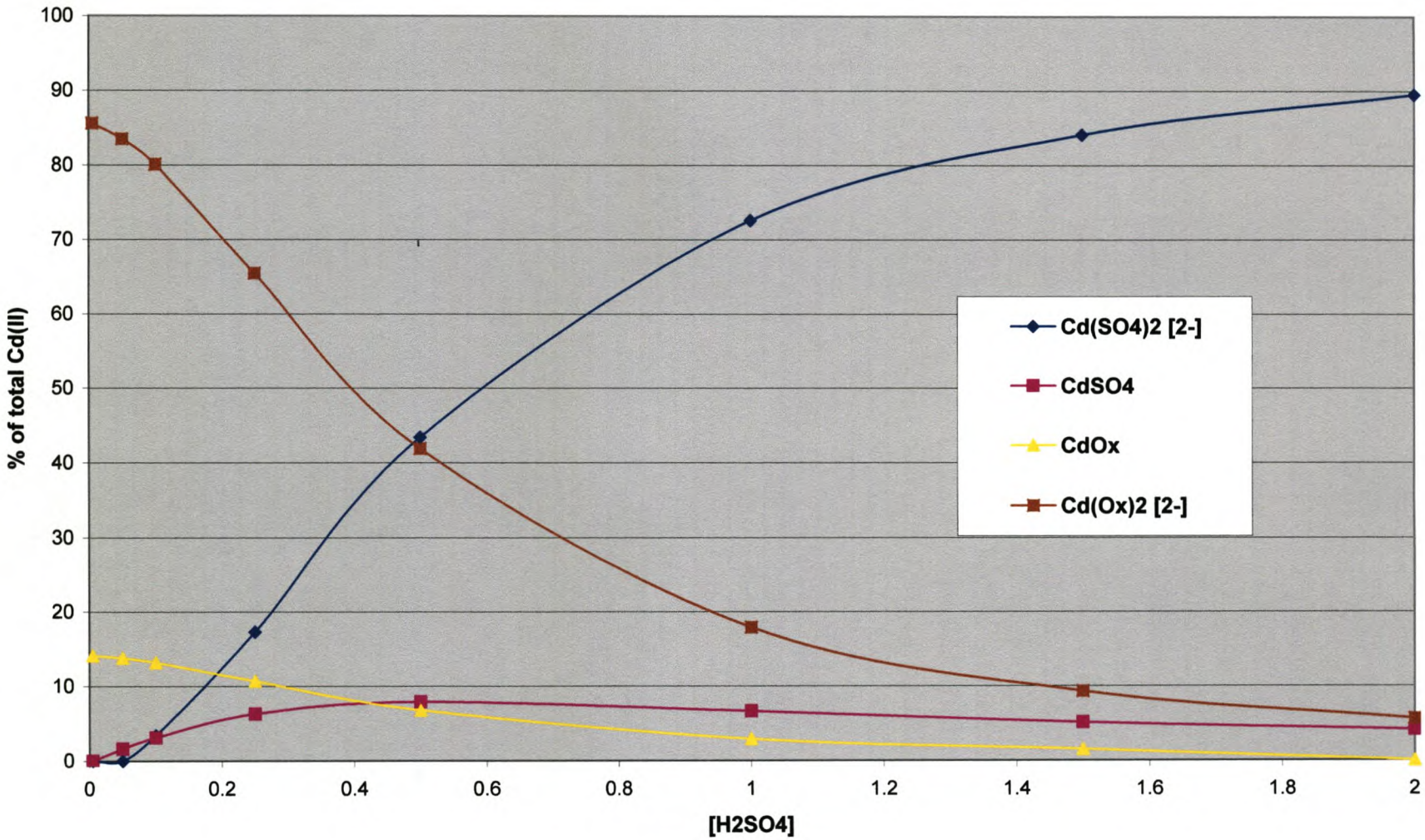

Figure 8.5 Distribution diagram of Cd(II) in 0.25 M oxalic acid in varying sulphuric acid concentrations (0.005 M – 2.00 M).

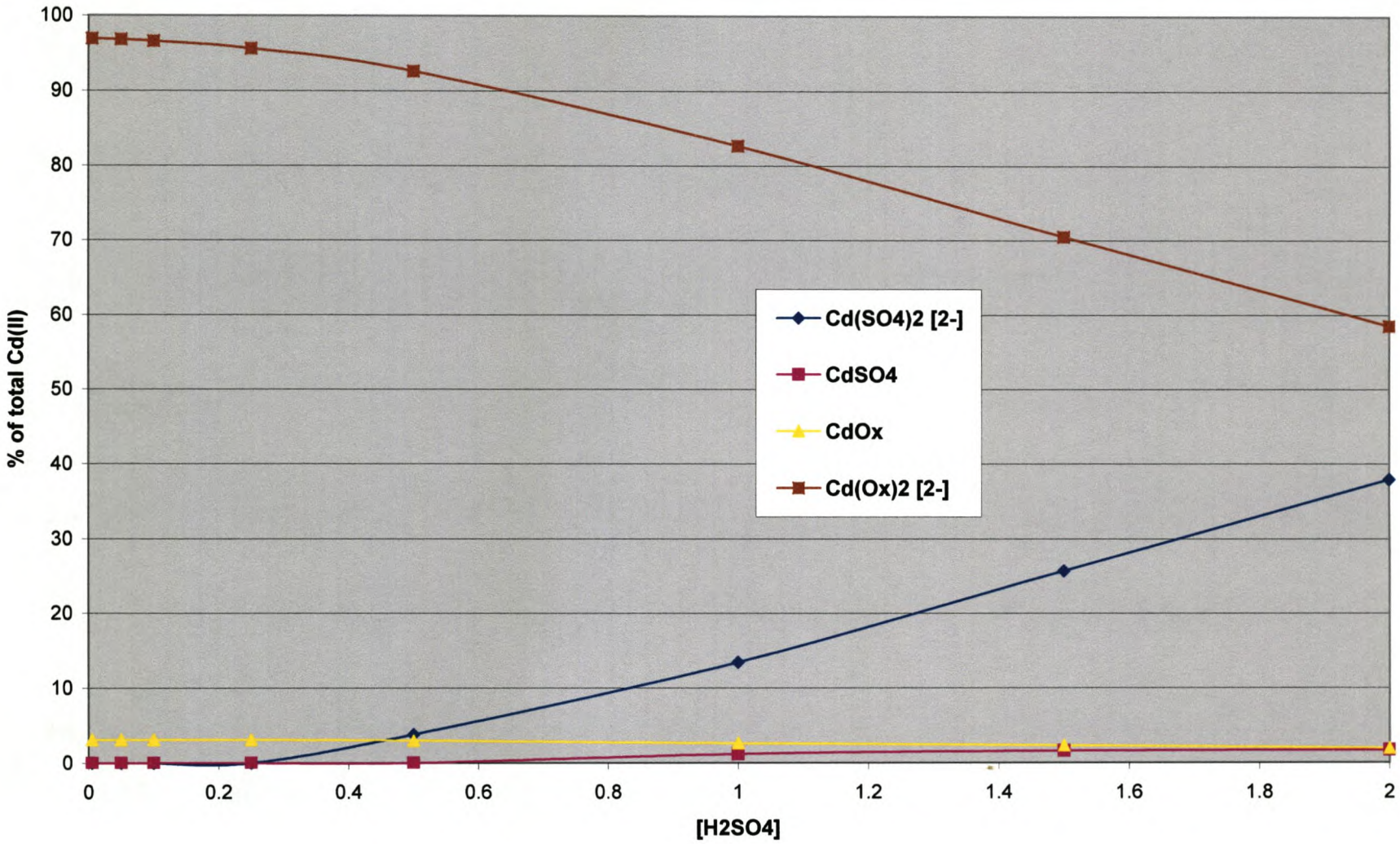

Journal of Radioanalytical and Nuclear Chemistry, Vol. 253, No. 2 (2002) 221–225

Cyclotron production of ^{68}Ge with a Ga_2O target

C. Naidoo,[1] T. N. van der Walt,[2] H. G. Raubenheimer[3]

[1] *Forensic Chemistry Laboratory, P.O. Box 668, Cape Town, 8000, South Africa*
[2] *National Accelerator Centre, P.O. Box 72, Faure, 7131, South Africa*
[3] *Department of Chemistry, University of Stellenbosch, Stellenbosch, South Africa*

(Received May 15, 2001)

Systematic information of exchange behavior of Ge(IV) and Ga(III) in varying oxalic acid (0.05M and 0.25M) and sulphuric acid (0.005M—2M range) mixtures is presented. These findings were used to develop a separation involving ^{68}Ge from a Ga_2O target material. A method based on acid dissolution of the target and chromatography on an anion exchange resin (Bio—Rad® AG1—X8) was developed. The separated ^{68}Ge has high radionuclidic purity and an acceptable chemical purity.

Introduction

^{68}Ge ($T_{1/2}=288$ d) decays by electron capture to give ^{68}Ga ($T_{1/2}=68$ m), which disintegrates mainly by positron emission (90.5%).[1] Its daughter ^{68}Ga emits β^+- and γ-rays (1077 keV) that last several months and is obtained by the use of ^{68}Ge in equilibrium with its daughter ^{68}Ga.[2] ^{68}Ge has many uses: for instance, ^{68}Ge has been used as a positron source in positron annihilation studies in nuclear physics and metal radiography in industry.[3] However, ^{68}Ge is used mainly as a ^{68}Ge–^{68}Ga generator for positron emission topography (PET) in nuclear medicine.[4,5] The growing use of ^{68}Ge–^{68}Ga generators for radiopharmaceutical purposes has increased the demand for ^{68}Ge.[6]

Various nuclear reactions leading to ^{68}Ge production is possible by either $^{66}Zn(\alpha, 2n)^{68}Ge$ (^{66}Zn abundance: 27.8%) or by the $^{69}Ga(p, 2n)^{68}Ge$ (^{69}Ge abundance: 60%) reaction. The former reaction has a yield of 1—2 $\mu Ci \cdot \mu Ah^{-1}$ whilst the latter reaction has as yield of 20 $\mu Ci \cdot \mu Ah^{-1}$.[7] For medical cyclotrons the second reaction is often used because of higher yields and because the chemical processing involves only two elements (germanium and gallium) in the separation, whereas the zinc target involves a third element (zinc) which introduces additional radionuclidic impurities.

Target matrices included the following: Ga metal (natural or enriched, melting point: 39 °C),[8,9] Ga_2O_3 (melting point: 1900 °C),[10] Ga_4Ni (melting point: 900 °C)[11] and RbBr (melting point: 682 °C).[12] The Ga_4Ni and RbBr targets were avoided because, again, additional components (Ni and Rb, respectively) were added to the system. The natural Ga metal (low melting point) and the isotopically enriched Ga metal (expensive material) were also not considered. Ga_2O_3 prohibited the use of high particle currents.

After irradiation of the target, ^{68}Ge may be separated from the target material by various methods. GRANT et al.[12] reported on the dissolution of a RbBr target in 6M HCl solution followed by quantitative distillation of ^{68}Ge from 6M HCl solution. GLEASON[8] reported on the distillation of ^{68}Ge from a ^{69}Ga target using CCl_4. PAO et al.[7] reported on the dissolution of Ga_2O_3 in 16M HNO_3 solution under reflux followed by ion exchange chromatography of ^{68}Ge on a hydrous zirconium oxide medium. LOC'H et al.[11] reported on the dissolution of Ga_4Ni in cold HNO_3 solution, followed by the recovery of ^{68}Ge by liquid-liquid extraction in a 9M HCl–CCl_4 system. BORONG[10] reported on the dissolution of Ga_2O_3 in concentrated H_2SO_4 solution, followed by liquid–liquid extraction of ^{68}Ge in H_2SO_4–HCl and H_2SO_4–KI systems. KOPECKY[13] also reported on the extraction of ^{68}Ge into CCl_4 from concentrated HCl solution using an α–particle irradiated Zn target.

At the National Accelerator Centre (NAC) the routine production of radioisotopes is carried out by means of a high energy proton (66 MeV) beam which has high beam currents (>65 μAh) available. For large-scale production, large targets (3–10 g) are normally used. At NAC an in-house Ga_2O target has been developed. No systematic information on distribution coefficients of Ge(IV) and Ga(III) in the oxalic acid–sulphuric acid mixture has been found in the literature. We have set out to investigate and develop a separation involving ^{68}Ge from the Ga_2O target.

Experimental

Reagents and apparatus

The reagents were of analytical grade. Deionized water was used and was obtained from a Millipore Milli-Z water system. Gallium metal (99.99%) and gallium oxide (99.99%) were obtained from Koch Chemicals Ltd., Heartford Hearts, England. The strongly basic quaternary ammonium anion exchanger, AG1–X8 (chloride form, 100–200 mesh particle size), was supplied by Bio–Rad® Laboratories, Richmond, California. Polyethylene tubes [25 mm inner diameter and 140 mm length (13 ml column) and 25 mm inner diameter and 110 mm length (10 ml column)] fitted with 70 μm polyethylene frits at the bottom were used as ion

0236–5731/2002/USD 17.00

Akadémiai Kiadó, Budapest
Kluwer Academic Publishers, Dordrecht

exchange columns. For elution curves and separations the columns were filled with a slurry of the resin until the settled resin reached the indicated mark. A 70 µm polyethylene frit was placed on top of the resin in the column. A plunger made of a Teflon® rod [25 mm diameter, 45 mm length, with a hole (1 mm bore) drilled through the length, fitted with an O-ring near the bottom and a luer-fitting at the top] was used to seal the column at the top end. The plunger was pushed firmly onto the frit until the resin column was compacted to the required volume.

Equilibrium distribution coefficients

Equilibrium distribution coefficients were obtained by equilibrating 100 ml of oxalic acid-sulphuric acid mixtures (at specified concentration ratios) containing various concentrations (0.1 or 1 mmol) of the specific element to be determined, with 1 g of the dry resin by shaking for 24 hours at 20 °C. After equilibration the resin was separated from the aqueous phase by filtration, the filtrate was collected in a 250 ml volumetric flask and diluted with water to volume, and the amount of the specific element in the aqueous phase determined by inductively coupled plasma emission spectrometry (Perkin Elmer 400). The element retained on the resin was eluted with 2M HNO_3 (50 ml) in a 250 ml volumetric flask, diluted with water to volume and the concentration of the element determined by emission spectrometry (as above). Equilibrium distribution coefficients (D) were calculated according to:

$$D = \frac{\text{mass of metal in resin (g)}}{\text{mass of metal in solution (g)}} \times 100 \text{ ml} \cdot \text{g}^{-1} \quad (1)$$

Elution curves

Elution curves were obtained by equilibrating the 10 ml (ca. 3.1 g dry resin) or 13 ml (ca. 4 g dry resin) with 50 ml of the appropriate solution. The sorption solution containing the dissolved elements in the appropriate media (50 ml) was passed through the resin column. The appropriate eluent was used to remove any impurities remaining on the column whilst the retained element was eluted with 2M HNO_3 (50 ml). The flow rate was 3±0.5 ml·min^{-1} and fractions (20 ml in volume) were collected from the sorption step. The excess acid was evaporated on a water bath, the residue was diluted with water to an appropriate volume, and the amounts of each element in all fractions were determined by emission spectrometry (as above). The experimental parameters for the elutions are presented in Table 1.

Target preparation and irradiations

Gallium oxide (1.874 g) and gallium metal (2.789 g) were heated at 60 °C until the gallium metal melted. The mixture was then heated at 700 °C for a further 15 minutes and mixed well (process repeated). The Ga_2O target (ca. 4.5 g) was prepared by unaxial pressing of the above mixture at a pressure of 523 MPa under vacuum by means of a suitable punch and die (machined from a high carbon and high chromium tool set).

Table 1. Experimental parameters of the various elution curves (column separations) on the anion exchange resin (AG1-X8)

Elution curve No.	Column size, ml	Equilibrating/eluting solution oxalic acid/sulphuric acid	Metals in the sorption solution
1	13	0.05M/0.25M	5 g Ga(III)/10 mg Ge(IV)
2	13	0.05M/0.5M	5 g Ga(III)/10 mg Ge(IV)
3	13	0.05M/1M	5 g Ga(III)/10 mg Ge(IV)
4	13	0.25M/0.5M	5 g Ga(III)/10 mg Ge(IV)
5	10	0.25M/1M	5 g Ga(III)/10 mg Ge(IV)
6	13	0.25M/1M	5 g Ga(III)/10 mg Ge(IV)
7[a]	13	0.25M/1M	ca. 4.5 g Ga_2O
8[a]	13	0.25M/1M	ca. 4.5 g Ga_2O
9[a]	13	0.25M/1M	ca. 4.5 g Ga_2O
10[b]	13	0.25M/1M	ca. 4.5 g Ga_2O
11[b]	13	0.25M/1M	ca. 4.5 g Ga_2O
12[b]	13	0.25M/1M	ca. 4.5 g Ga_2O

[a] Inactive Ga_2O target with radiotacer ^{67}Ga and ^{69}Ge
[b] Proton-irradiated Ga_2O target.

The disc (20 mm diameter and 1 mm thick) was encapsulated in an aluminium canister, which was sealed by a cold welding process. The targets were bombarded with a proton beam (energy window: 2–34 MeV; current 65 μA) for 10–15 minutes. High resolution γ-ray spectrometric analyses were performed with a high purity germanium detector and a multichannel analyzer (Silena Cicero-8K channel). Radiotracers ^{67}Ga ($T_{1/2}$ = 72.4 h) and ^{69}Ge ($T_{1/2}$ = 39 h) were readily available on site (NAC) and were used in the preliminary experiments. The radiotracers were dissolved in a 0.01M H_2SO_4 solution.

Chemical processing

Initial column separations were done using the inactive Ga_2O target. The target was gently heated and stirred in 5M H_2SO_4 solution (50 ml). After complete dissolution, the solution was heated to dryness (8 h). The residue was then dissolved in deionised water (25 ml) and again evaporated to dryness. The resultant residue was dissolved in 10M H_2SO_4 solution (10 ml), followed by 0.5M oxalic acid (50 ml) and deionized water (40 ml) in succession. The sorption solution was spiked with the ^{67}Ga and ^{69}Ge radiotracer (0.1 ml). The solution was pumped with a peristaltic pump at a rate of 3± 0.5 ml·min^{-1} onto a preconditioned AG1-X8 (13 ml) resin column as described above. The gallium (and ^{67}Ga) was eluted with 0.25M oxalic acid-1M sulphuric acid (450 ml), followed by deionized water (50 ml). The ^{69}Ge radionuclide was then eluted with 5M HNO_3 (100 ml). The ^{69}Ge eluate was evaporated to dryness and finally dissolved in deionized water (10 ml).

Proton irradiated Ga_2O target

The bombarded Ga_2O disc was recovered from the aluminium canister after a decay period (10 d) and processed using chemical steps similar to those described above (Fig. 1).

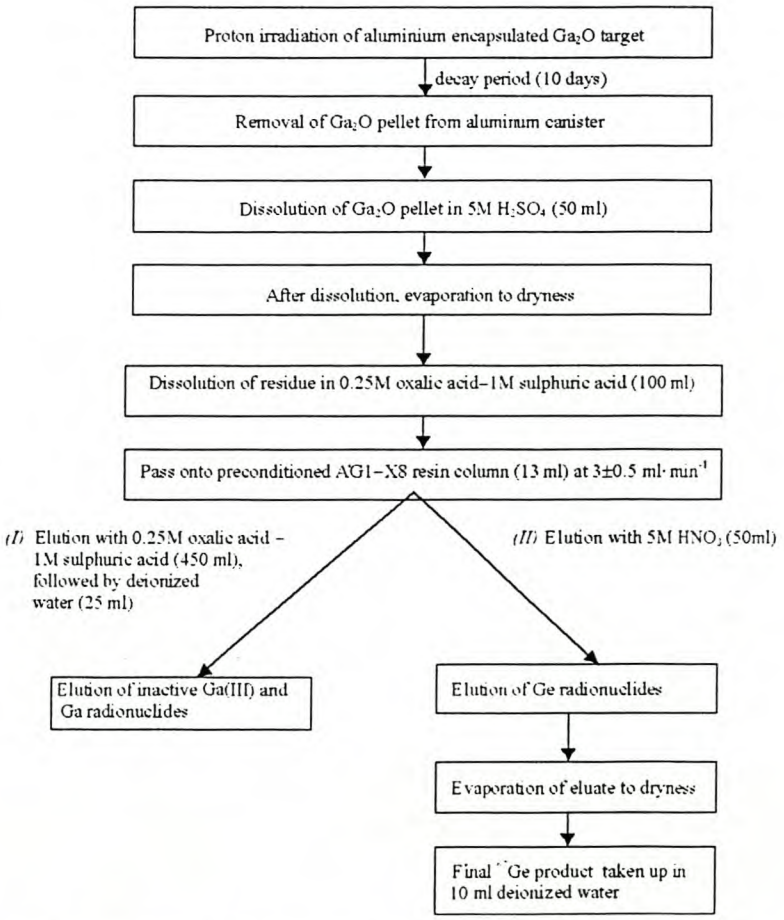

Fig. 1. Schematic diagram for the separation of high purity ^{68}Ge from a proton-irradiated Ga_2O

Table 2. Equilibrium distribution coefficients and separation factor for Ge(IV) and Ga(III) in varying oxalic acid-sulphuric acid concentration

H_2SO_4, M	0.005	0.05	0.1	0.25	0.5	1.0	1.5	2.0
0.05M oxalic acid								
Ge(IV)	7430	2710	1150	425	120	34.1	5.4	<0.5
Ga(III)	3500	1000	140	30.1	6.2	<0.5	<0.5	<0.5
α^{Ge}_{Ga}	2.1	2.7	8.2	14.1	19.4	68.2	10.8	1.0
0.25M oxalic acid								
Ge(IV)	$>10^4$	6410	3035	1215	520	175	104	45
Ga(III)	9700	6100	1150	140	42.1	10.1	3.5	<0.5
α^{Ge}_{Ga}	1.3	1.1	2.6	8.7	12.4	17.3	29.7	90

Table 3. Results of various elution curves (column separations) on the anion exchange resin (AG1-X8)

Elution curve No.	Breakthrough of metals (inactive or active) in sorption step, %	Breakthrough of metals (inactive or active) in eluting step, %	Total contaminant in the retained metal eluate
1	Ga(93.1%)–Ge(0%)	Ga(6.7%)–Ge(0%)	190 µg Ga(III)
2	Ga(96.2%)–Ge(1.5%)	Ga(3.9%)–Ge(0.01%)	105 µg Ga(III)
3	Ga(98.4%)–Ge(5.9%)	Ga(1.9%)–Ge(0.9%)	85 µg Ga(III)
4	Ga(92.3%)–Ge(0%)	Ga(7.9%)–Ge(0%)	195 µg Ga(III)
5	Ga(97.1%)–Ge(0.9%)	Ga(2.7%)–Ge(0.01%)	35 µg Ga(III)
6	Ga(95.1%)–Ge(0%)	Ga(2.7%)–Ge(0%)	75 µg Ga(III)
7[a]	Ga(95.1%)–Ge(0%)	Ga(4.9%)–Ge(0%)	90 µg Ga(III)
8[a]	Ga(96.1%)–Ge(0%)	Ga(3.7%)–Ge(0%)	75 µg Ga(III)
9[a]	Ga(95.1%)–Ge(0%)	Ga(4.9%)–Ge(0%)	85 µg Ga(III)
10[b]	Ga(95.1%)–Ge(0%)	Ga(4.7%)–Ge(0%)	90 µg Ga(III)
11[b]	Ga(96.1%)–Ge(0%)	Ga(4.1%)–Ge(0%)	80 µg Ga(III)
12[b]	Ga(95.1%)–Ge0%)	Ga(4.9%)–Ge(0%)	90 µg Ga(III)

[a] Inactive Ga_2O target with radiotacer ^{67}Ga and ^{69}Ge
[b] Proton-irradiated Ga_2O target.

Results and discussion

The equilibrium distribution coefficients (Table 2) show that Ge(IV) is higher than Ga(III) in both oxalic acid concentrations (0.05M and 0.25M). Increasing oxalic acid concentrations leads to higher coefficients for both metals. For a fixed oxalic acid concentration, both Ga(III) and Ge(IV) show a decrease in distribution coefficient with increasing sulphuric acid. This behavior can be ascribed to a combination of two factors: first, the increasing suppression of the dissociation of oxalic acid, and second, the increasing competition of the sulphate ion for exchange sites.

The separation factor ($\alpha^{Ge}_{Ga} = D_{Ge}/D_{Ga}$) for Ge(IV) and Ga(III) at varying oxalic acid-sulphuric acid concentrations is summarized in Table 2. The separation factor is optimum in the 1M sulphuric acid containing 0.05M oxalic acid or the 2M sulphuric acid containing 0.25M oxalic acid. However, at these sulphuric acid concentrations the distribution coefficients are relatively low and the separation of Ge from Ga is not feasible. By observing the distribution coefficients the best options seem to be either using 0.5M sulphuric acid containing 0.05M oxalic acid or 1M sulphuric acid containing 0.25M oxalic acid as sorption medium and eluent for Ga. The latter mixture was chosen as sorption medium and eluent for Ga because the distribution coefficient for Ge is higher. This was experimentally confirmed by elution curves (1)–(6) with 5 g Ga and 10 mg Ge, summarized in Table 3. Elution (6) showed a complete retention of Ge(IV) and easy elution of Ga(III) in the sorption and eluting steps. The retained Ge(IV) was easily eluted from the column and the inactive Ga(III) carrier (<75 µg) in the Ge eluate was at acceptable levels. The elution profile of elution curve (6) is depicted in Fig. 2. Elution (5) used similar conditions as elution (6) except for the use of a 10 ml column that resulted in breakthrough of Ge(IV) in the sorption and eluting steps. Elutions (2) and (3) also showed a breakthrough of Ge(IV) in the sorption and eluting steps. Elutions (1) and (4) showed no breakthrough of Ge(IV) but strong retention of Ga(III) on the column that resulted in tailing in the eluting step and, as expected, a higher inactive Ga(III) carrier (>190 µg) in the Ge eluate.

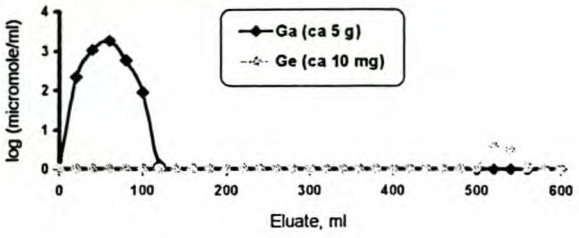

Fig. 2. Elution curve (6) for Ge—Ga on AG1-X8 resin (13 ml column) in 0.25M oxalic acid-1M sulphuric acid mixture

The conditions (0.25M oxalic acid-1M sulphuric acid mixture) of elution (6) were chosen for further work and adapted for the chemical processing of the inactive Ga_2O target (spiked with ^{67}Ga and ^{69}Ge radiotracer) and the proton-irradiated Ga_2O target.

Various dissolution methods of the target material (inactive Ga_2O) were investigated. Dissolution with concentrated and diluted HNO_3 solution (15M and 5M, respectively) was avoided because it required refluxing. Dissolution with concentrated HCl solution (10M) was also avoided because of vaporization of $GeCl_4$ at 83 °C. Complete dissolution of the target material was possible with 5M H_2SO_4 solution, but this was a lengthy (8 h) process. The results of the column separations of both the inactive target with radiotracers and that of the proton-irradiated target are presented in Table 3. The proton-irradiated target was processed after a decay period (10 d) when only the long-lived Ga and Ge radionuclides were present. During the separation again ^{67}Ga and ^{69}Ge radionuclides were again used to follow the efficiency of the separation, because β^+- and γ-rays were present for ^{68}Ge. The findings of the initial work were very similar to the results obtained with the inactive target with the radiotracers as well as with the proton-irradiated targets. The Ga radionuclides were very easily eluted during the sorption (>94%) and the eluting (>4%) steps. The final Ge radionuclide product was recovered from the resin column with high yield (>95%). The final ^{68}Ge product had acceptable levels of inactive Ga(III) present (<100 μg). The ^{68}Ge was detected by assaying the ^{68}Ga in the final ^{68}Ge product. This was performed at calibration time (15 days after the end of bombardment) when all the original ^{68}Ga had decayed and the remaining ^{68}Ga was due to the ^{68}Ge–^{68}Ga parent-daughter equilibrium. No ^{69}Ge (1107 keV) or other radionuclidic impurities were detected at calibration time. The ^{68}Ge had a radionuclidic purity of >99.99% at calibration time. The irradiation yield (15.1 $\mu Ci \cdot \mu A \cdot h^{-1}$) was of similar order to the theoretical yield (20 $\mu Ci \cdot \mu A \cdot h^{-1}$). Losses could be attributed to volatilization of the Ge radionuclides during the dissolution of the target. This could, however, be minimized if a closed system existed. The conversion of ^{68}Ge (deionized water matrix) into a 1M HCl solution matrix enables the production of a ^{68}Ge–^{68}Ga generator, by simply passing the radioactive solution through a tin dioxide column under conditions described in the literature.[14]

Conclusions

Purification of ^{68}Ge from the proton-bombarded Ga_2O target material has been achieved easily by the proposed method based on acid dissolution and column chromatography on a Bio-Rad® AG1-X8 resin column. The method is relatively simple, requires unsophisticated facilities, and has given consistent results. Adaptation to large-scale production in a hot-cell should be accomplished with ease.

References

1. Y. IWATA, M. KAWAMOTO, Y. YOSHIZAWA, Intern. J. Appl. Radiation Isotopes, 31 (1983) 1537.
2. G. R. CHOPPIN, J. RYDBERG, Nuclear Chemistry, Theory and Applications, New York, Pergamon Press, 1985.
3. E. HUGHES, Mat. Eng., 2 (1980) 34.
4. R. M. LAMBRECHT, M. SAJJAD, Radiochim. Acta, 43 (1988) 171.
5. R. M. LAMBRECHT, Radiochim. Acta, 34 (1988) 9.
6. S. M. QAIM, IAEA-SR-131/5, Vienna Austria, 13-17 October, 1986.
7. P. J. PAO, D. J. SILVESTER, S. L. WATERS, J. Radioanal. Chem., 64 (1981) 267.
8. G. I. GLEASON, Intern. J. Appl. Radiation Isotopes, 8 (1960) 90.
9. S. MIRZADEH, M. KAHN, P. M. GRANT, H. A. O'BRIEN, Radiochim. Acta, 28 (1981) 47.
10. B. BARONG, W. YINSONG, Nucl. Sci. Tech., 3 (1992) No. 3, 202.
11. C. LOC'H, B. MAZIERE, D. COMAR, R. KNIPPER, Intern. J. Appl. Radiation Isotopes, 33 (1982) 267.
12. P. M. GRANT, D. A. MILLER, J. S. GILMORE, H. A. O'BRIEN, Intern. J. Appl. Radiation Isotopes, 33 (1982) 415.
13. P. KOPECKY, B. MUDROVA, K. SVOBODA, Intern. J. Appl. Radiation Isotopes, 24 (1973) 73.
14. R. O. NEIRINCKX, M. A. DAVIS, J. Nucl. Med., 21 (1980) 81.